the LENSES project

LEarning and action alliances for NexuS EnvironmentS in an uncertain future

LENSES

WP7

D7.2 Fit for Nexus Climate Projections and Climate Risk Assessments (v6.0)

Christina Papadaskalopoulou,

Marina Antoniadou, Dimitris Tassopoulos (DRAXIS)

21 September 2023

Project coordinator

crea

Project partners

ecoadapta SWRI Technical University of Crete DRAXIS MIGAL NARC agriSat Ea-Tek

Project Website

www.lenses-prima.eu

This project is part of the PRIMA programme supported by the European Union.
GA n° [2041] [LENSES] [Call 2020 Section 1 Nexus IA]

Project no. 2041

Project acronym: LENSES

Project title: Learning and action alliances for NEXUS environments in an uncertain future

Call: PRIMA call Section 1 – Nexus 2020, Topic 1.4.1-2020 (IA).

Start date of project: 01.05.2021

Duration: 36 months

Deliverable title: D7.2 Fit for Nexus Climate Projections and Climate Risk Assessments

Due date of deliverable: April 2023

Project Coordinator: Stefano Fabiani, Council for Agricultural Research and Economics (CREA)

Organisation name of lead contractor for this deliverable: DRAXIS

Lead Authors Christina Papadaskalopoulou, Dimitris Tassopoulos, Marina Antoniadou

Email dtassopoulos@draxis.gr

Contributions from -

Internal Reviewer 1 **Gülay Onuşluel Gül (EA-TEK)**

Internal Reviewer 2 **Maria Llanos Lopez (AGRISAT)**

Dissemination level		
PU	**Public**	**PU**
CO	**Confidential, restricted under conditions set out in Model Grant Agreement**	
CI	**Classified, information as referred to in Commission Decision 2001/844/EC**	

History

Version	Date	Reason	Revised by
01	31/05/2021	TOC	Leon Kapetas
02	31/08/2021	First draft	Leon Kapetas, George Kefalas, Marina Antoniadou
05	30/09/2021	Second draft	Leon Kapetas, George Kefalas, Marina Antoniadou
08	31/10/2021	Third draft	Christina Papadaskalopoulou, George Kefalas, Marina Antoniadou
1.0	15/11/2021	Prefinal	Christina Papadaskalopoulou, George Kefalas, Marina Antoniadou
2.0	20/12/2021	Final	Christina Papadaskalopoulou, George Kefalas, Marina Antoniadou, Ali Gül, Filiz Barbaros
3.0	07/04/2023	Revised Draft	Christina Papadaskalopoulou, Dimitris Tassopoulos, Marina Antoniadou

This project is part of the PRIMA programme supported by the European Union.
GA n° [2041] [LENSES] [Call 2020 Section 1 Nexus IA]

History			
Version	**Date**	**Reason**	**Revised by**
4.0	04/08/2023	Prefinal	Christina Papadaskalopoulou, Dimitris Tassopoulos, Marina Antoniadou
5.0	18/09/2023	Prefinal	Christina Papadaskalopoulou, Dimitris Tassopoulos, Marina Antoniadou, Gülay Onuşluel Gül, Maria Llanos Lopez
6.0	21/09/2023	Final	Christina Papadaskalopoulou, Dimitris Tassopoulos, Marina Antoniadou

Executive summary

The water and food sectors are inextricably linked so that actions in one policy area commonly have impacts on the other, as well as on the ecosystems that natural resources and human activities ultimately depend upon. All three elements – water, food, ecosystems – are crucial for human well-being, poverty reduction, and sustainable socio-economic development. Climate is strongly connected to the Water-Ecosystem-Food (WEF) systems as it provides vital sources for their functionality while a changing climate may have adverse effects on them. The thorough analysis of the WEF and Climate nexus not only needs to account for the interactions taking place today but also to consider how future climate will affect the three sectors in isolation or in combination (e.g., compounding/cascade effects). As such, climate projections for different climatic variables are necessary.

This deliverable is entitled "Fit-for-Nexus climate projections and Climate Risk Assessments" (Del.7.2) and is aimed to provide the LENSES project partners (scientific and pilot teams) as well as the broader project stakeholders with valuable information on the expected changes in the main climate variables as well as on the fit-for-nexus climate risk assessments for the seven project pilot areas. In specific, an ensemble of global and regional climate models is utilized to examine the climate variables of mean temperature, total precipitation, and potential evapotranspiration based on two Representative Concentration Pathways, the RCP4.5 and the RCP8.5. The analysis takes place for the period from 2011 to 2100 where the simulations for future projections are available, while the period 1971 to 2000 is used as the reference period. Following, the information on future climate changes is used in combination with other relevant information on exposure and vulnerabilities associated to the nexus sectors of food, water, and ecosystems, in order to produce fit-for-nexus climate risk assessments for the pilot areas. Once the climate risk is estimated, adaptive capacity is evaluated based on the larger economic and social context prevailing at the pilot areas.

Overall, the upcoming increase in mean temperature is reflected in the analysis made for all pilots with a maximum increase of up to 5.9°C in the Middle East pilots (Jordan and Israel), where the mean temperature is expected to reach 28°C in the case of Jordan for the RCP8.5 scenario and for the long term. Regarding precipitation, the model signal varies per period and per pilot. In general, there is a decrease for both the dry and wet periods, with the decrease being more pronounced for the latter and this is strongly linked to the climate change. Finally, in the case of actual evapotranspiration, there is an increase in four of the seven pilots with the maximum increase in the case of the Gediz pilot (+60 mm) for the mid- and long-term period and according to RCP8.5. In three of the pilots, there is a strong decrease in all periods for both scenarios up to -110 mm. Most likely, the combined effects of decreasing precipitation and increasing temperature have led to reductions in actual evapotranspiration, because the reduction in water availability (due to lower precipitation) outweighed the increase in evaporation and transpiration (due to higher temperature).

As a review of the results of the overall climate risk assessment for the LENSES pilot sites, in the food system, the majority shows Medium-High risk. Exceptions to this are the Hula region in Israel, where the risk is High, and in Deir Alla, Jordan, for the RCP4.5 scenario, it is Medium. In the ecosystem sector, the results are more uneven between pilots. For the majority of the pilot areas, the results of the risk are Medium-High; however, the risk is estimated as High in the case of RCP8.5 for the Doñana and Pinios pilots. Additionally, in the Gediz basin in Turkey, the risk is estimated Low-Medium for both scenarios, while the risk is Medium for the RCP4.5

for the Tarquinia plain in Italy. Lastly, the adaptive capacity is estimated as Low-Medium for most of the pilots, while it is Medium for the Doñana and Tarquinia and Low for Deir Alla in Jordan.

The current report is produced under Task 7.2 “Climate Projections & Climate Risk Assessments” of WP7 “Nexus operationalization for SDG delivery” of the LENSES project.

Contents

List of figures

List of tables

Abbreviations

Abbreviation	Definition
AI	Aridity Index
BEDD	Biologically Effective Degree Days
C3S	Copernicus Climate Change Service
CMIP5	Coupled Model Intercomparison Project - Phase 5
CORDEX	Coordinated Regional Climate Downscaling Experiment
EFFIS	European Forest Fire Information System
ESGF	Earth System Grid Federation
FWI	Fire Weather Index
GCM	Global Climate Model
GDD	Growing Degree Days
GHG	Greenhouse Gases
IPCC	Intergovernmental Panel on Climate Change
LPIS	Land Parcel Identification System
LULC	Land Use/Land Cover
PRB	Pinios River Basin
PRD	Pinios River Delta
RCM	Regional Climate Model
RCP	Representative Concentration Pathways
SDG	Sustainable Development Goals
SSP	Shared Socioeconomic Pathways
WCRP	World Climate Research Program
WEF	Water-Ecosystem-Food

1 Introduction

The water and food sectors are inextricably linked so that actions in one policy area commonly have impacts on the other, as well as on the ecosystems that natural resources and human activities ultimately depend upon**.** For example, concerns over access to water are highly interdependent with issues of food insecurity and malnutrition as well as with the degradation of ecosystems. Water is an input for agricultural production and related value chains, as the largest user of water at a global level is agriculture. Consequently, agriculture may contribute to negative water budgets, aquifer depletion and water quality degradation. Ecosystems, such as forests, wetlands, and grasslands, are at the heart of the global water cycle, while their degradation is a multidimensional issue. Demographic, economic, social, and climatic changes are all exerting increasing pressures on natural resources, threatening the well-being of the ecosystems we rely upon. All three elements – water, food, ecosystems – are crucial for human well-being, poverty reduction and sustainable socio-economic development (Bervoets et al., 2018; Strasser and Stec, n.d.).

The climate is strongly connected to the Water-Ecosystem-Food (WEF) systems as it provides vital sources for their functionality while a changing climate may have adverse effects on them. In specific for the Mediterranean region, climate change is expected to be experienced through an increase in temperature, a decrease in precipitation and an increase in the frequency and duration of droughts which may have detrimental effects on water availability, agricultural production and may also lead to ecosystem degradation (EEA, 2017; IPCC,2021). Therefore, a thorough analysis of the WEF Nexus not only needs to account for the interactions taking place today but also to consider how future climate will affect the three sectors in isolation or in combination (e.g., compounding/cascade effects).

The general objective of the LENSES project is to contribute to improved water allocation and enhanced food security while preserving ecosystems and aiding climate change adaptation, by supporting the operationalization of the Nexus paradigm (from Nexus Thinking to Nexus Doing) through a collective learning process. This approach integrates the concepts of sustainable Nexus management with a resilience-oriented approach, leading decision-makers in accepting uncertainty as an integral part of management and decision-making. The project is implemented at seven demonstration pilot sites across the Mediterranean basin, which cover a wide range of environmental, socio-economic and socio-technical conditions. All pilots represent typical Mediterranean conditions, in terms of climate conditions, potentially conflicting uses of the resources, relevance of agricultural activities, types of crops, social context and stakeholders. The seven pilot cases are: the Middle Jordan Valley (Jordan); the Hula Valley, Galilee (Israel); the Doñana national park area, Guadalquivir basin (Spain); the Tarquinia plain (Italy); the Gediz basin & delta (Turkey) and finally, the Koiliaris Critical Zone Observatory (Greece) and the Pinios River Basin Hydrologic Observatory (Greece), which belong to the International Long-Term Ecological Research Network Sites.

The current report is entitled "Fit-for-Nexus climate projections and Climate Risk Assessments" and is produced as Deliverable 7.2 under Task 7.2 "Climate Projections & Climate Risk Assessments" of WP7 "Nexus operationalization for SDG delivery" of the LENSES project. This task, led by DRAXIS, aims at examining the climatic trends foreseen for the project pilot areas based on the available climate projections of the global and regional climate models. In addition, with this task it is aimed that the climate change information is used in combination with other relevant information on exposure and vulnerabilities associated to the Nexus sectors of food, water and ecosystems, in order to produce fit-for-Nexus climate risk assessments for the pilot areas.

1.1 Relation to other Work Packages of LENSES

Task 7.2 on Climate Projections & Climate Risk Assessments is designed so as to directly convey to the pilot partners valuable information on the expected future climate and risks for the pilot areas through WP2 "Learning & Action Alliances", as well as to provide input to other scientific tasks. In addition, the task is built on the requirements of the pilot partners and the local stakeholders, as the climate risk indicators will be selected based on their needs and tailored to the local conditions of the pilot areas, which will take place in the framework of Task 4.1 Nexus structure and Nexus Indicators. Furthermore, Task 7.2 outputs are going to be exploited within Task 4.2 "Participatory System Dynamics Modelling", where the knowledge acquired from a range of multidisciplinary scientific models will be integrated in order to support shifting from the individual WEF perspectives to the definition of a "System" picture. Finally, Task 7.2 will provide input with respect to the climate projections on precipitation and potential evapotranspiration for the examined climate scenarios, which will feed into the simulations of the hydrologic and water supply/allocation models to be set-up and run for the pilot cases in the framework of Task 7.4 "Water accounting, allocation and planning".

1.2 Structure of the document

In the Section that follows Section 2 ("Description of LENSES pilot areas"), a description of each LENSES pilot area is provided including topography, climatic conditions, and economic activities in relation to the Nexus systems under examination. In Section 3 ("Methodology"), the methodology for carrying out the climate projections is laid down, as well as the conceptual framework for climate risk assessments. In Section 4 ("Climate projections results for the LENSES pilots"), the outputs of the climate projections are presented in the form of maps, diagrams, and tables. In section 5 ("Climate Risk Assessment for the LENSES pilots"), the outputs of the climate risk assessment are presented for all pilots in the form of maps and tables. Section 6 is the Conclusions section, where the main findings of the analysis are summarized.

2 Description of LENSES pilot areas

In this section, a description of the seven pilot areas participating at the LENSES project is provided including information on the topography of the area, the economic activities in relation to the Nexus systems under examination and the climatic conditions prevailing at the area.

In the following table the coordinates of the pilot areas are presented while in Figure 1 the location of the pilots across the Mediterranean basin is depicted.

Table 1: Pilot area description by coordinates and resolution.

Pilot area name	Country	Coordinates
Koiliaris Critical Zone Observatory	Greece	35.6°N, 24°E, 35.2°N, 24.3°E
Pinios River Basin Hydrologic Observatory	Greece	40°N, 22.48°E, 39.56°N, 22.95°E
Gediz Basin & Delta	Turkey	38.7°N, 26.66°E, 38.5°N, 27.28°E
Tarquinia plain	Italy	42.65°N, 11.47°E, 42.11°N, 12.15°E
Doñana national park area, Guadalquivir basin	Spain	37.8°N, 6.9°W, 36.8°N, 6.0°W
Hula Valley, Galilee	Israel	33.05°N, 35.60°E, 33.01°N, 35.62°E
Middle Jordan Valley	Jordan	32.26°N, 35.5°E, 32.16°N, 35.6°E

Figure 1: Location of the pilots across the Mediterranean basin.

2.1 Pinios River Basin Hydrologic Observatory (Greece)

The Pinios River Basin (PRB) is situated in central Greece, covering an approximate area of 11,000 km^2. It is considered one of Greece's most productive basins and serves as the national Water Framework Directive (WFD) pilot basin. The Agia watershed forms the heart of the Pinios Hydrologic Observatory, which is a part of both the Greek and International Long Term Ecosystem Research networks. Within the LENSES project, the research and implementation efforts will be directed toward the two watersheds within the PRB, as illustrated in Figure 2. The Pinios River Delta (PRD) is located at the downstream end and encompasses an area of approximately 75 km^2. PRD holds significant socio-economic and environmental importance, as it sustains thriving agricultural and tourism activities that greatly benefit the local community. Additionally, the basin has been designated as part of the NATURA2000 network (GR1420002).

Regarding the climate conditions in this region, similar to the PRB, both the Agia watershed and PRD endured severe droughts from 1988 to 1993, which had a substantial impact on the PRB and the broader Mediterranean Basin (Loukas, 2010). The microclimatic conditions in the basin lead to temperature inversions and result in frost conditions that can only be accurately observed and recorded through an extensive network of climate monitoring stations.

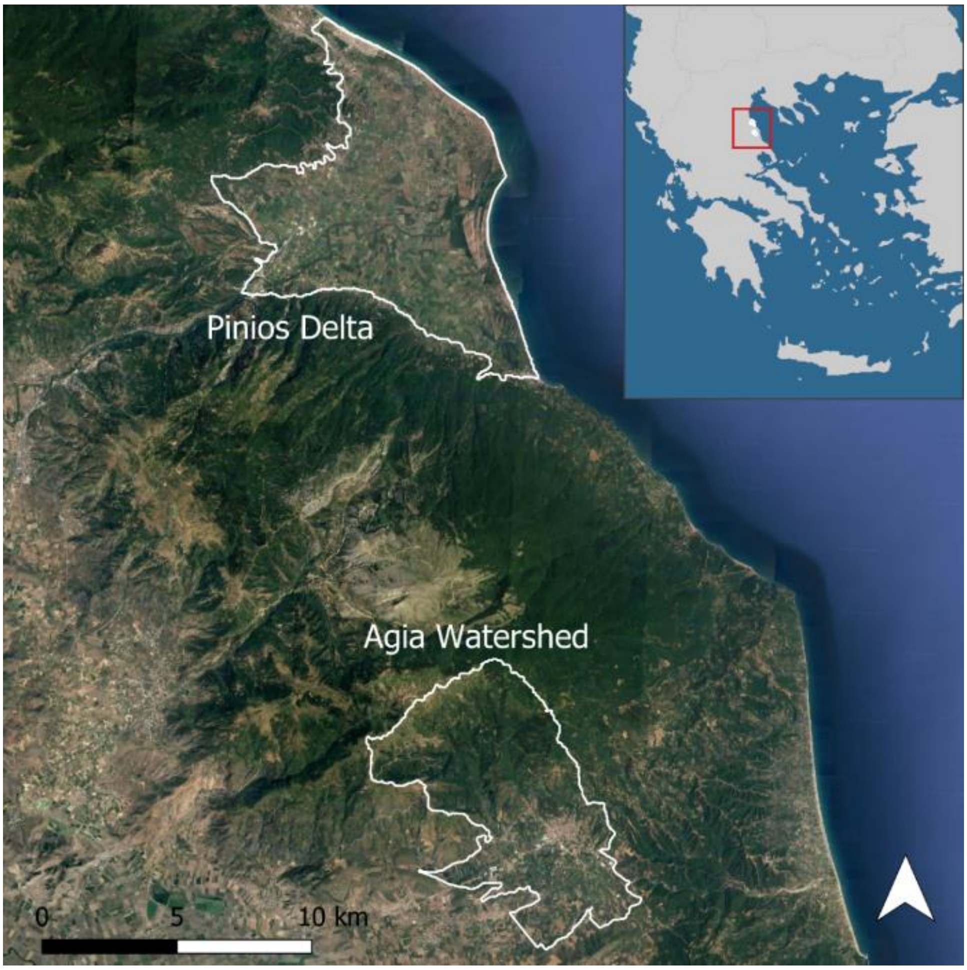

Figure 2. Pinios pilot in Greece. Source: SWRI, 2021.

2.2 Doñana national park area, Guadalquivir basin (Spain)

The Doñana national park area (hereafter called Doñana) is located in Andalusia, southwestern Spain. Doñana consists of a large system of marshes, dunes, and beaches associated with the coastal dynamic of the mouth of the Guadalquivir River (Gómez-Baggethun, 2010). The total extent of Doñana pilot area is about 3,723 km^2 and encompasses the distribution of the different components in the WEF nexus critical to understanding the current conflicts for the use of resources. Some oceanic influence in the climate of Doñana results in milder temperatures, higher air moisture and rainfall than further inland. The Mediterranean type of climate with the harsh summer drought is moderate by the humid masses of air arriving from the ocean (Garcia Novo, 1997). Doñana is broadly considered a very threatened area by climate change. Several recent studies and scientific publications warn of the big climatic threats for Doñana, e.g., desertification, sea-level rise, changes in climatic conditions affecting endangered species, etc. (Iglesias et al., 2017).

In the following figure the Doñana pilot area is presented. The pilot was divided into the North part and the South part to separately assess the Doñana Natural Park (South part) and the agricultural areas that are mostly located at the northern area of the pilot. The borders of this division were based on the boundaries of ground water bodies, that were provided by the pilot.

Figure 3: Doñana national park area with North and South divisions

2.3 Koiliaris Critical Zone Observatory (Greece)

The Koiliaris River watershed is designated as a Critical Zone Observatory (CZO) and can be accessed at www.koiliaris-czo.tuc.gr. It is situated on the island of Crete and is an integral part of the European Long Term Ecological Research (LTER) Network as well as the LTER-Greece Network. This watershed has been the subject of extensive research for the past 15 years. The Koiliaris River watershed is noteworthy for its severely degraded soils, which have been impacted by centuries of intensive agricultural activities, including grazing.

These soils exemplify Mediterranean soil conditions that face an imminent threat of desertification, particularly with regard to soil carbon loss. This concern arises due to the climate change projections made by the United Nations Intergovernmental Panel on Climate Change (IPCC) for the region in the coming century.

The Koiliaris CZO is situated in the northwestern region of Crete, near Chania, Greece. In the following figure the topography and location of the Koiliaris Critical Zone Observatory pilot area are presented.

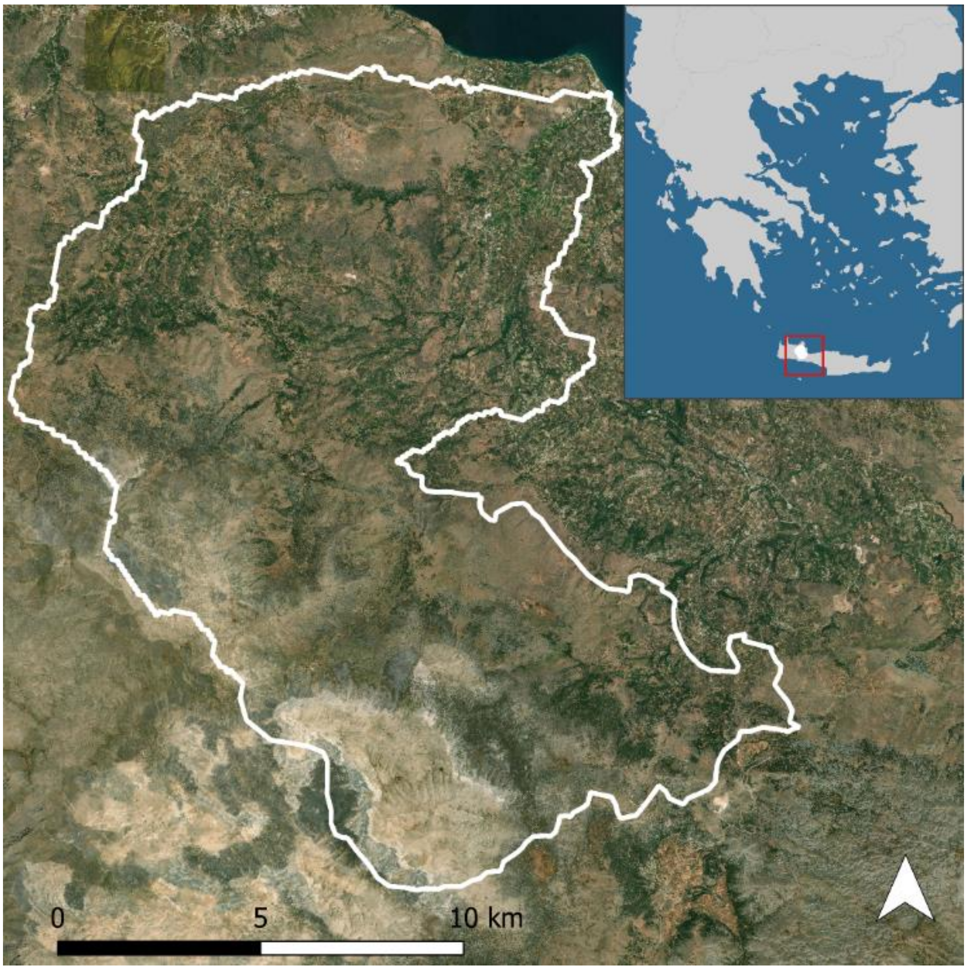

Figure 4: Schematic of the regional geology, the drainage network, and the monitoring network of Koiliaris CZO. Source: Lilli et al., 2020

2.4 Gediz Basin & Delta (Turkey)

The Gediz River Basin, covering an expansive area of 17,500 km^2, stands as one of the most significant basins in Western Turkey, constituting 2.2% of Turkey's total land area. Within this basin, the Menemen Plain emerges as a sub-region with the highest agricultural potential in the entire area. This fertile plain, situated in the Lower Gediz River Basin, falls within the borders of the Izmir Province.

The climate characteristics of the Gediz Basin exhibit notable variations between the upper and lower regions of the basin. In the lower parts of the basin, the Mediterranean climate prevails, while in the upper reaches, the climate exhibits more transitional patterns influenced by various climatic factors such as temperature, pressure, wind, and precipitation. In the following figure the topography and location of the Gediz Basin & Delta pilot area are presented.

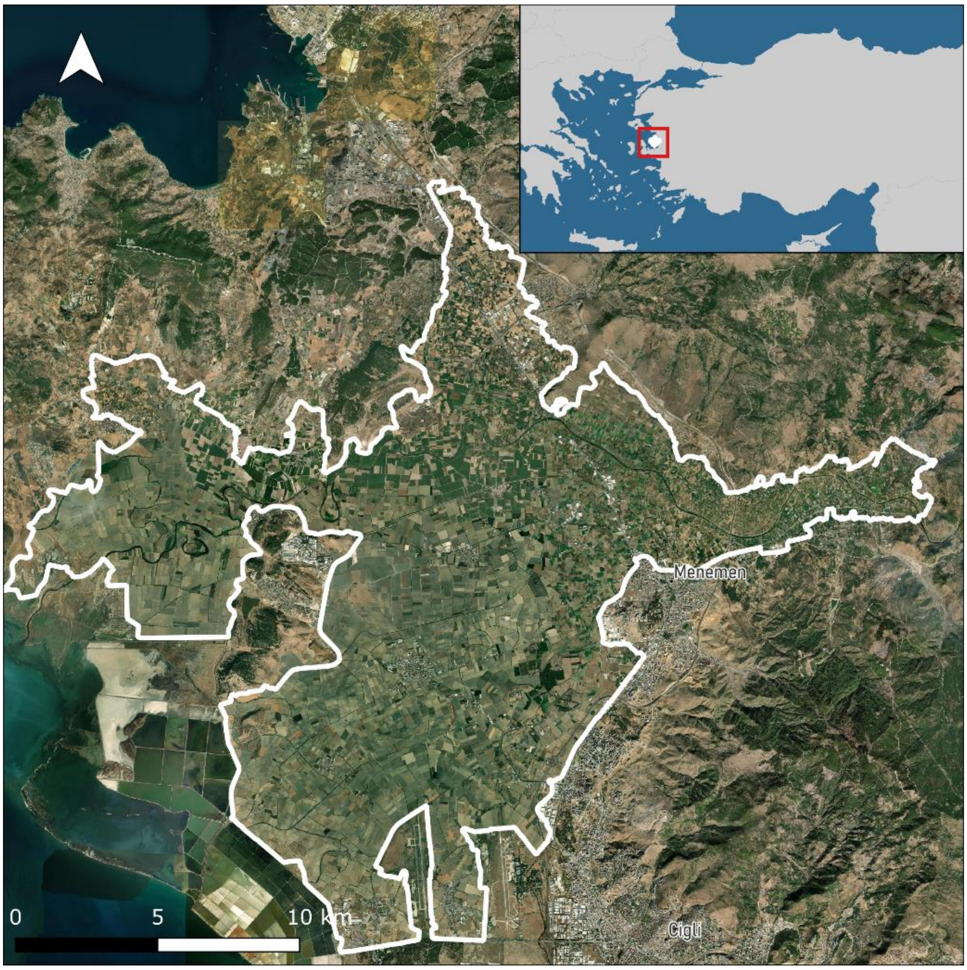

Figure 5: Gediz River Basin. Source: UTAEM, 2021

2.5 Galilee, Hula Valley (Israel)

The Galilee region constitutes the northernmost periphery of Israel, extending from the Mediterranean Sea in the west to the Golan Heights massif and the Jordan River in the east, with Syria and Jordan lying beyond. The Upper Galilee, which comprises the northern highland part of the Galilee, is bordered to the north by the political boundary with Lebanon. The principal town in this region is Safed, situated towards the eastern edge of the highlands. The area, referred to as the Eastern Galilee and depicted on the map, spans approximately 2,000 km2 and is home to approximately 180,000 residents. The steep slopes of the Golan Heights to the east and the Naphtali Mountains in the west (Upper Galilee mountains) rise 400-900 meters above sea level, forming natural boundaries that run in a narrow north-south orientation along the Hula Valley. The Hula Valley is situated within the northern portion of the Dead Sea Rift Valley, approximately 70 meters above mean sea level. This valley occupies a significant portion of the Jordan River's course to the north of the Sea of Galilee.

In terms of climate, the region experiences hot, dry winds originating from the inland desert during the summer months, while the winter months are characterized by wet, cool westerlies from the ocean.

However, unlike the moderate Mediterranean climate found along the coastal plains, the enclosed topography of the Hula Valley results in more pronounced seasonal and daily temperature fluctuations.

For a visual representation of the topography and the precise location of the Galilee and Hula Valley pilot area, please refer to Figure 6.

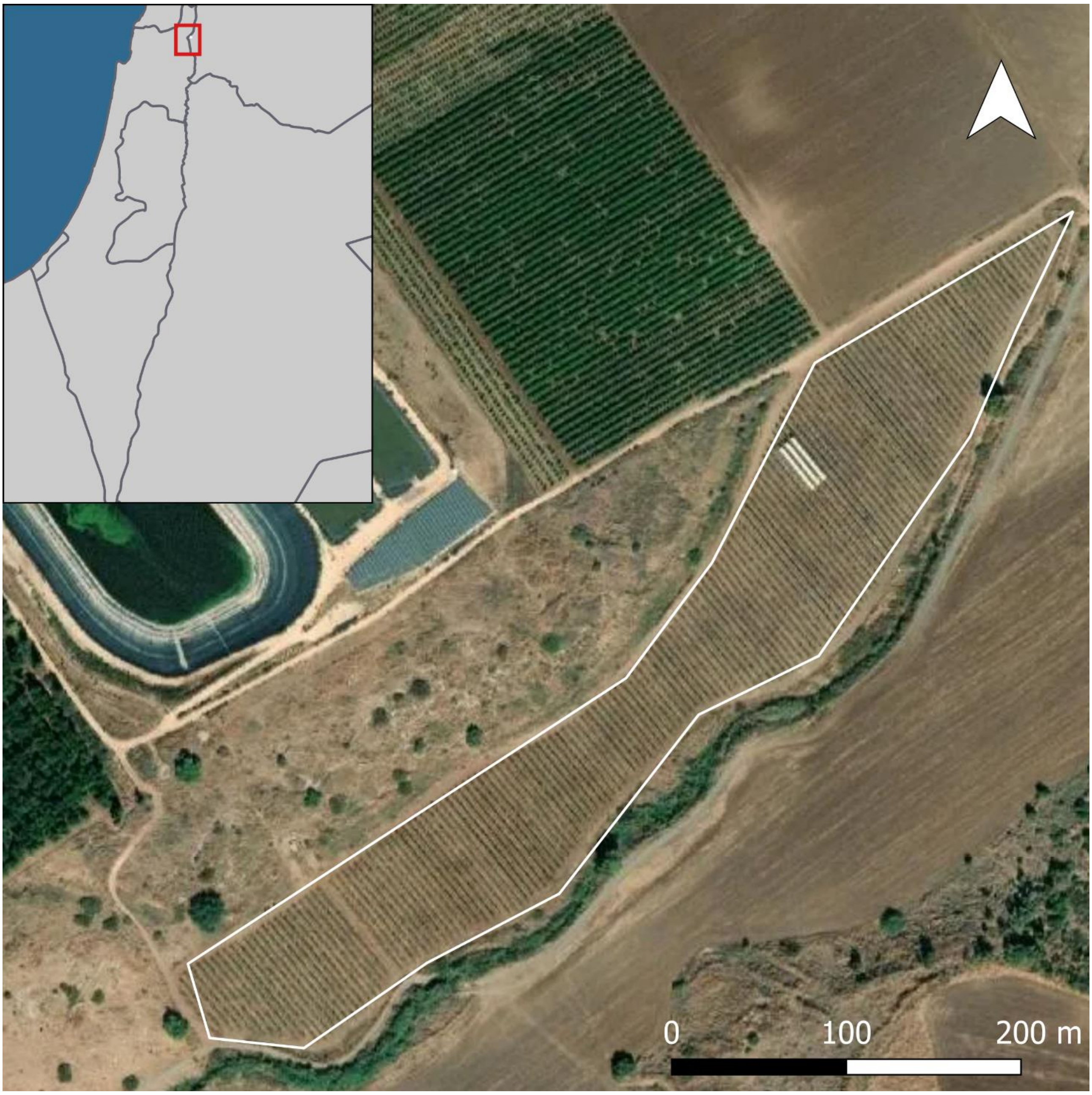

Figure 6: Hula Valley, Galilee region. Source: MIGAL, 2021

2.6 Middle Jordan Valley, Deir Alla (Jordan)

The Jordan Valley stretches from Lake Tiberias, situated at an elevation of 212 m southward to the Dead Sea, which presently stands at a height of about 429 m. Its width at the northern end of the Dead Sea measures approximately 20 km, whereas it narrows to about 10 km as it extends toward Lake Tiberias, with its minimum width in the central part being around 4 km.

The prevailing climate in the Jordan Valley area is distinct and sharply contrasts with the climate of its surrounding regions. Specifically, the Jordan Valley is characterized by hot, dry summers and mild, wet winters. As one moves southward through the valley toward the Dead Sea, the climate becomes progressively drier. In the following figure the topography and location of the Middle Jordan Valley, Deir Alla pilot area are presented.

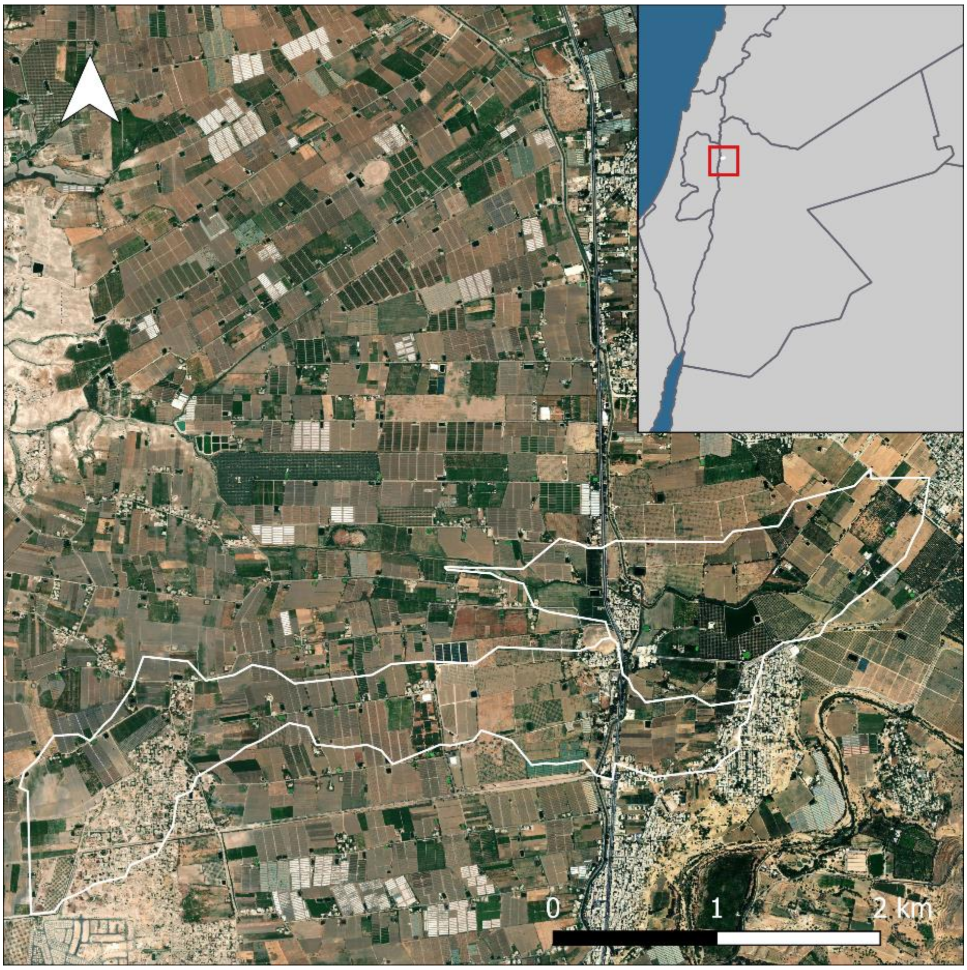

Figure 7: Middle Jordan Valley, Deir Alla. Source: NARC, 2021

2.7 Tarquinia plain (Italy)

Tarquinia is situated in central Italy within the Lazio Region, approximately 90 km to the north of Rome. The primary economic activities in this region revolve around tourism, as Tarquinia has been included on the UNESCO World Heritage list since 2004, and agriculture. The pilot area boasts a flat topography and serves as an intensive agricultural zone, with approximately 85% of the site designated as a vulnerable nitrate zone. The potential risks associated with severe weather patterns resulting from climate change could have detrimental and irreversible impacts on agricultural activities and the local economy.

The climate in Tarquinia aligns with the typical Mediterranean pattern, characterized by warm, dry summers and mild winters. In the following figure the topography and location of the Tarquinia plain pilot area are presented.

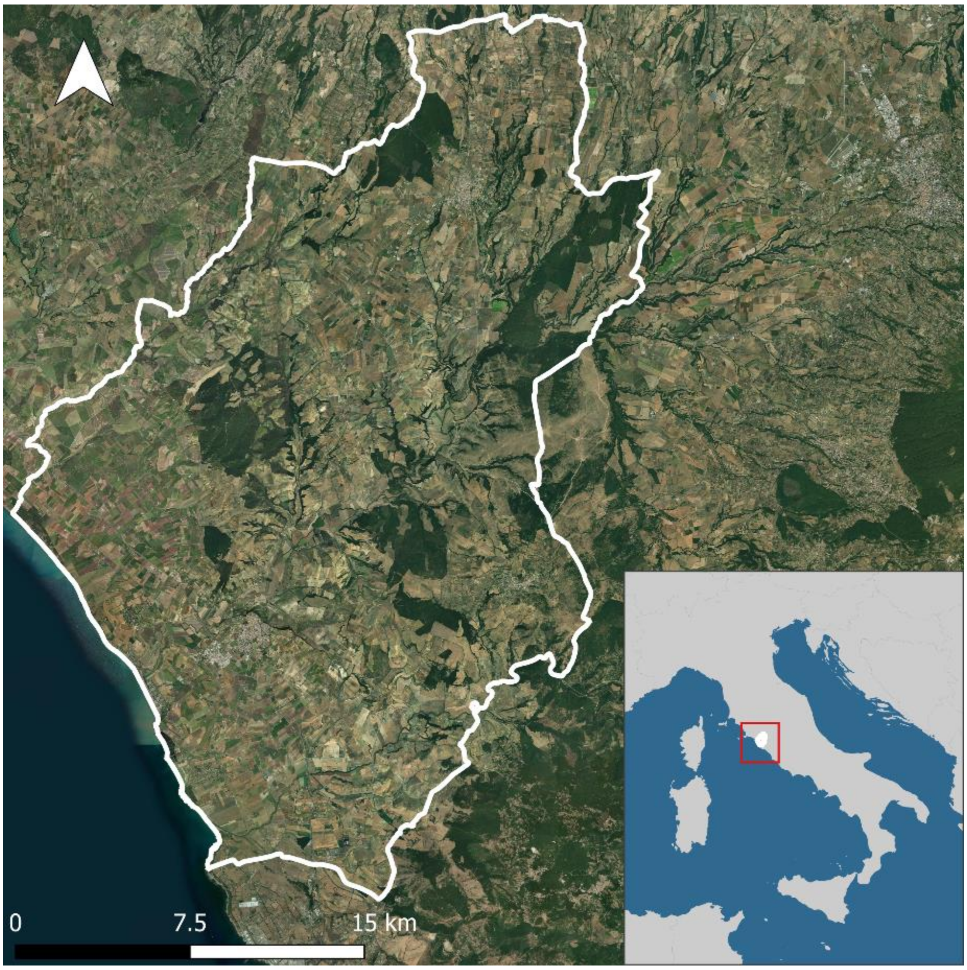

Figure 8: Tarquinia Plain in central Italy. Source: CREA, 2021

3 Methodology

3.1 Climate Projections

There are two types of models used to produce climate projections, namely the Global Climate Models (GCMs) which simulate the climate at a global scale, and the Regional Climate Models (RCMs) which simulate the climate for a specific region (Mc Sweeney & Hausfather, 2018). GCMs have a typical spatial resolution from 50 to 250 km and require large computational power and time. RCMs were essentially developed with the aim of downscaling climate fields produced by coarse resolution GCMs, thereby providing information at fine, sub-GCM grid scales more suitable for studies of regional phenomena and application to climate risk assessments. The results of RCMs and GCMs are different because the former describes global circulation, taking into account large-scale factors such as greenhouse gases (GHGs) or fluctuations in solar radiation, while the latter improves this information both spatially and temporally, taking into account smaller-scale information such as topography, coastlines, inland water bodies, and land cover or mid-range dynamic processes (Giorgi, 2019) (Figure 9).

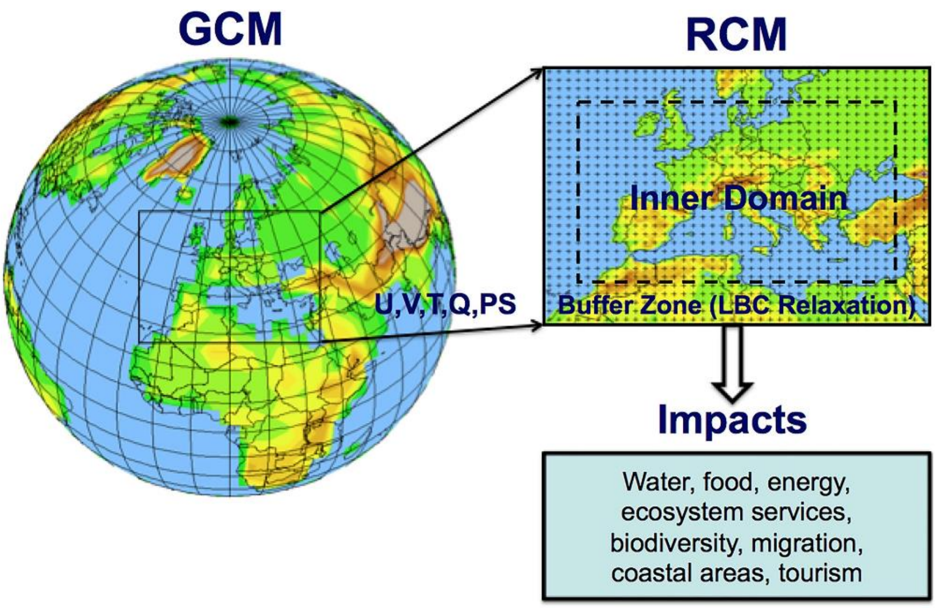

Figure 9: An RCM domain embedded in a GCM grid. Application to vulnerability, impacts, and adaptation studies (Source: Giorgi, 2019).

Climate projections are presented for a range of plausible pathways for the future state of greenhouse gas emissions, land use, and atmospheric aerosols, among others. In 2013, the IPCC in its fifth Assessment Report (AR5) presented for the first time the Representative Concentration Pathways (RCPs) (IPCC, 2013). Following AR5, the 5th phase of the Coupled Model Intercomparison Project (CMIP5) was launched with the simulations of GCMs based on the RCPs. A few years later, the CMIP5 GCM's simulations were downscaled to the regional level with the use of RCMs, through the Coordinated Regional Climate Downscaling Experiment (CORDEX).

Since 2014, research efforts have focused in parallel on the further evolution of the RCPs into the Shared Socioeconomic Pathways (SSPs) (O'Neill et al., 2014; O'Neill et al., 2015; Kriegler et al., 2016; Riahi et al., 2017), with the aim to incorporate them into the 6th IPCC Assessment Report (AR6) (IPCC, 2021). The 6th phase of the Coupled Model Intercomparison Project (CMIP6) was launched in 2021 with the first data of CMIP6 global simulations driven by the SSPs. However, the CORDEX database has not yet published any regional simulations from CMIP6 data.

The spatial resolution of GCM simulations that is currently available for CMIP6 (based on the SSPs) is considered suitable for a climate analysis at a wider geospatial level (European, Mediterranean, etc.), but not at the pilot level (e.g. the case of the LENSES pilots which are quite small in size, ranging within 0.7 - 80km), as the average climatic conditions in a wider area (e.g. 100×100 km) are usually very different from the ones prevailing in a specific small area. As a result, the analysis for the LENSES pilots would not be representative of the local conditions, and therefore it was decided to carry out a detailed analysis at pilot level with the use of RCM simulations based on the RCPs.

Additionally, to provide an insight on the differences expected at wider Mediterranean level among the projections of the successive generation scenarios (RCPs, SSPs), the results of the GCM simulations for the Mediterranean basin are presented in the Discussion section.

Among the four RCPs of the IPCC (2013), RCP2.6 is a scenario with very strict measures regarding GHG emissions, RCP4.5 and RCP6.0 are both intermediate scenarios and RCP8.5 is a scenario that captures the GHG emissions, in case no mitigation measures are implemented (IPCC, 2013). The scenarios which do not assume additional efforts to constrain emissions ('baseline scenarios') lead to pathways ranging between RCP6.0 and RCP8.5. The primary factors affecting emission projections are population projections, economic development, energy use and land-use change (IPCC, 2013).

For the current analysis at pilot level, the RCP4.5 and RCP8.5 were selected, the former serving for examining a more realistic mitigation scenario (compared to RCP2.6) and the latter representing a business-as-usual scenario, against which a comparison may be made. In specific,

- RCP4.5 is a scenario that assumes stabilization of radiative forcing at 4.5 W/m² in the year 2100 without ever exceeding that value (Thomson et al., 2011) and
- RCP8.5 assumes that radiative forcing will exceed 8.5 W/m² by 2100 and will continue to rise for some amount of time (Riahi et al., 2011).

As for the analysis at Mediterranean level, the respective to RCP4.5 and RCP8.5 combined scenarios are selected which are the SSP3-4.5 and SSP5-8.5.

The data used in the following analysis were retrieved from the Copernicus Climate Change Service (C3S, 2019). More specifically, the dataset was the outcome of the Coordinated Regional Climate Downscaling Experiment (CORDEX) database. CORDEX is a framework, under the World Climate Research Program (WCRP), to evaluate regional climate model performance through a set of experiments aiming at producing regional climate projections (Giorgi et al., 2009).

An ensemble of climate models is performed consisting of different RCMs that are driven by different GCMs, with the necessary model information given in Table 2. The selection of GCMs was based on the study of McSweeney et al. (2015), which illustrates a methodology for selecting from available models in order to identify a set of 4-5 GCMs for use in regional climate change assessments. The selection in this mentioned study focuses on their suitability across multiple regions. The selection of the RCMs was based on the studies of Kotlarski et al. (2014) and Katragkou et al. (2015), to ensure that the simulations selected are plausible and representative of future climate. Those analyses confirm the ability of RCMs to capture the basic features of the climate, including its variability in space and time.

The examined climate variables are the mean temperature, precipitation, and actual evapotranspiration. For the mean temperature, the data represent the mean ambient air temperature at 2m above the surface and the initial unit of the variable was Kelvin (°K), nevertheless a unit conversion has been applied to Celsius (°C). With respect to the precipitation, the variable of the precipitation flux is used, after a conversion to mm·day^{-1}. Actual evapotranspiration is defined as a positive vector component indicating energy transfer from the surface to the atmosphere. The unit of the actual evapotranspiration was kg·m^{-2}·s^{-1}, but a conversion to mm·day^{-1} was applied as well. As for the spatial resolution of the datasets, the best available resolution was chosen, i.e., 5 km for the mean temperature and total precipitation and 12.5 km for the actual evapotranspiration, while the initial temporal resolution of the input data was daily. It is important to note that for the variables of mean temperature and total precipitation, a bias-adjusted dataset was used, also based on CORDEX data. In particular, an ensemble of EURO-CORDEX (daily mean temperature and precipitation) was bias-adjusted using EFAS-Meteo and a new bias adjustment method developed by SMHI.

Table 2: Ensemble of models used for each climatic variable and area under study

MODELS		VARIABLES		
Global Climate Models (GCMs)	Regional Climate Models (RCMs)	Mean Temperature	Total Precipitation	Actual Evapotranspiration
ICHEC-EC-EARTH	KNMI-RACMO22E	-	-	✓
MPI-M-MPI-ESM-LR	CLMcom-CLM-CCLM4-8-17	-	-	✓
MPI-M-MPI-ESM-LR	MPI-CSC-REMO2009	✓	✓	✓
NCC-NorESM1-M	DMI-HIRHAM5	-	-	✓
HadGEM2-ES	KNMI-RACMO22E	✓	✓	-

It is important to mention that there is a variety of uncertainty sources in climate projections, such as sampling uncertainty, model uncertainty, scenario uncertainty and the natural variability or internal variability of the climate system (Tebaldi & Knutti, 2007). To address the uncertainty due to climate model selection, the ensemble of climate models is utilized as according to various studies, multi-model ensembles produce more accurate results than single models (Kiktev et al., (2007); Mullen and Buizza, (2002)).

With respect to the selected periods of the analysis, these are broken down into the baseline (or reference) period and the future period. The baseline period is based on the period covered by the historical experiments, which is the period for which modern climate observations exist (1850 or 1950 up to 2005). These experiments, that follow the observed changes in climate forcing, show how the Regional Climate Models (RCMs) perform for the past climate when forced by Global Climate Models (GCMs) and can be used as a reference period for comparison with scenario runs for the future. Thus, from 2006 to 2100, the available model climatic data refer to model projections. The period of analysis selected was decided to be in consistency with the predefined periods available through the Copernicus Climate Change Service (i) the baseline period: 1971-2000 and (ii) three future sub-periods: 2011-2040, 2041-2070, 2071-2100, as these indicators will be used in the climate risk assessment part of the deliverable.

3.2 Climate Risk Assessment Conceptual Framework

The Sixth Assessment Report of the Intergovernmental Panel on Climate Change (Reisinger et al., 2020) defines **risk** as "*the potential for adverse consequences for human or ecological systems, recognising the diversity of values and objectives associated with such systems"*. The aforementioned adverse consequences for the Water-Ecosystem-Food sectors can refer to health and well-being, economic assets and investments, services, ecological integrity, ecosystems and species, and others. In the framework of the current assessment, the term "risk" is used in the context of climate change impacts, as this is defined by IPCC, i.e., "risks *result from dynamic interactions between climate-related* ***hazards*** *with the* ***exposure*** *and* ***vulnerability*** *of the affected human or ecological system to the hazards".* As it may be noticed from the aforementioned definition, risk refers only to the adverse consequences of climate change.

While risk refers to the potential for adverse consequences, the term "**impact**" is used to describe the consequences of realized risks, while impacts can also be beneficial as shown in the relevant definition of IPCC "*The consequences of realized risks on natural and human systems, where risks result from the interactions of climate-related hazards (including extreme weather and climate events), exposure, and vulnerability...Impacts may be referred to as consequences or outcomes, and can be adverse or beneficial".*

In the framework of the LENSES Project, a methodology was developed for the assessment of climate risks on the Water – Ecosystem – Food nexus, based on the conceptual framework of the IPCC (Cardona et al., 2012) and of the World Bank (The World Bank, 2021). In specific, for the assessment of climate risk, a qualitative formula is used for depicting the relationship of risk with hazard, exposure and vulnerability:

$$Risk\ = Hazard * Exposure * Vulnerability \qquad (1)$$

Each variable in the above equation is defined as a composite indicator consisting of one or more individual indicators. A set of hazard indicators is used to reflect the climate-dependent information for each impact and is calculated with the use of information on the climate projections for climate-based indexes (see subchapter "Hazard"). Exposure is estimated with the use of spatial data on landscape characteristics, such as land use/cover, agricultural land management, essential ecosystems etc. (see subchapter "Exposure"). Regarding the vulnerability aspect, a series of indices is adopted for assessing the predisposition and susceptibility of certain critical elements of the nexus sectors in climatic hazards (see subchapter "Vulnerability").

Once the climate risk is estimated, adaptive capacity is evaluated based on the economic capacity of the pilots. Finally, overall risk is estimated based on the synthesis of the aforementioned indicators, as shown in the figure below which is adopted by IPCC and further specified for the needs of the LENSES project.

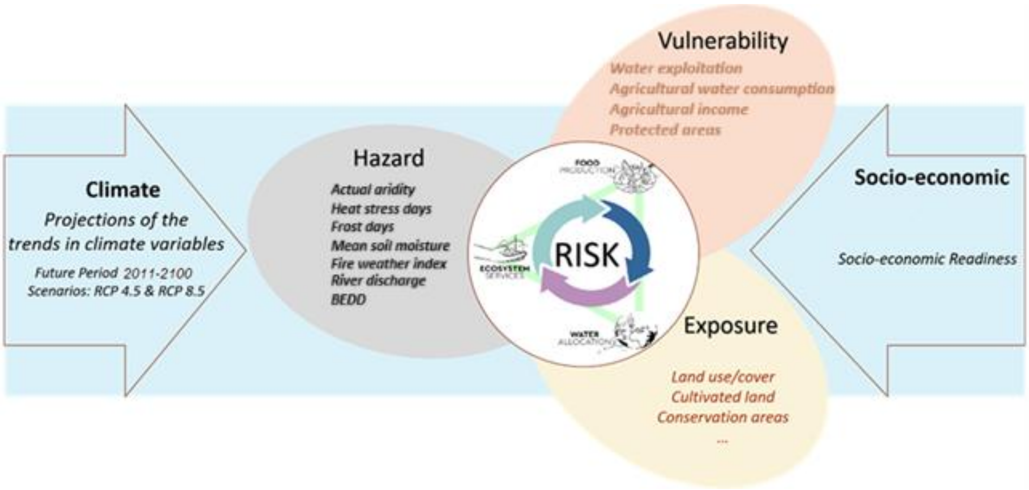

Figure 10: Conceptual framework of the Climate Risk Assessment in the LENSES project.

The formulation of the indicators includes the stages of normalization, weighting, and aggregation. As shown in Table 3, in the normalization stage, the values of indicators expressed in different measurement units are adjusted to a common scale 0-5 to be comparable. The weighting stage includes the assignment of weights to the variables to express the contribution and the relevant importance of each sub-indicator in a composite index.

It is noted that in the case of the hazard sub-indicators, negative values are also used where a climate trend turns to have beneficial effect for the WEF system under examination (e.g., increase in the number of days with temperature conditions suitable for crop growth).

Table 3. Rating scale of risk indicators

Qualitative scale	Numerical scale
Low	**0 < Risk ≤1**
Low to Medium	**1 < Risk ≤2**
Medium	**2 < Risk ≤ 3**
Medium to High	**3 < Risk ≤ 4**
High	**4 < Risk ≤ 5**

The indicators were normalized and rescaled to the new range [0-5]**,** by applying the min-max method (OECD 2008) according to the following formula.

$$x' = a + \frac{(x - \min(x))(b - a)}{\max(x) - \min(x)} \quad (2)$$

where x' is the normalized value, x is the original value and a, b are respectively the minimum and maximum values of the selected new range.

The weighting stage includes the assignment of weights to the variables in order to express the contribution and the relevant importance of the individual risk components and of their sub-indicators in the composite risk index. For the aggregation of the risk components, it was considered appropriate to select the geometric aggregation method (OECD, 2008), according to which each sub-indicator is raised to its weight and then multiplied with the other indicators, to form the composite indicator, as shown in the following formula:

$$R = \prod_{q=1}^{Q} C_R^{w} \tag{3}$$

where R is the composite risk indicator, C_R the individual risk components (i.e., hazard, exposure, vulnerability), Q the number of indicators comprising the composite indicator (i.e., 3) and w the weight assigned to each risk component. The sum of the weights for all risk components equals to 1. This method was selected as, based on the conceptual framework of IPCC (2014), there is no compensability in the performance of the risk components, i.e., a zero exposure of elements cannot be compensated for by a high hazard.

$$R = H \times a + E \times b + V \times C \tag{4}$$

where H stands for the hazard component, E for exposure and V for vulnerability, while a, b and c are the weights, which are set to 0.6, 0.2 and 0.2 respectively for the current assessment.

For the aggregation of the risk component sub-indicators, it was considered more appropriate to apply a method which allows for compensability. This is achieved with the linear, or else, *weighted arithmetic aggregation method* (OECD 2008), which is recommended also in the Vulnerability Sourcebook of GIZ (Fritzsche et al., 2014). According to this method, individual indicators are multiplied by their weights and then summed to form the composite indicator, as indicated in the following formula:

$$C_R = \sum_{q=1}^{Q} w \times I_C \tag{5}$$

where C_R is the composite risk component, I_C the individual sub-indicators of the risk components (i.e. heat stress, frost), Q the number of sub-indicators comprising the composite risk component (i.e. 3) and w the weight assigned to each sub-indicator. The sum of the weights for all sub-indicators equals to 1. In the current assessment, equal weights are assigned to each-sub-indicator.

For the WEF sectors, a set of hazard, exposure and vulnerability indicators is employed to assess risk, with clear interconnections between the systems reflecting the Nexus dependencies. In particular, some of the indicators are used for the assessment of more than one system so as to effectively take into account the WEF Nexus.

3.2.1 Hazard

According to the Intergovernmental Panel on Climate Change, the hazard is "*the potential occurrence of a natural or human-induced physical event or trend or physical impact that may cause loss of life, injury, or other health impacts, as well as damage and loss to property, infrastructure, livelihoods, service provision, ecosystems, and environmental resources*" (IPCC, 2018). In the LENSES Project, the CRA study the potential risks that are triggered by climate change in the frame of the WEF Nexus, and for this reason, the examined hazards are related to each of the WEF sectors. The potential hazards are assessed through a set of indicators estimated with the use of information on climatic variables. As in the case of Climate projections (Section 3.1), the respective datasets is sourced from the Copernicus Climate Change Service (C3S, 2021) and further processed to produce the hazard indicators that address the requirements of the current study. It is worth noting that the critical values of the climate indicators provided by the aforementioned datasets in most of the cases are predetermined. However, in the cases that the critical values of certain indicators are not representative of the local conditions prevailing at the pilot areas, the indicators are calculated based on the case-specific critical values with the use of raw data will be able to set the appropriate thresholds according to areas' unique characteristics. The selected thresholds for each pilot are confirmed from the pilot leaders.

The datasets provided by the Copernicus Climate Change Service are products that have been estimated using a range of algorithms and models. The primary input in these algorithms and models are climate datasets for historical and future periods. The climatic products (datasets) are categorized based on the subject (e.g., agroclimatic, bioclimatic, hydrologic, etc.) and sector (agriculture, water resources, biodiversity, etc.). The temporal and spatial resolution as well as the spatial coverage may differ among the available products, a fact which played an important role in the selection of the datasets for the present study. The datasets related to the WEF Nexus were further examined in order to assess the suitability of the individual indicators for use in the climate risk assessment, in the form of hazard indicators. The relevant datasets are presented next:

- Agroclimatic indicators dataset (Nobakht et al., 2019)
- Hydrology-related climate impact indicators dataset (Berg et al., 2021)
- Fire Weather Index dataset (Giannakopoulos & Karali, 2019)

Specifically, the agroclimatic indicators are produced to represent features of the climate that are used to assess plant-climate interactions. These indicators help convey climate variability and change in terms that are meaningful to agriculture and are often used in species distribution modelling to study the phenological developments of plants under varying climate conditions (Nobakht et al., 2019). Thus, the provided information is particularly important for many agricultural community users to assess crop growth for the current or future cropping seasons. The estimation of the agroclimatic indicators is based on the Inter-Sectoral Impact Model Intercomparison Project (ISIMIP) products, containing daily, bias-corrected climate data from CMIP5 General Circulation Models covering the period 1951-2099 (historical data run up to 2005).

The hydrology-related climate impact indicators are fundamental for a wide range of users that study not only the water sector but also the other WEF nexus sectors, such as agriculture and ecosystems. These indicators have been estimated using the E-HYPEcatch multi-model system, E-HYPEgrid and VIC-WUR (Berg et al., 2021). As input data, the aforementioned models consider an ensemble of EURO-CORDEX for the variables of daily mean temperature and precipitation that were further bias-adjusted using EFAS-Meteo and a new bias adjustment method developed and applied by the Swedish Meteorological and Hydrological Institute (SMHI). The dataset includes a set of water-related climate impact indicators for the period of 1971 - 2100 based on an ensemble of hydrological models at both catchment and grid scales. The calculations take into account the annual or seasonal means over the reference period, and for the future periods (Berg et al., 2021).

Finally, with respect to the Fire Weather Index dataset, this includes a set of indicators based on the Fire Weather Index (FWI). The FWI has been used worldwide to estimate Fire Weather Index in a generalized fuel type (mature pine stands). The estimation of FWI is based on the Canadian FWI System (Giannakopoulos & Karali, 2019), providing fire behaviour indices that determine the ease of spread and intensity of fire events.

For future projection, FWI uses the dataset developed from the GCM/RCM pairs within the EURO-CORDEX framework.

Below, the selected climate indicators for the WEF systems are presented.

Biologically effective degree days

The indicator “Biologically effective degree days” (BEDD) is used to estimate biological effectiveness and specifically crop growth. It is based on heat accumulation and is calculated as the sum of daily mean temperatures above 0°C and less than 30°C, over 10 days, providing information about the duration of the growing season. Finally, it has been calculated as a relative change compared to the reference period (1970-2000) to represent the increase in the growing season and reflect the possibility of increased agricultural production in some areas, as an alternative positive effect of climate change.

$$BEDD = \sum_{i=1}^{I} min\left[max\left[TG_{ij} - T_{low}, 0\right], T_{high} - T_{low}\right] \tag{6}$$

Coverage: Global
Temporal coverage: From 1951 to 2090
Spatial resolution: 12.5km×12.5Km
Temporal aggregation: Monthly/seasonal/annual
Data availability/suitability: Ready-to-use index/Calculated using the specific thresholds provided by the LENSES pilot partners.
Dataset: Agroclimatic indicators dataset (Nobakht et al., 2019)

Heat stress days

“Heat stress days” is a crucial indicator in the agricultural sector as it provides essential information regarding the occurrence of heat stress which can be detrimental to crop growth. The units of Heat stress days are the number of days per ten days, where the maximum daily temperature is above a given threshold (e.g., 35°C or other temperature thresholds defined by pilot partners as critical values for specific crops of high importance).

Coverage: Global
Temporal coverage: From 1951 to 2090
Spatial resolution: 12.5km×12.5Km
Temporal aggregation: Days per year/season/month
Data availability: Ready-to-use index/Calculated using the specific thresholds provided by the LENSES pilot partners.
Dataset: Agroclimatic indicators dataset (Nobakht et al., 2019)

Frost days

Damage caused by frost is considered one of the most important economically harmful weather-related phenomena (Snyder & De Melo-Abreu, 2005), and occurs when freezing temperatures are lower than critical damage temperatures of the plant tissues. “Frost days” counts/estimates the days per ten days where the minimum daily temperature is below 0°C (*TN<0°C*).

Coverage: Global

Temporal coverage: From 1951 to 2090
Spatial resolution: 12.5km×12.5Km
Temporal aggregation: Days per year/season/month
Data availability: Ready-to-use index/Calculated using the specific thresholds provided by the LENSES pilot partners.
Dataset: Agroclimatic indicators dataset (Nobakht et al., 2019)

Mean soil moisture

Soil moisture is the water stored in the soil and is affected by several climatic and soil characteristics of a given area. In the hydrological model that the Copernicus climate change service system has been used, soil moisture is defined as the moisture in the root zone as a fraction of the field capacity volume. The soil moisture indicator is provided as annual mean values, averaged over a 30-year period. Soil moisture is essential for the development of plants, it regulates soil structure and soil temperature, and it contributes to preventing soil erosion thus this indicator is crucial for agriculture and natural ecosystems.

Coverage: Global
Temporal coverage: From 1951 to 2090
Spatial resolution: 12.5km×12.5Km
Temporal aggregation: Days per year/season/month
Data availability: Ready-to-use index/Calculated using the specific thresholds provided by the LENSES pilot partners.
Dataset: Hydrology-related climate impact indicators dataset (Berg et al., 2021)

Fire Weather Index

The indicator "Fire Weather Index" shows the mean annual days over a 30-year period, with a daily FWI at a high level and thus it represents the days with a high probability of fire. This indicator is crucial for the natural ecosystem's safety and reflects the risk of fire.

The FWI is used to measure the fire risk based on meteorological conditions. This index is formulated from the integration of different components that assess the effects of fuel moisture and wind on fire behavior and spread. The essential information needed to calculate this index is: a) the temperature in the middle of the afternoon (when it has its highest value), b) the 24-hour total precipitation (from noon to noon), c) the maximum speed of the average wind.

Based on the European Forest Fire Information System (EFFIS), the FWI is classified into 6 classes (Table 4).

Table 4: FWI classes, according to EFFIS.

Fire Weather Index Classes	FWI
Very low	<5.2
Low	5.2 to 11.2
Moderate	11.2 to 21.3
High	21.3 to 38.0
Very high	38.0 to 50.0
Extreme	>50.0

Coverage: Global
Temporal coverage: From 1951 to 2090

Spatial resolution: 12.5km×12.5Km
Temporal aggregation: Days per year/season/month
Data availability: Ready-to-use index/Calculated using the specific thresholds provided by the LENSES pilot partners
Dataset: Fire Weather Index dataset (Giannakopoulos & Karali, 2019)

Actual aridity

The actual aridity is a numerical indicator of the degree of dryness of the climate at a given location. This indicator is calculated as the annual mean of the ratio between actual evapotranspiration and precipitation over a 30-year period, therefore it is dimensionless.

Coverage: Global
Temporal coverage: From 1970 to 2100
Spatial resolution: 5km × 5km and catchment level
Temporal aggregation: Seasonal
Data availability: Ready-to-use index
Dataset: Hydrology-related climate impact indicators dataset (Berg et al., 2021)

River discharge

The river discharge is calculated as the annual mean values of daily runoff ($m^3 \times s^{-1}$) averaged over a 30-year period. For future periods the indicator is presented as a relative change against the reference period (1971-2000). Low river discharge can have impacts on species relying on the ecosystem, thus this indicator is reflecting the possible impact of lower precipitation and water availability on ecosystems relevant to the streams.

Coverage: Europe
Temporal coverage: From 1970 to 2100
Spatial resolution: 5km × 5km and catchment level
Temporal aggregation: Seasonal
Data availability: Ready-to-use index
Dataset: Hydrology-related climate impact indicators dataset (Berg et al., 2021)

3.2.2 Exposure

In this section, the selected exposure sub-indicators for the Food, Water and Ecosystems Nexus sectors are presented.

- Share of area cultivated with crops;
- Share of area covered with forests and natural area.

Exposure refers to *"the inventory of elements in an area where hazard events might occur"* (IPCC, 2018). Therefore, in our nexus system, if the croplands, water bodies and ecosystems were not located in (exposed to) potentially dangerous areas, the disaster risk would not exist. In order to identify, map and assess the exposure of the pilot areas to climate change, several geographical datasets will be used such as the CORINE Land Cover maps (CLC, 2018).

Share of area cultivated with crops

This indicator aims to show the actual exposure of the crops of the pilot area to climate change through the share of the area cultivated with crops to the total pilot area, as shown next.

$$Share\ of\ area\ cultivated\ with\ crops = \frac{Area\ cultivated\ with\ crops\ (ha)}{Total\ area\ of\ the\ pilot\ (ha)} \quad (7)$$

The source used for this indicator is the CORINE Land Cover maps (CLC, 2018) provided by the Copernicus Land Monitoring Service, while for the case of the Greek pilots, more detailed, crop-specific data at land parcel level were provided by the pilot through the Greek Payment Authority of Common Agricultural Policy (C.A.P.) Aid Schemes (OPEKEPE).

Share of area covered with forests and natural areas

This indicator aims to show the actual exposure of the ecosystems of the pilot area to climate change through the share of the natural areas covered mainly by forests, grasslands, water bodies etc. to the total pilot area, as shown next.

$$Share\ of\ area\ covered\ with\ forests\ and\ natural\ areas = \frac{Forest\ and\ natural\ areas\ of\ the\ pilot\ (ha)}{Total\ area\ of\ the\ pilot\ (ha)} \quad (8)$$

The source used for this indicator is the CORINE Land Cover maps (CLC, 2018) provided by the Copernicus Land Monitoring Service.

3.2.3 Vulnerability

In this section, the selected vulnerability sub-indicators for the Food, Water and Ecosystems Nexus sectors are presented.

- Water exploitation index
- Agricultural water consumption
- Agricultural income
- Share of protected areas

According to IPCC's glossary, "*vulnerability refers to the propensity of exposed elements such as human beings, their livelihoods, and assets to suffer adverse effects when impacted by hazard events*". Therefore, the term is used to describe the predisposition, susceptibility, fragility and weakness of elements on climate change and the hazard that might be triggered (IPCC, 2018).

Water Exploitation Index

The water exploitation index serves as a proxy for water stress on socio-economic systems and ecosystems, by providing an indication of how the total water demand puts pressure on the water resource. The higher the water stress, the higher the vulnerability of water resources to a reduction in water availability due to climate change. The index is calculated as the ratio of water use to total water resources.

$$WEI = \frac{Water\ use}{Available\ freshwater\ resources} \quad (9)$$

For the numerator, the Eurostat dataset on water use from all NACE activities and households is used, while for the denominator, the Eurostat dataset on freshwater resources is used, Eurostat (2022). Specifically, the available freshwater resources are calculated based on the following equation.

$$Available\ freshwater\ resources = External\ inflow + Precipitation - Actual\ evapotranspiration \quad (10)$$

Values above 20 % indicate that water resources are under water stress, and values above 40 % indicate that water stress is severe and the use of freshwater resources is clearly unsustainable (Raskin et al., 1997). For this assessment, the following threshold values/ranges have been used: (a) no stress < 10%; (b) low stress 10 to < 20%; (c) stress 20% to < 40%; and (d) severe water stress ≥ 40%.

The indicator is estimated at a river basin district level based on the data provided at an annual time frequency. For our analysis, a 5-year average of the most recent data was used. In the case of the Thessaly river basin district in Greece where there were missing data in Eurostat datasets, the respective data were sourced directly from the River Basin Management Plan of Thessaly (Special Secretary for Water, 2014) and reviewed by the pilot. In the case of the Middle Apennines River basin district in Italy where there were missing data in Eurostat datasets, the water exploitation index was sourced from the European Environment Agency (EEA, 2019). In the pilot cases of Turkey, Israel and Jordan due to the lack of available data at the annual level, the water exploitation index data was sourced from the Mediterranean countries dataset of the European Environment Agency (EEA, 2015) at the national level.

Agricultural water consumption

Water plays a crucial role in food production and agriculture in general. The intensity of water use in agriculture in relation to the water use in the other sectors (industry, services, households) is considered a proxy of the vulnerability of the food sector in relation to water and climate, as the higher the share of water consumption in agriculture, the highest the vulnerability of the food system to a reduction in water availability due to climate change. This indicator is estimated at the river basin district level based on the data provided by Eurostat (2022) on water use from public water supply. The data are provided in million cubic meters at an annual time frequency, while for our analysis a 5-year average of the most recent data was used. The indicator is available at the national level for the pilot cases in Jordan (USAID, 2020) and Turkey (OECD, 2020).

$$Share\ of\ agricultural\ water\ consumption = \frac{Water\ use\ in\ agriculture}{Total\ water\ use} \quad (11)$$

Agricultural income

The indicator of Agricultural income is intended to reflect the dependency of the country on the agricultural income of the region where the pilot area is located. Therefore, the higher the agricultural income of the region, the higher the vulnerability, as climatic hazards in the agricultural sector of the region would also have important impacts on the country. The data are provided in Euros at an annual time frequency, while for our analysis a 5-year average of the most recent data was used. The normalization of this indicator was based on the position of the regional agricultural income in relation to the national average agricultural income of all regions, using the following equation.

$$Agricultural\ income\ index = \frac{Regional\ agricultural\ income}{National\ average\ agricultural\ income} \quad (12)$$

This project is part of the PRIMA programme supported by the European Union.
GA n° [2041] [LENSES] [Call 2020 Section 1 Nexus IA]

If the regional agricultural income is close to the national average (i.e. the value of the index is 80-120%), then the vulnerability related to this indicator is considered moderate. Higher values (>120%) indicate high vulnerability and lower values (<80%) low vulnerability.

This indicator is calculated based on the Eurostat dataset "Economic accounts for agriculture" and Specifically on the crop output value at current prices, which is available at the regional level (NUTS2) (Eurostat, 2022). In the pilot case of Turkey, Israel and Jordan the agricultural income indicator was calculated based on the value added of agriculture as percent of the national GDP compared to the Mediterranean countries' average. The respective data were sourced from the relevant dataset of the World bank (World Bank, 2022).

Share of protected areas

For assessing the vulnerability of the ecosystems to climate change impacts, the share of protected areas to the total pilot area was calculated based on the spatial data provided by the World Database on Protected Areas (WDPA) from the UN Environment Programme World Conservation Monitoring Centre (UNEP-WCMC). This indicator is intended to reflect the importance of the ecosystems of the pilots. Therefore, the higher the percentage of the pilot area that is covered by protected areas regulated by national laws, the higher the vulnerability of the ecosystems.

$$Share\ of\ protected\ areas\ = \frac{Protected\ areas\ of\ the\ pilot\ (ha)}{Total\ area\ of\ the\ pilot\ (ha)} \tag{13}$$

3.2.4 Adaptive capacity

The national Gross Domestic Product is employed as indicator to assess the larger economic and social context of the region of the pilot and how this may influence the level of risk.

The Gross Domestic Product (GDP) is a commonly used index for evaluating a nation´s economic situation and welfare. It reflects the total value of all goods and services produced less the value of goods and services used for intermediate consumption in their production. The data are provided in Euros per capita at an annual time frequency, while for our analysis a 5-year average of the most recent data was used. The normalization of this indicator was based on the position of the national GDP in relation to the regional average, using the following equation.

$$Economic\ capacity\ = \frac{National\ GDP}{EU\ average\ GDP} \tag{14}$$

If the national GDP is close to the EU average (i.e., the value of the index is 80-120%), then the adaptive capacity related to this indicator is considered moderate. Higher values (>120%) indicate high adaptive capacity and lower values (<80%) low adaptive capacity.

This indicator is calculated for the European pilots based on the Eurostat dataset "Gross domestic product at market prices" and compared with the EU average. In the case of Turkey, Israel and Jordan pilots the respective data were sourced from the relevant dataset of the World Bank (World Bank, 2022) and compared to the Mediterranean countries average GDP.

4 Climate projections results for the LENSES pilots

In this Section, the results of the climate projections for the RCP4.5 and RCP8.5 are provided. The Section is broken down into individual sub-sections for each pilot area, where in each sub-section, the results are presented for each variable in the following form:

1. Graphs with the annual timeseries. The graphs depict average values for the whole pilot area and the examined period.

2. Tables providing the average values of the examined climate variables for the reference period and three 30-year future periods (2011-2040, 2041-2070, 2071-2100), as well as the relative change compared to the reference period 1971-2000.

3. Maps showing the spatial distribution of the values of the climatic variables for the reference period (1971-200) and the future period (2041-2070) for both RCP4.5 and RCP8.5.

4.1 Pinios River Basin Hydrologic Observatory (Greece)

Mean Temperature

The projected annual mean temperature for the period 2011-2100 is presented in the form of time series in Figure 11. As it may be observed, there is a clear tendency of temperature increase during the 90-year period in both scenarios. Based on the findings for the RCP4.5, the trend over the period 2011-2100 indicates a rise of up to 1.5°C, whereas under the RCP8.5 scenario, the trend shows a significantly higher increase, up to 4.6°C. Additionally, the mean temperature for both scenarios is above 13°C throughout the 90-year period. The maximum value of annual mean temperature is observed in the case of the RCP8.5 and in specific during the last years of the time series, when it reaches the value of about 19.2°C.

This project is part of the PRIMA programme supported by the European Union.
GA n° [2041] [LENSES] [Call 2020 Section 1 Nexus IA]

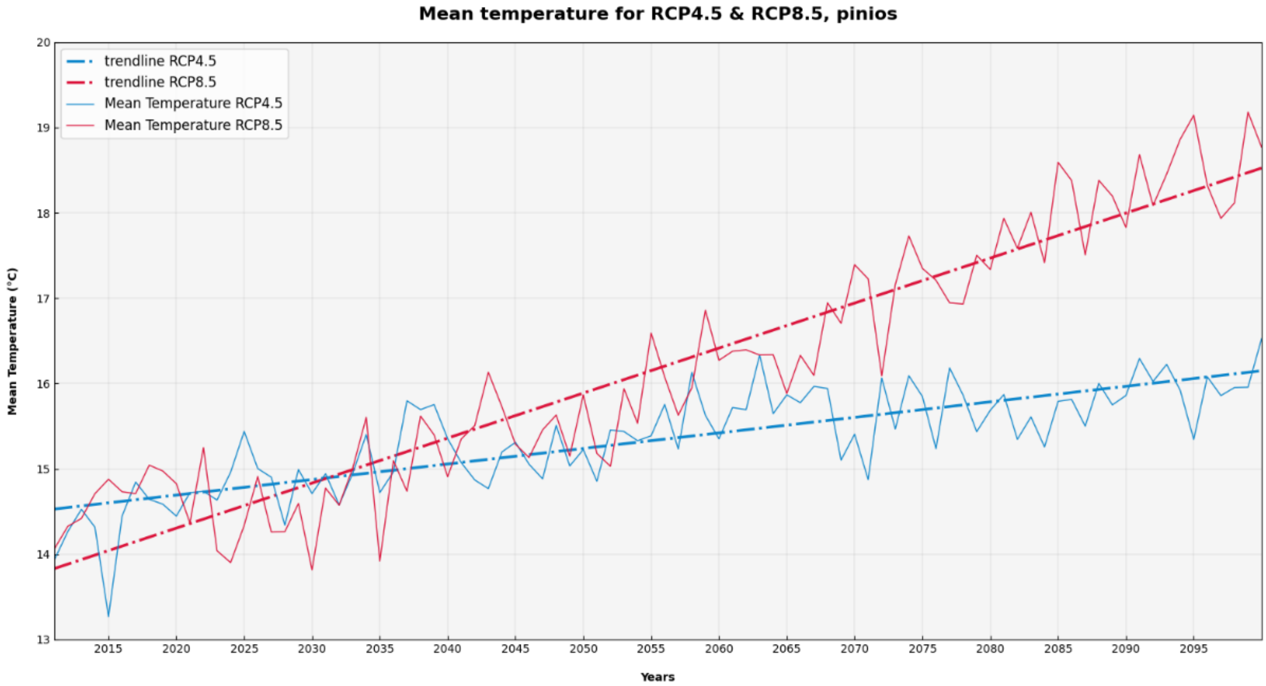

Figure 11: Ensemble mean of mean temperature of the period 2011-2100 for the RCP4.5 (blue line) and RCP8.5 (red line), Pinios pilot.

The mean temperature of the examined reference and future periods is shown in Table 5, for the Pinios pilot area. It may be seen that the absolute change of the mean temperature compared to the reference period is +1.2°C and +1.1°C for the near-term period, while in the long-term period it is expected to reach up to +2.2°C and +4.3°C, for the RCP4.5 and RCP8.5 respectively. In addition, for the near-term period (2011-2040) the absolute value of the mean temperature is expected to be around 14.8°C for both scenarios. These values gradually increase until they reach 15.8°C and 17.9°C in the long-term period (2071-2100), for RCP4.5 and RCP8.5 respectively.

Table 5: Ensemble mean temperature for the reference period and the future sub-periods based on the RCP4.5 and RCP8.5. Values are presented as absolute change from the reference period 1971-2000 and as absolute value in °C, Pinios pilot.

Mean Temperature	2011-2040		2041-2070		2071-2100	
	RCP4.5	RCP8.5	RCP4.5	RCP8.5	RCP4.5	RCP8.5
absolute change (°C)	+1.2	+1.1	+1.8	+2.4	+2.2	+4.3
absolute value (°C)	*14.8*	*14.7*	*15.4*	*16.0*	*15.8*	*17.9*

Regarding the spatial distribution of the mean temperature range (Figure 12), it is observed that during the reference period the mean temperature range ranges from 9-11°C at the more mountainous area of the pilot (Agia region) and reaches up to 15-17°C at the Pinios delta region. During the period 2041-2070, it is expected that the mean temperature will range from 11-17°C in Agia region to 15-18.3°C in Pinios Delta, according to RCP4.5. Similar, according to scenario RCP8.5, the maximum mean temperature in Agia region will reach up to 18.3°C, while this is expected to be the highest mean temperature for the greatest part of the Pinios delta area.

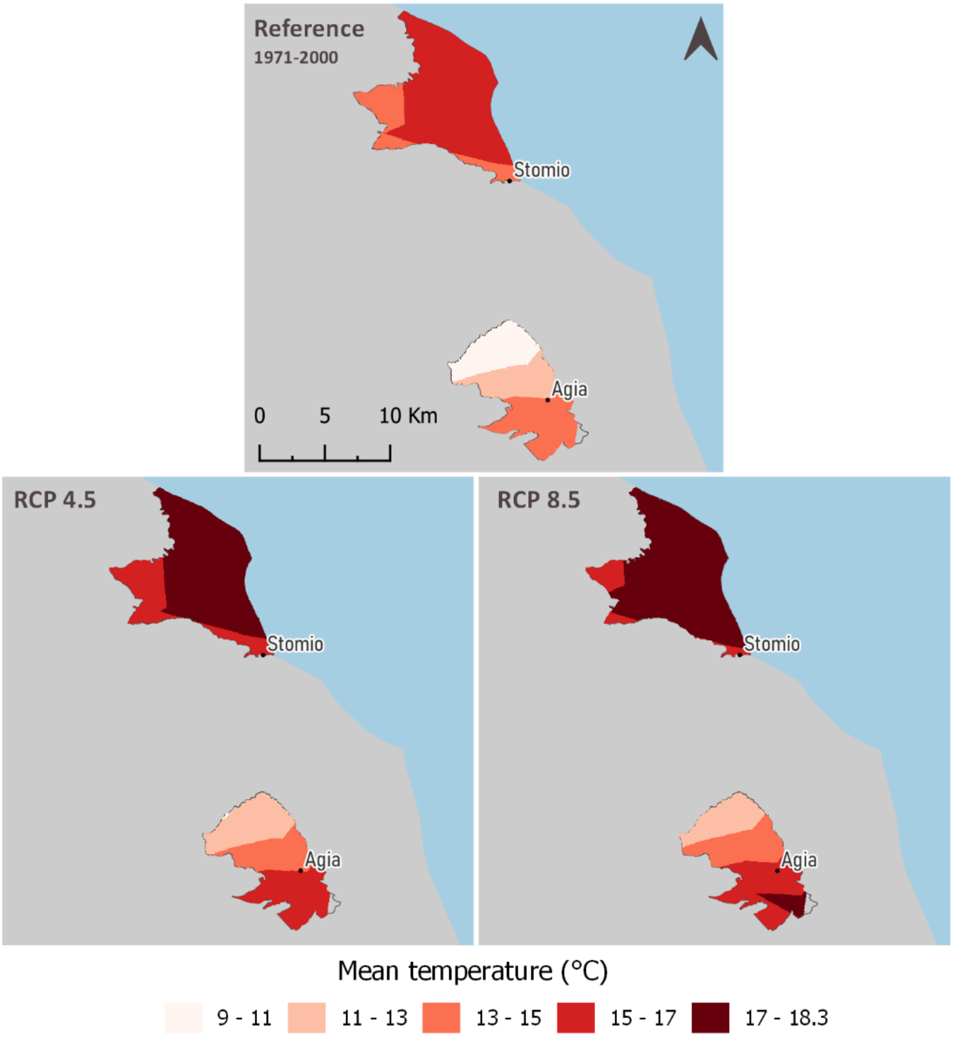

Figure 12: Spatial distribution of the mean annual temperature, for the reference period (top) and the future period 2041-2070, based on the RCP4.5 and RCP8.5 (bottom), Pinios pilot.

Total Precipitation

The projected mean annual total precipitation for the period 2011 to 2100 for the two scenarios at Pinios pilot area, is presented in the form of annual time series in Figure 13. As it may be seen, total precipitation tends to be stable over the 90-year period for both scenarios. Additionally, the minimum annual total precipitation value is expected to be around 300 mm, while the maximum value is expected around 700 mm for both scenarios.

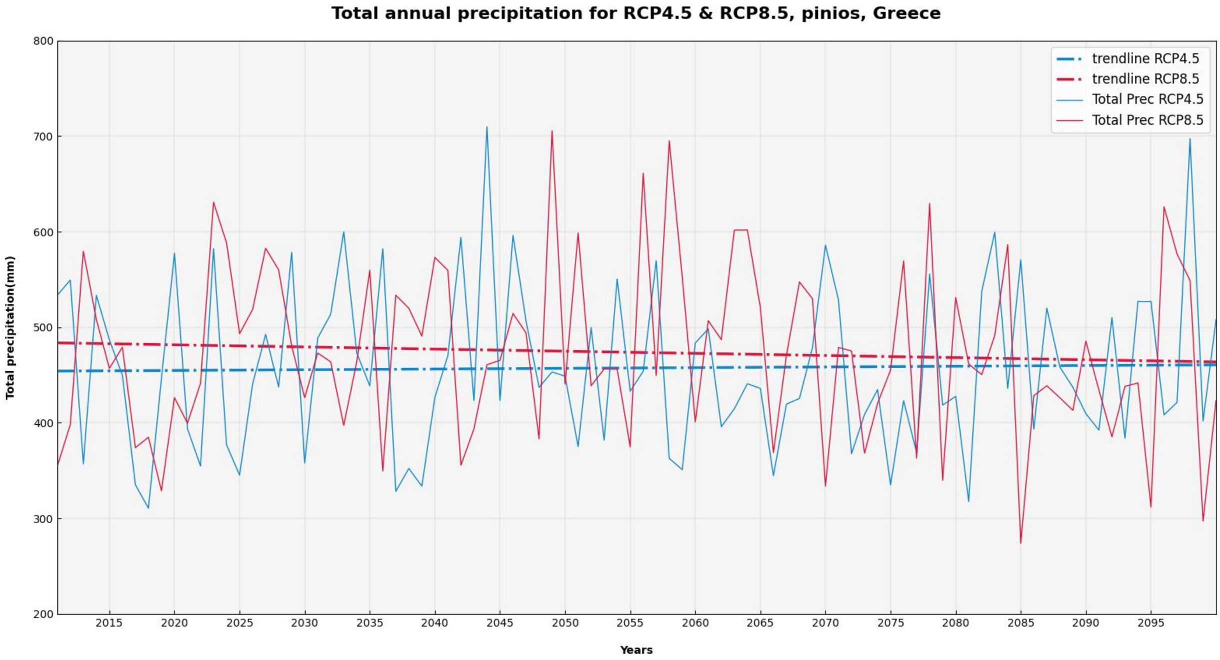

Figure 13: Ensemble mean of total precipitation of the period 2011-2100 for the RCP4.5 (blue line) and RCP8.5 (red line), Pinios pilot.

In Table 6, the projected average annual total precipitation for the examined future sub-periods is provided, divided in the dry and wet periods of the year. In the case of the Pinios pilot area, the selected dry months include the period from May to September while the selected wet period starts from October until April. It may be seen that the total precipitation is expected to show a decrease for the dry period of the year in relation to the reference period. The only exception is the short- and mid-term periods for the RCP8.5 where an increase of 15 mm is expected on average. Regarding the wet period of the year an increase is expected during all the subperiods and for both scenarios. The highest increase is expected during the mid-term period with an increase of 20.5 mm on average for the two scenarios.

Table 6: Ensemble mean of total precipitation for the future sub-periods based on the RCP4.5 and RCP8.5 divided in dry and wet period. Values are presented as absolute change from the reference period 1971-2000 and as absolute value in mm, Pinios pilot.

Total Precipitation		**2011-2040**		**2041-2070**		**2071-2100**	
		RCP4.5	**RCP8.5**	**RCP4.5**	**RCP8.5**	**RCP4.5**	**RCP8.5**
Dry period	absolute change (mm)	-10	14	-7	16	-4	-8
	absolute value (mm)	*120*	*144*	*123*	*147*	*126*	*123*
Wet period	absolute change (mm)	5	6	18	23	7	6
	absolute value (mm)	*329*	*330*	*342*	*347*	*331*	*330*

Figure 14, shows the geospatial variation of the total precipitation for the periods 1971-2000 and 2041-2070, for both the dry and wet periods of the year. As shown, the maximum amount of precipitation (up to 340 mm) is observed during the wet season for the reference period at the Pinios delta, while in the rest of the study area the value of the precipitation is 320 to 330 mm. As for the dry season, the study area experiences a range of precipitation amounts, starting at 115 mm in the Agia area and gradually increasing towards the delta, reaching up to 135 mm. The changes for both RCPs in relation to the reference period for dry and wet seasons are noticeable. In the future period, the precipitation is expected to increase during the wet season under both scenarios. On the contrary, a decrease is expected under RCP8.5 for the greatest part of the Pinios pilot area during the dry season, while an increase is expected in the case of RCP4.5.

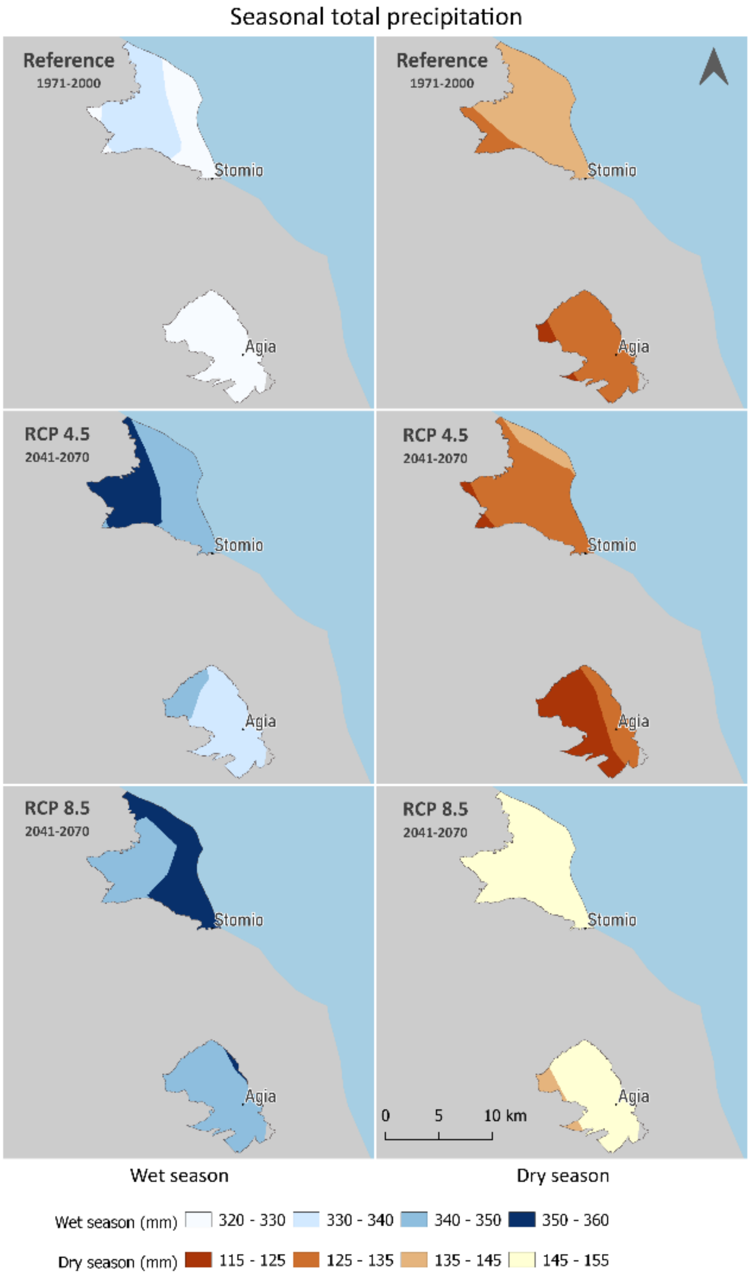

Figure 14: Spatial distribution of the mean total precipitation during the reference period (top) and the future period based on the RCP4.5 (middle) and RCP8.5 (bottom), for the dry (right) and the wet (left) periods, Pinios pilot.

Actual Evapotranspiration

The total annual actual evapotranspiration for the period 2011-2100 is presented in Figure 15 for both RCP4.5 and RCP8.5. As it may be observed, there is a tendency of increase during the 90-year period in both scenarios. According to the results for the RCP4.5, the trend for the period 2011-2100 shows a small increase of around 10 mm, while for the RCP8.5 the increase is expected to be higher, up to 40mm. Additionally, the actual evapotranspiration for both scenarios is above 600 mm for almost all the 90-year period. The maximum value of annual actual evapotranspiration is around 750 mm, and it is observed in the case of the RCP8.5.

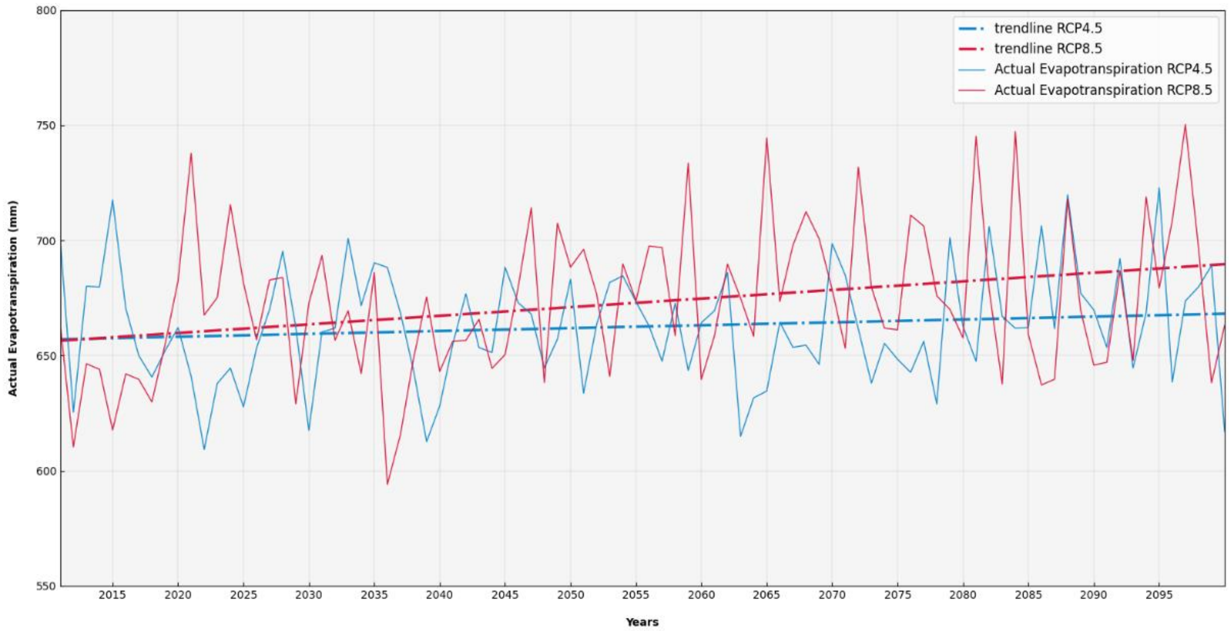

Figure 15: Ensemble mean of actual evapotranspiration of the period 2011-2100 for the RCP4.5 (blue line) and RCP8.5 (red line), Pinios pilot.

The expected total actual evapotranspiration for the examined future periods under RCP4.5 and RCP8.5 for the Pinios pilot area, is presented in Table 7. The values are presented as the absolute change from the reference period 1971-2000 and as absolute values. It may be observed that the absolute change of the evapotranspiration compared to the reference period is +28 mm for the near-term period for both scenarios, while in the long-term period is expected to increase even more, up to 43 mm on average for the two scenarios. In addition, for the near-term period (2011-2040) the mean evapotranspiration is expected to be 659 mm for both scenarios and gradually increase up to 674 mm on average in the long-term period (2071-2100).

Table 7: Actual evapotranspiration per sub-period for RCP4.5 and RCP8.5. Values are presented as absolute change from the reference period 1971-2000 and as absolute value in mm, Pinios pilot.

Actual Evapotranspiration	2011-2040		2041-2070		2071-2100	
	RCP4.5	RCP8.5	RCP4.5	RCP8.5	RCP4.5	RCP8.5
absolute change (mm)	28	28	30	49	37	50
absolute value (mm)	*659*	*659*	*661*	*680*	*668*	*681*

Regarding the spatial distribution of the total actual evapotranspiration (Figure 16), it is observed that during the reference period the evapotranspiration ranges from 400 mm to 800 mm with the lowest values being observed for the Agia region. As it is shown, during the future period, the actual evapotranspiration tends to increase up to 900 mm for both scenarios for the Delta region, while the values in Agia region remain similar.

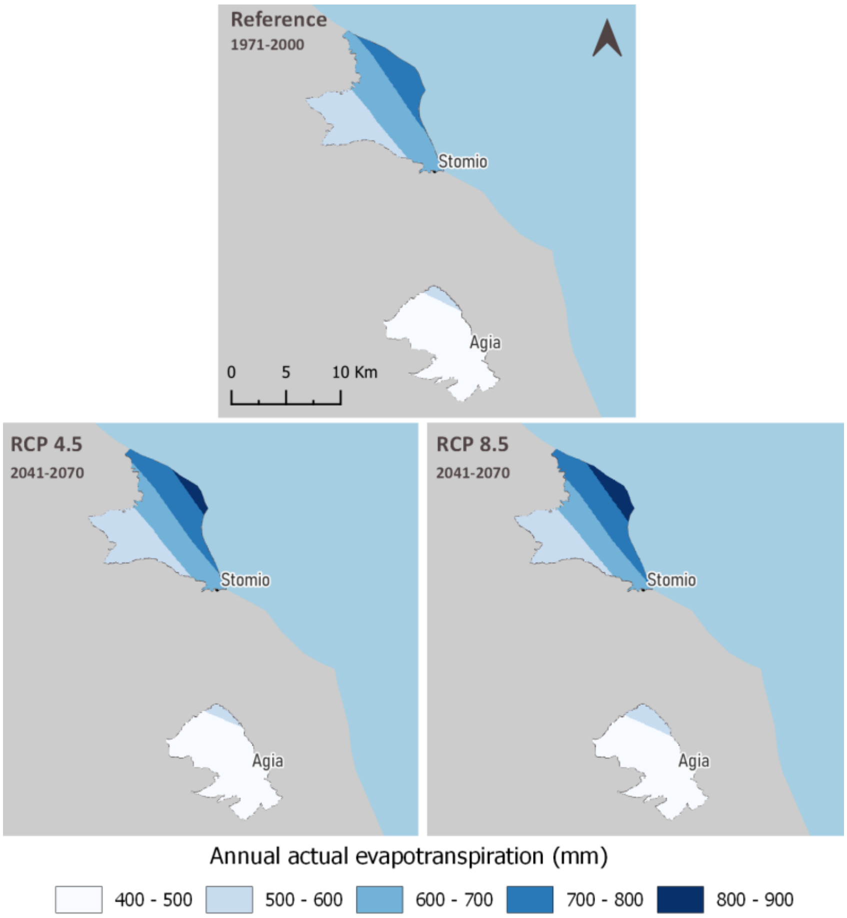

Figure 16: Spatial distribution of the mean annual actual evapotranspiration, for the reference period (top) and the future period 2041-2070, based on the RCP4.5 and RCP8.5 (bottom), Pinios pilot.

4.2 Doñana national park area (Spain)

Temperature

The projected annual mean temperature for the period 2011-2100 is presented in the form of time series in Figure 17. As it may be observed, there is a clear tendency of temperature increase during the 90-year period in both scenarios. Based on the findings for the RCP4.5, the trend over the period 2011-2100 indicates a rise of up to 2.2°C, whereas under the RCP8.5 scenario, the trend shows a significantly higher increase, up to 4.5°C. Additionally, the mean temperature for both scenarios is above 18°C throughout the 90-year period. The maximum value of annual mean temperature is observed in the case of the RCP8.5 and in specific during the last years of the time series, when it reaches the value of about 23.5°C.

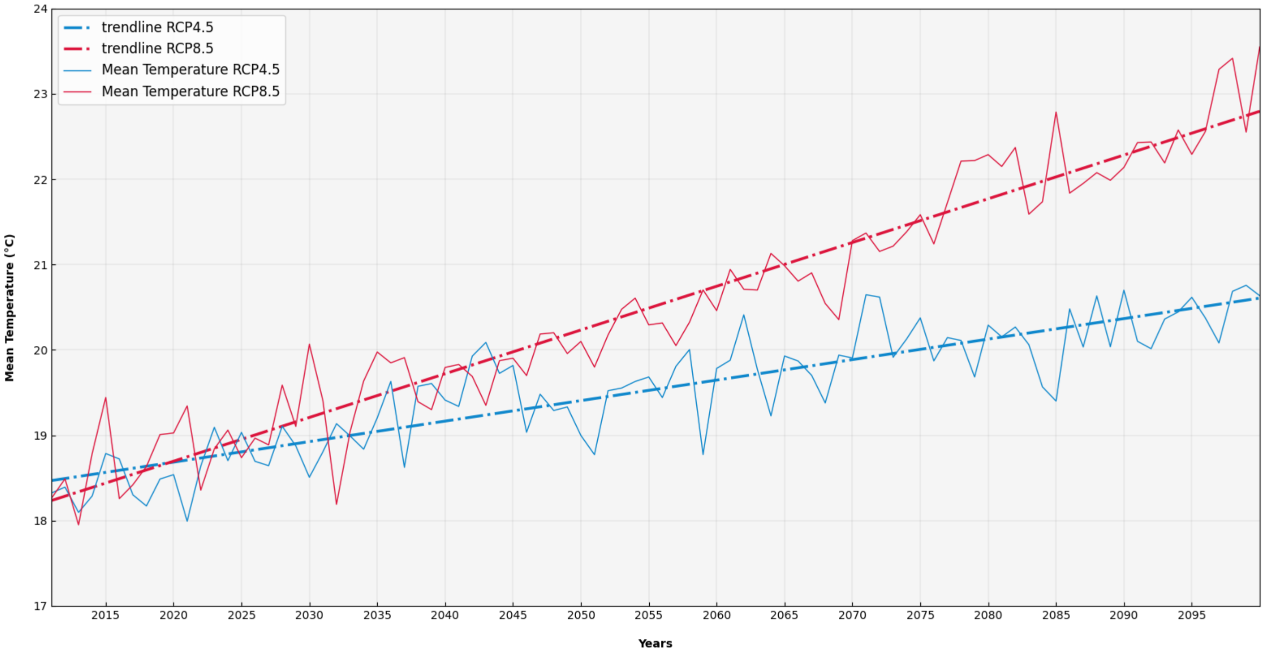

Figure 17: Ensemble mean of mean temperature of the period 2011-2100 for the RCP4.5 (blue line) and RCP8.5 (red line), Doñana pilot.

The mean temperature of the examined reference and future periods is shown in Table 8, for the Doñana pilot area. It may be seen that the absolute change of the mean temperature compared to the reference period is +0.9°C and +1.2°C for the near-term period, while in the long-term period it is expected to reach up to +2.4°C and +4.3°C, for the RCP4.5 and RCP8.5 respectively. In addition, for the near-term period (2011-2040) the absolute value of the mean temperature is expected to be around 18.8°C for the RCP4.5 and slightly higher for the RCP8.5, around 19.1°C. These values gradually increase until they reach 20.2°C and 22.1°C in the long-term period (2071-2100), for RCP4.5 and RCP8.5 respectively.

Table 8: Ensemble mean temperature for the reference period and the future sub-periods based on the RCP4.5 and RCP8.5. Values are presented as absolute change from the reference period 1971-2000 and as absolute value in °C, Doñana pilot.

Mean Temperature	2011-2040		2041-2070		2071-2100	
	RCP4.5	RCP8.5	RCP4.5	RCP8.5	RCP4.5	RCP8.5
absolute change (°C)	+0.9	+1.2	+1.7	+2.5	+2.4	+4.3
absolute value (°C)	*18.8*	*19.1*	*19.6*	*20.3*	*20.2*	*22.1*

Regarding the spatial distribution of the mean temperature range (Figure 18), it is observed that during the reference period the mean temperature range ranges from around 16°C at the more mountainous area of the pilot (northern part) and reaches up to 18-19°C at the eastern part. During the period 2041-2070, it is expected that the mean temperature will range from 18-19°C to 20-21.5°C according to RCP4.5. On the other hand, according to scenario RCP8.5, the greatest part of the pilot is expected to experience a mean temperature of 20-21.5 °C.

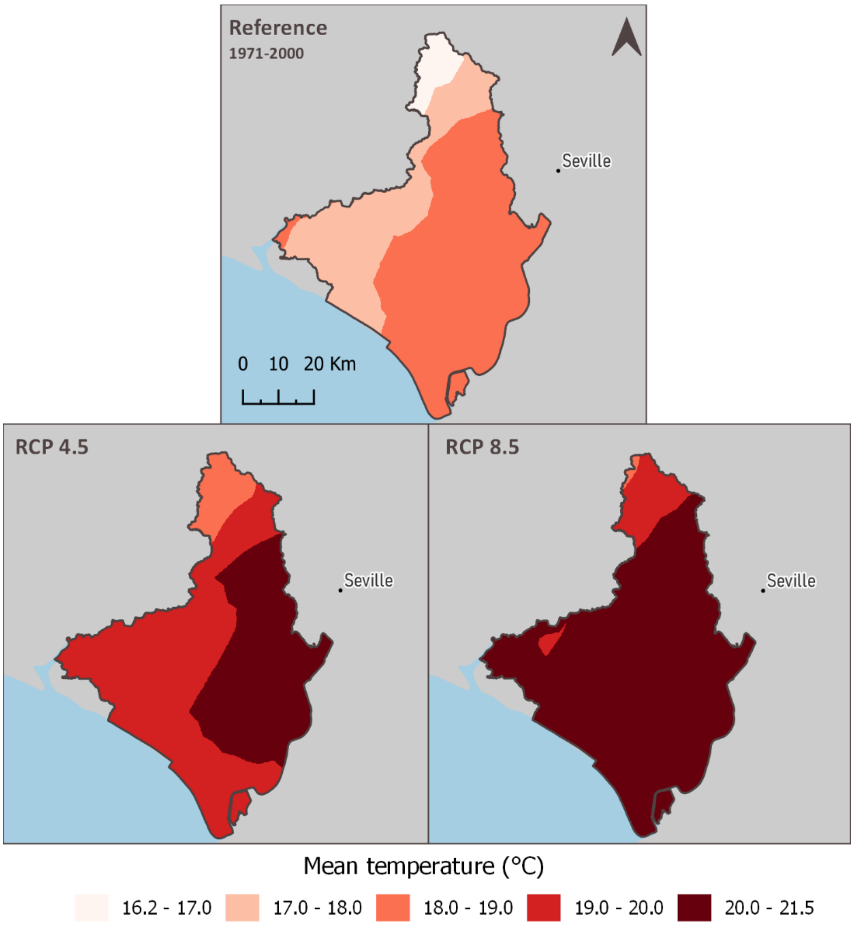

Figure 18: Spatial distribution of the mean annual temperature, for the reference period (top) and the future period 2041-2070, based on the RCP4.5 and RCP8.5 (bottom), Doñana pilot.

Precipitation

The projected mean annual total precipitation for the period 2011 to 2100 for the two scenarios at Doñana pilot area, is presented in the form of annual time series in Figure 19. As it may be seen, total precipitation tends to decrease over the 90-year period for both scenarios. Regarding RCP4.5, the trend is expected to be reduced by up to 70 mm, while for the RCP8.5 up to 110 mm. Additionally, the minimum annual total precipitation value is expected to be around 450 mm for the RCP4.5 and 390 mm for the case of RCP8.5; values which are observed during the last years of the period under study.

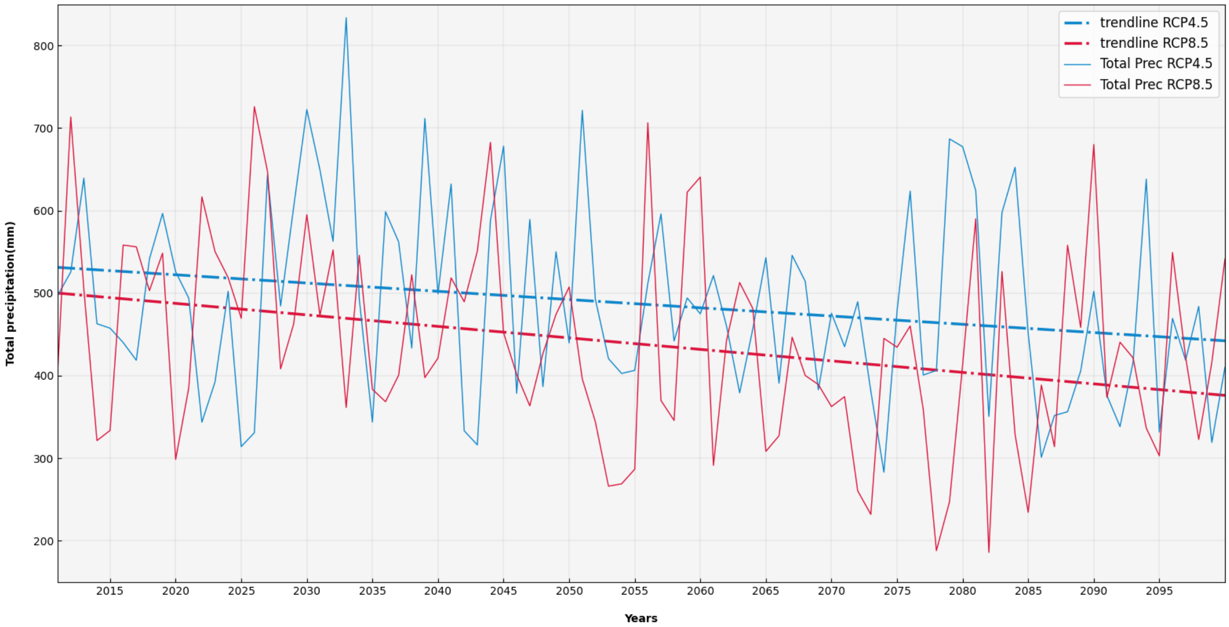

Figure 19: Ensemble mean of total precipitation of the period 2011-2100 for the RCP4.5 (blue line) and RCP8.5 (red line), Doñana pilot.

In Table 9, the projected average annual total precipitation for the examined future sub-periods is provided, divided in the dry and wet periods of the year. In the case of the Doñana pilot area, the selected dry months include the period from April to September while the selected wet period starts from October until March. It may be seen that the total precipitation is expected to show a decrease for most subperiods, for both scenarios, in the dry and wet seasons of the year in relation to the reference period. The only exception is the period 2011-2070 for RCP4.5 in the wet period where an increase of 9.5 mm on average is observed compared to the reference period. The maximum reduction is expected in the wet season of 2071-2100, for RCP8.5, where it reaches -63 mm compared to the 1971-2000 period, while this value is very similar for the corresponding dry season decrease (-61 mm).

Table 9: Ensemble mean of total precipitation for the future sub-periods based on the RCP4.5 and RCP8.5 divided in dry and wet period. Values are presented as absolute change from the reference period 1971-2000 and as absolute value in mm, Doñana pilot.

Total Precipitation		2011-2040		2041-2070		2071-2100	
		RCP4.5	RCP8.5	RCP4.5	RCP8.5	RCP4.5	RCP8.5
Dry period	absolute change (mm)	-9	-16	-38	-52	-47	-61
	absolute value (mm)	*117*	*110*	*88*	*74*	*79*	*65*
Wet period	absolute change (mm)	13	-15	6	-29	-15	-63
	absolute value (mm)	*404*	*375*	*397*	*361*	*376*	*328*

Figure 20, shows the geospatial variation of the total precipitation for the periods 1971-2000 and 2041-2070, for both the dry and wet periods of the year. As shown, the maximum amount of precipitation (up to 430 mm) is observed during the wet season for the reference period at the northern part of the area as well as at the south-eastern part, where the climate is influenced by the high altitude, while the minimum amount (340-360 mm) is observed at the western part of the study area. As for the dry season, the study area experiences a range of precipitation amounts, starting at 100 mm in the southern part and gradually increasing towards the north, reaching up to 150 mm. The changes for both RCPs in relation to the reference period for dry and wet seasons are noticeable. In the future period, the precipitation is expected to increase during the wet season under RCP4.5. On the contrary, a decrease is expected under RCP8.5 for the greatest part of the Doñana pilot area during the wet season. Regarding the precipitation during the dry period, this is expected to decrease in the future according to both scenarios, with the reduction being even more pronounced in the case of the RCP8.5.

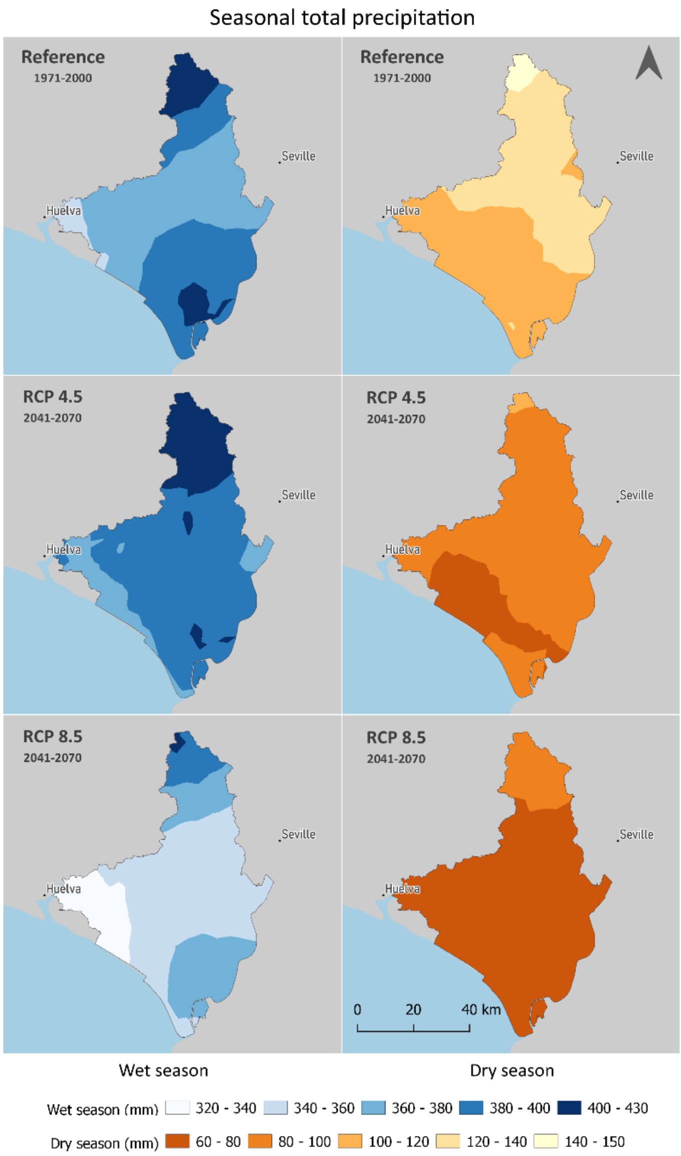

Figure 20: Spatial distribution of the mean total precipitation during the reference period (top) and the future period based on the RCP4.5 (middle) and RCP8.5 (bottom), for the dry (right) and the wet (left) periods, Doñana pilot.

This project is part of the PRIMA programme supported by the European Union.
GA n° [2041] [LENSES] [Call 2020 Section 1 Nexus IA]

Actual evapotranspiration

The total annual actual evapotranspiration for the period 2011-2100 is presented in Figure 21 for both RCP4.5 and RCP8.5. As it may be observed, there is a tendency for the evapotranspiration to decrease during the 90-year period in both scenarios. According to the results for the RCP4.5, the trend for the period 2011-2100 shows a decrease of 40 mm, while for the RCP8.5 the decrease is expected to be double, up to 80 mm. Additionally, the actual evapotranspiration for both scenarios is above 500 mm for almost all the 90-year period. The maximum value of annual actual evapotranspiration is around 700 mm, and it is observed in the case of the RCP4.5.

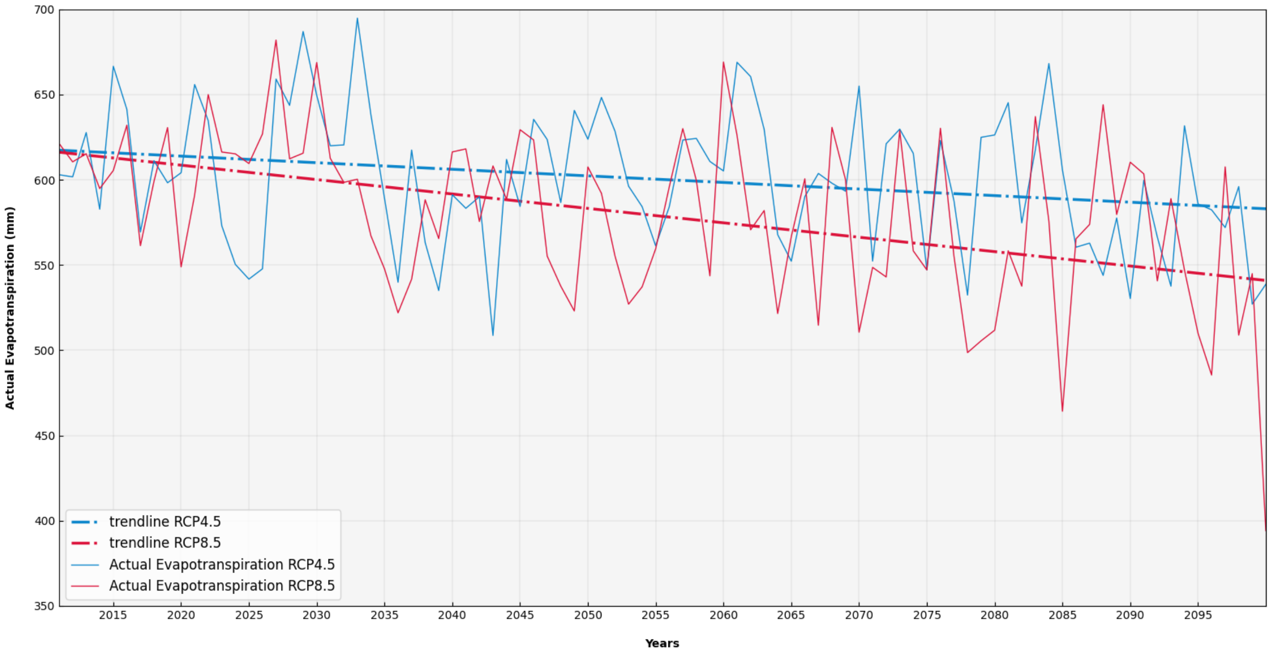

Figure 21: Ensemble mean of the total annual actual evapotranspiration for the period 2011-2100, RCP4.5 (blue line), RCP8.5 (red line), Doñana pilot.

The expected total actual evapotranspiration for the examined future periods under RCP4.5 and RCP8.5 for the Doñana pilot area, is presented in Table 10. The values are presented as the absolute change from the reference period 1971-2000 and as absolute values. It may be observed that the absolute change of the evapotranspiration compared to the reference period is -21 mm on average for the near-term period, while in the long-term period is expected to decrease even more, up to -41 mm and -73 mm, for the RCP4.5 and RCP8.5 respectively. In addition, for the near-term period (2011-2040) the mean evapotranspiration is expected to be 606 mm on average for the RCP4.5 and RCP8.5 and gradually decrease up to 570 mm on average in the long-term period (2071-2100).

Table 10: Actual evapotranspiration per sub-period for RCP4.5 and RCP8.5. Values are presented as absolute change from the reference period 1971-2000 and as absolute value in mm, Doñana pilot.

Actual Evapotranspiration	2011-2040		2041-2070		2071-2100	
	RCP4.5	RCP8.5	RCP4.5	RCP8.5	RCP4.5	RCP8.5
absolute change (mm)	-18	-24	-21	-47	-41	-73
absolute value (mm)	*609*	*602*	*606*	*580*	*586*	*554*

Regarding the spatial distribution of the total actual evapotranspiration (Figure 22), it is observed that during the reference period the evapotranspiration ranges from 500 mm at the greater part of the pilot area and reaches up to 1200 mm at the coastal areas. As it is shown, during the future period, the actual evapotranspiration remains similar to the reference period for both future climate scenarios.

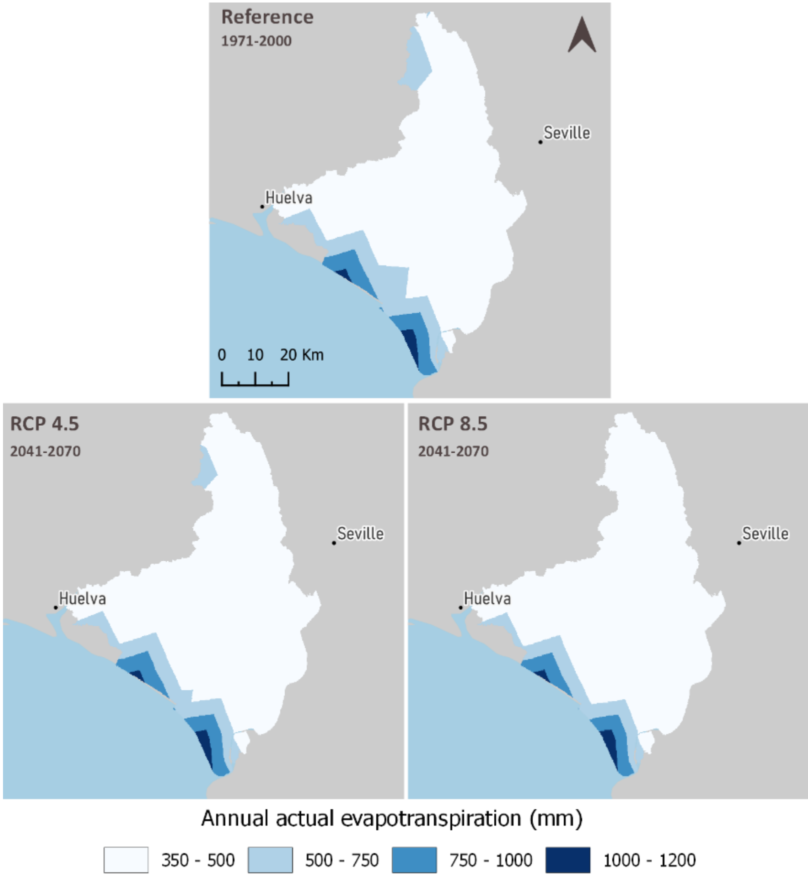

Figure 22: Spatial distribution of the mean annual actual evapotranspiration, for the reference period (top) and the future period 2041-2070, based on the RCP4.5 and RCP8.5 (bottom), Doñana pilot.

4.3 Koiliaris Critical Zone Observatory (Greece)

Mean Temperature

The projected annual mean temperature for the period 2011-2100 is presented in the form of time series in Figure 23. As it may be observed, there is a clear tendency of temperature increase during the 90-year period in both scenarios. Based on the findings for the RCP4.5, the trend over the period 2011-2100 anticipates a rise of up to 1.6°C, whereas under the RCP8.5 scenario, the trend shows a significantly higher increase, reaching 4.2°C. Additionally, the mean temperature for both scenarios is above 14°C throughout the 90-year period. The maximum value of annual mean temperature is observed in the case of the RCP8.5 and in specific during the last years of the time series, when it reaches the value of about 19.3°C.

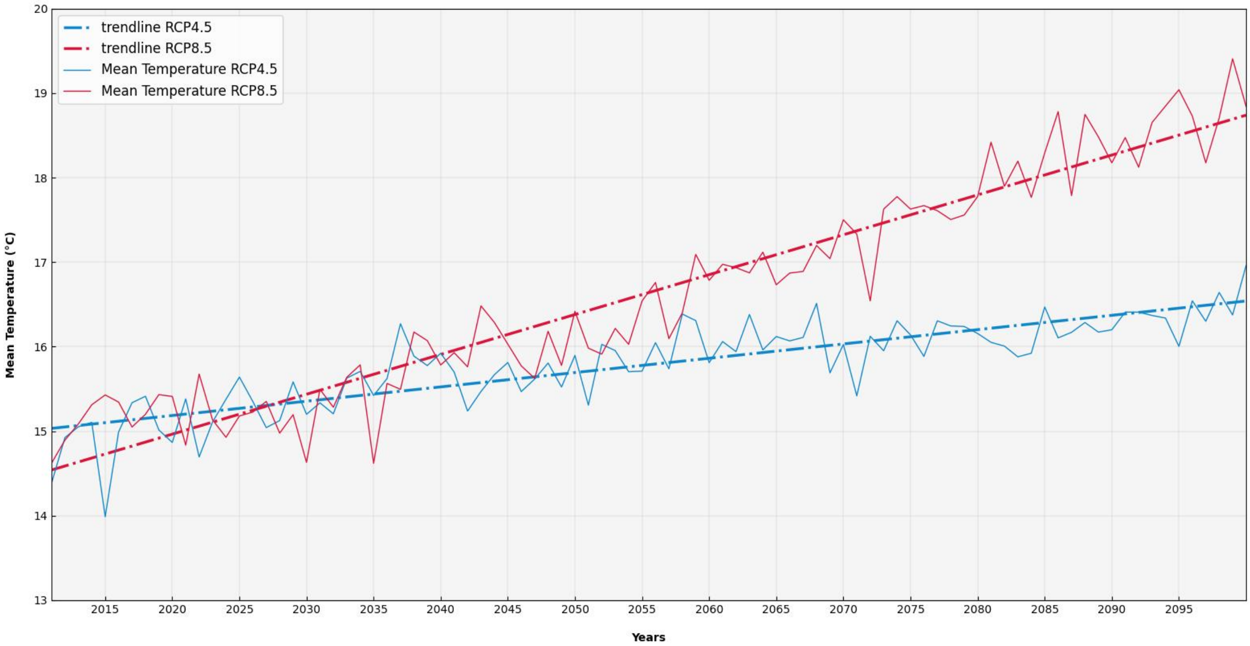

Figure 23: Ensemble mean of mean temperature of the period 2011-2100 for the RCP4.5 (blue line) and RCP8.5 (red line), Koiliaris pilot.

The mean temperature of the examined reference and future periods is shown in Table 11, for the Pinios pilot area. It may be seen that the absolute change of the mean temperature compared to the reference period is +1.2°C and +1.1°C for the near-term period, while in the long-term period it is expected to reach up to +2.2°C and +4.3°C, for the RCP4.5 and RCP8.5 respectively. In addition, for the near-term period (2011-2040) the absolute value of the mean temperature is expected to be around 14.8°C for both scenarios. These values gradually increase until they reach 15.8°C and 17.9°C in the long-term period (2071-2100), for RCP4.5 and RCP8.5 respectively.

Table 11: Ensemble mean temperature for the reference period and the future sub-periods based on the RCP4.5 and RCP8.5. Values are presented as absolute change from the reference period 1971-2000 and as absolute value in °C, Koiliaris pilot.

Mean Temperature	2011-2040		2041-2070		2071-2100	
	RCP4.5	RCP8.5	RCP4.5	RCP8.5	RCP4.5	RCP8.5
absolute change (°C)	+1.1	+1.2	+1.7	+2.3	+2.1	+4.0
absolute value (°C)	*15.3*	*15.3*	*15.9*	*16.5*	*16.2*	*18.2*

Regarding the spatial distribution of the mean temperature range (Figure 24), it is observed that during the reference period the mean temperature range ranges from around 8°C at the more mountainous area of the pilot (southern part) and reaches up to 20°C at the very northern part. During the period 2041-2070, it is expected that the mean temperature will have the same range according to RCP4.5, however the extend of the area covered with the highest values is greater. On the other and, according to scenario RCP8.5, the temperature expected to range from 10 to 20°C.

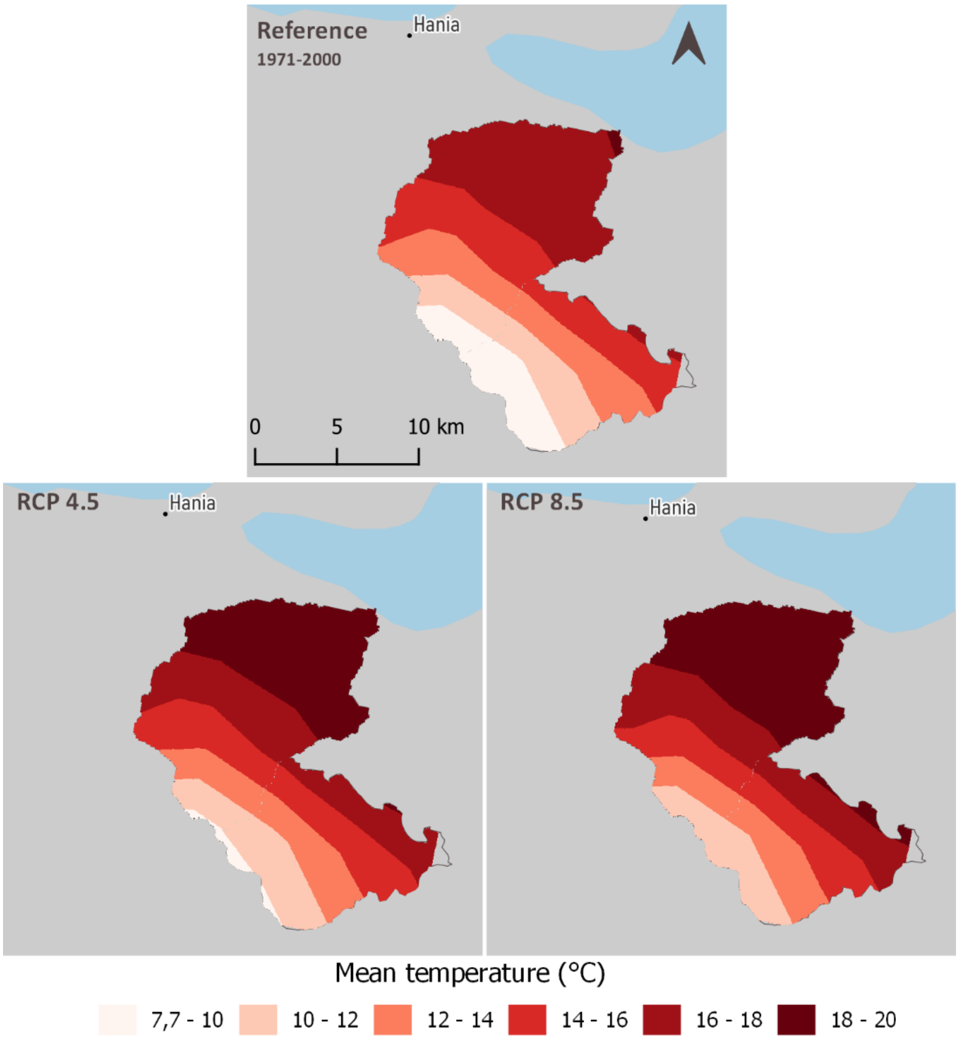

Figure 24: Spatial distribution of the mean annual temperature, for the reference period (top) and the future period 2041-2070, based on the RCP4.5 and RCP8.5 (bottom), Koiliaris pilot.

Total Precipitation

The projected mean annual total precipitation for the period 2011 to 2100 for the two scenarios at Koiliaris pilot area, is presented in the form of annual time series in Figure 25. As it may be seen, total precipitation tends to decrease over the 90-year period for RCP8.5 and it is expected to be stable for RCP4.5. Regarding RCP8.5, the trend is expected to be reduced by up to 190 mm. Additionally, the minimum annual total precipitation value is expected to be around 300 mm for both scenarios, while maximum values expected to reach up to 1000 mm.

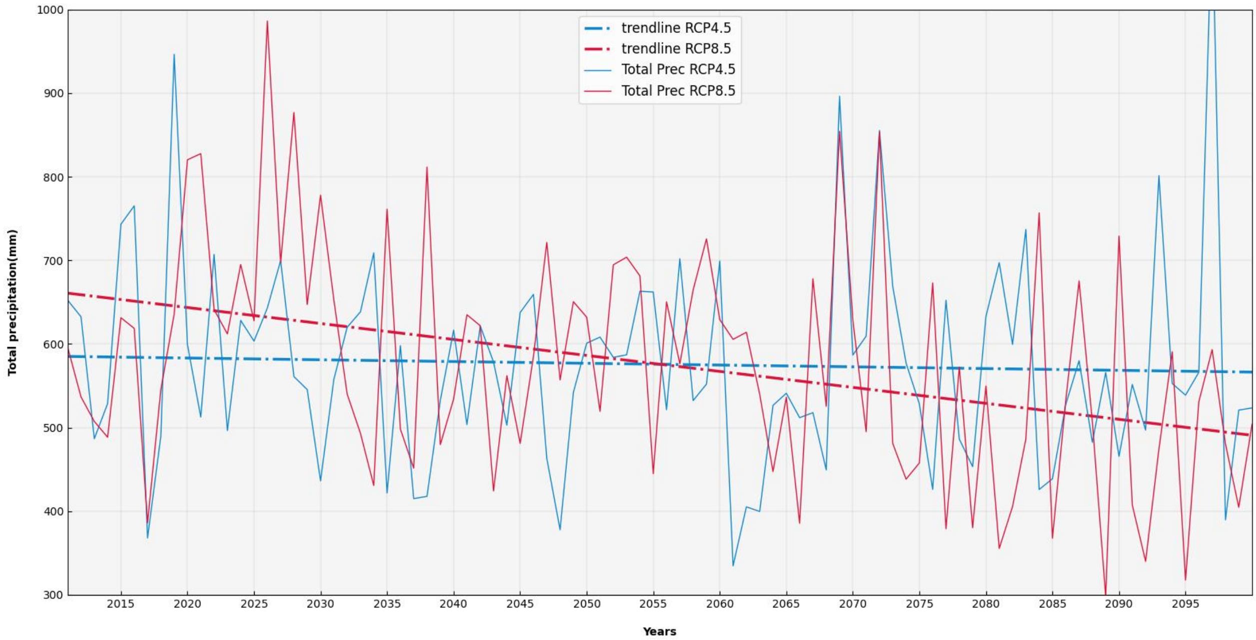

Figure 25: Ensemble mean of total precipitation of the period 2011-2100 for the RCP4.5 (blue line) and RCP8.5 (red line), Koiliaris pilot.

In Table 12, the projected average annual total precipitation for the examined future sub-periods is provided, divided in the dry and wet periods of the year. In the case of the Koiliaris pilot area, the selected dry months include the period from May to September while the selected wet period starts from October until April. It may be seen that the total precipitation is expected to show a decrease for most subperiods, for both scenarios, in the dry and wet seasons of the year in relation to the reference period. The exceptions to this are, the period 2011-2040 for RCP4.5 in the wet period where an increase of 8 mm is observed compared to the reference period, the period 2041-2070 for the RCP8.5 where the increase is expected to be 12 mm, and a small increase is also expected for the long-term period for the RCP4.5. The maximum reduction is expected in the wet season of 2071-2100, for RCP8.5, where it reaches -111 mm compared to the 1971-2000 period.

Table 12: Ensemble mean of total precipitation for the future sub-periods based on the RCP4.5 and RCP8.5 divided in dry and wet period. Values are presented as absolute change from the reference period 1971-2000 and as absolute value in mm, Koiliaris pilot.

Total Precipitation		2011-2040		2041-2070		2071-2100	
		RCP4.5	RCP8.5	RCP4.5	RCP8.5	RCP4.5	RCP8.5
Dry period	absolute change (mm)	-9	-9	-12	12	4	-16
	absolute value (mm)	*25*	*24*	*21*	*45*	*37*	*17*
Wet period	absolute change (mm)	-34	8	-57	-41	-50	-111
	absolute value (mm)	*561*	*603*	*538*	*554*	*545*	*484*

Figure 26, shows the geospatial variation of the total precipitation for the periods 1971-2000 and 2041-2070, for both the dry and wet periods of the year. As shown in Koiliaris pilot area, during the wet period about 580-600 mm of precipitation per year are estimated for the reference period, while for during the dry period, only 30 to 40 mm are estimated for the whole pilot area. The changes for both RCPs in relation to the reference period for dry and wet seasons are noticeable. In the future period, the precipitation is expected to decrease during the wet season under both scenarios. On the contrary, an increase is expected under

RCP4.5 for the greatest part of the Koiliaris pilot area during the dry season, while a decrease is expected in the case of RCP8.5.

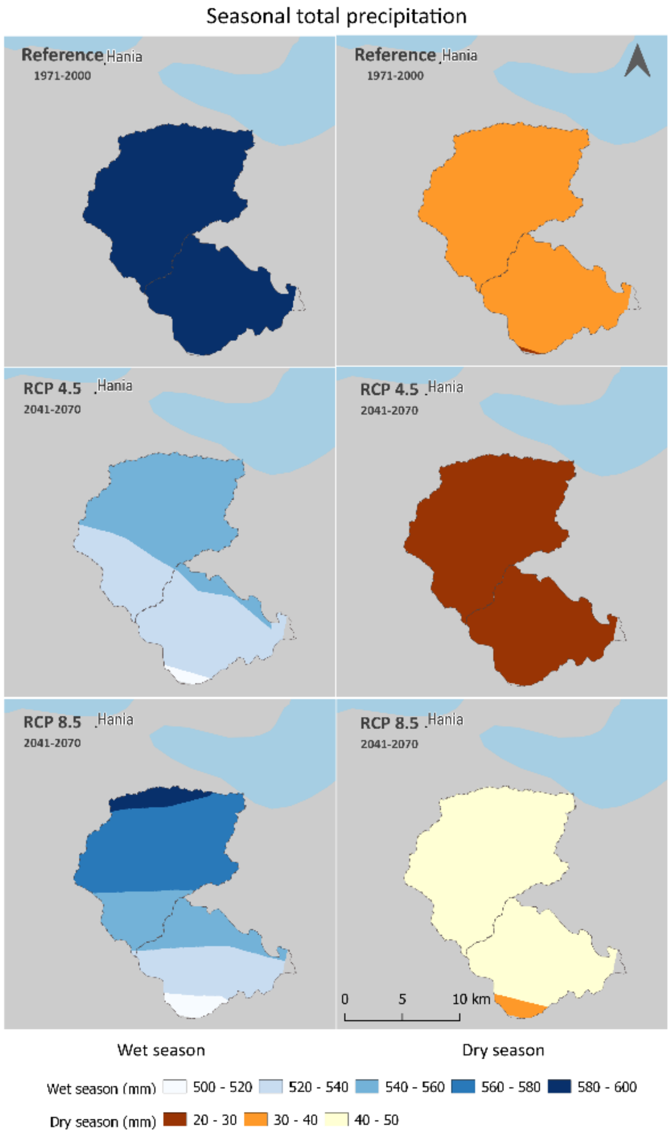

Figure 26: Spatial distribution of the mean total precipitation during the reference period (top) and the future period based on the RCP4.5 (middle) and RCP8.5 (bottom), for the dry (right) and the wet (left) periods, Koiliaris pilot.

Potential Evapotranspiration

The total annual actual evapotranspiration for the period 2011-2100 is presented in Figure 27 for both RCP4.5 and RCP8.5. As it may be observed, there is a tendency for the evapotranspiration to increase during the 90-year period in both scenarios. According to the results for both RCPs, the trend for the period 2011-2100 shows a small increase of around 20 mm, with the values of RCP8.5 expected to be slightly higher. Additionally, the actual evapotranspiration for both scenarios is above 750 mm for almost all the 90-year period. The maximum value of annual actual evapotranspiration is around 950 mm, and it is observed in the case of the RCP8.5.

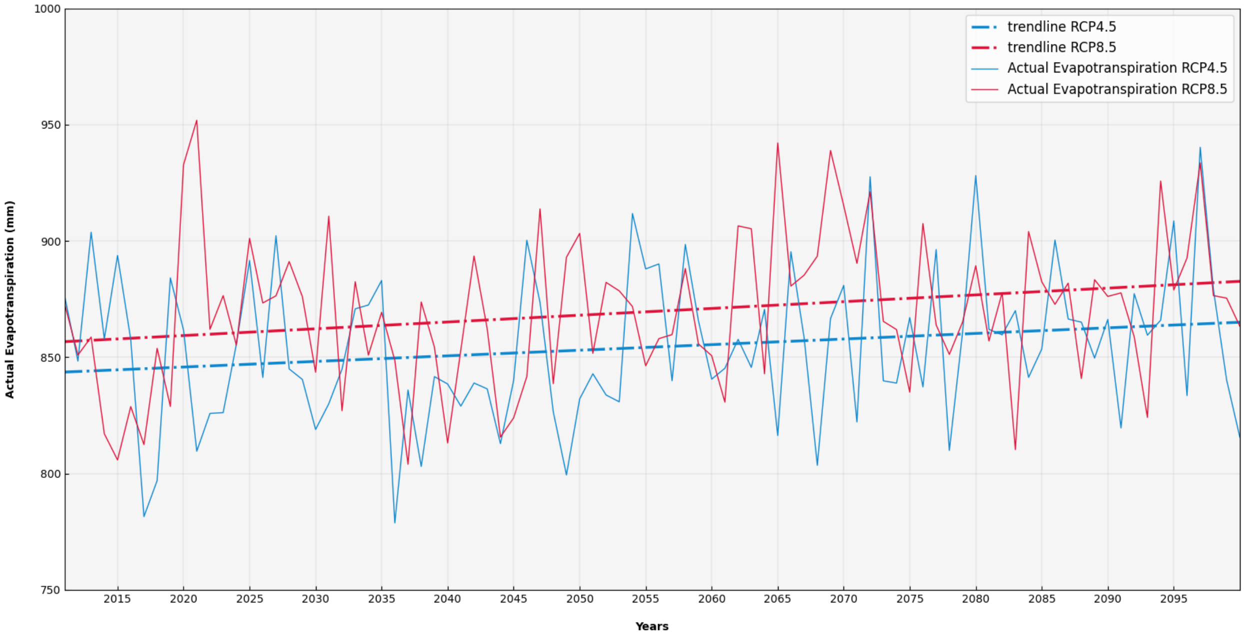

Figure 27: Ensemble mean of actual evapotranspiration of the period 2011-2100 for the RCP4.5 (blue line) and RCP8.5 (red line), Koiliaris pilot.

The expected total actual evapotranspiration for the examined future periods under RCP4.5 and RCP8.5 for the Koiliaris pilot area, is presented in Table 13. The values are presented as the absolute change from the reference period 1971-2000 and as absolute values. It may be observed that the absolute change of the evapotranspiration compared to the reference period is +25 mm average for the near-term period for both scenarios, while in the long-term period is expected to increase even more, up to 41 mm on average for the two scenarios.

Table 13: Actual evapotranspiration per sub-period for RCP4.5 and RCP8.5. Values are presented as absolute change from the reference period 1971-2000 and as absolute value in mm, Koiliaris pilot.

Actual Evapotranspiration	**2011-2040**		**2041-2070**		**2071-2100**	
	RCP4.5	**RCP8.5**	**RCP4.5**	**RCP8.5**	**RCP4.5**	**RCP8.5**
absolute change (mm)	19	32	24	46	35	47
absolute value (mm)	*847*	*860*	*852*	*874*	*863*	*875*

Regarding the spatial distribution of the total actual evapotranspiration (Figure 28), it is observed that during the reference period the evapotranspiration ranges from 400 mm to 900 mm, with the highest values being observed closer to the coast. As it is shown, during the future period, the actual evapotranspiration tends to remain very similar for both scenarios.

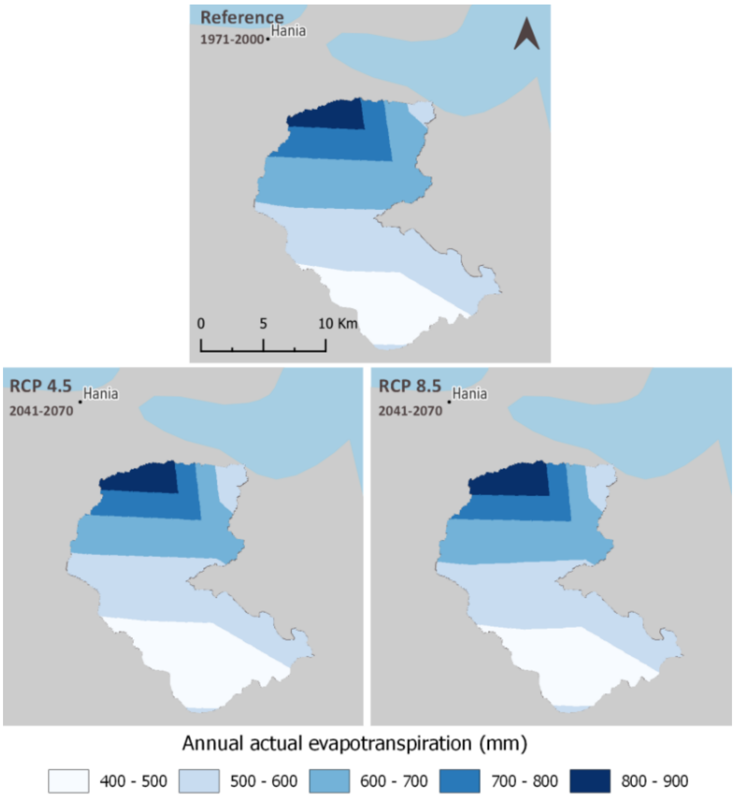

Figure 28: Spatial distribution of the mean annual actual evapotranspiration, for the reference period (top) and the future period 2041-2070, based on the RCP4.5 and RCP8.5 (bottom), Koiliaris pilot.

4.4 Gediz Basin & Delta (Turkey)

Mean Temperature

The projected annual mean temperature for the period 2011-2100 is presented in the form of time series in Figure 29. As it may be observed, there is a clear tendency of temperature increase during the 90-year period in both scenarios. Based on the findings for the RCP4.5, the trend over the period 2011-2100 indicates a rise of up to 1.6°C, whereas under the RCP8.5 scenario, the trend shows a significantly higher increase, upto 4.6°C. Additionally, the mean temperature for both scenarios is above 16°C throughout the 90-year period. The maximum value of annual mean temperature is observed in the case of the RCP8.5 and in specific during the last years of the time series, when it reaches the value of about 22.4°C.

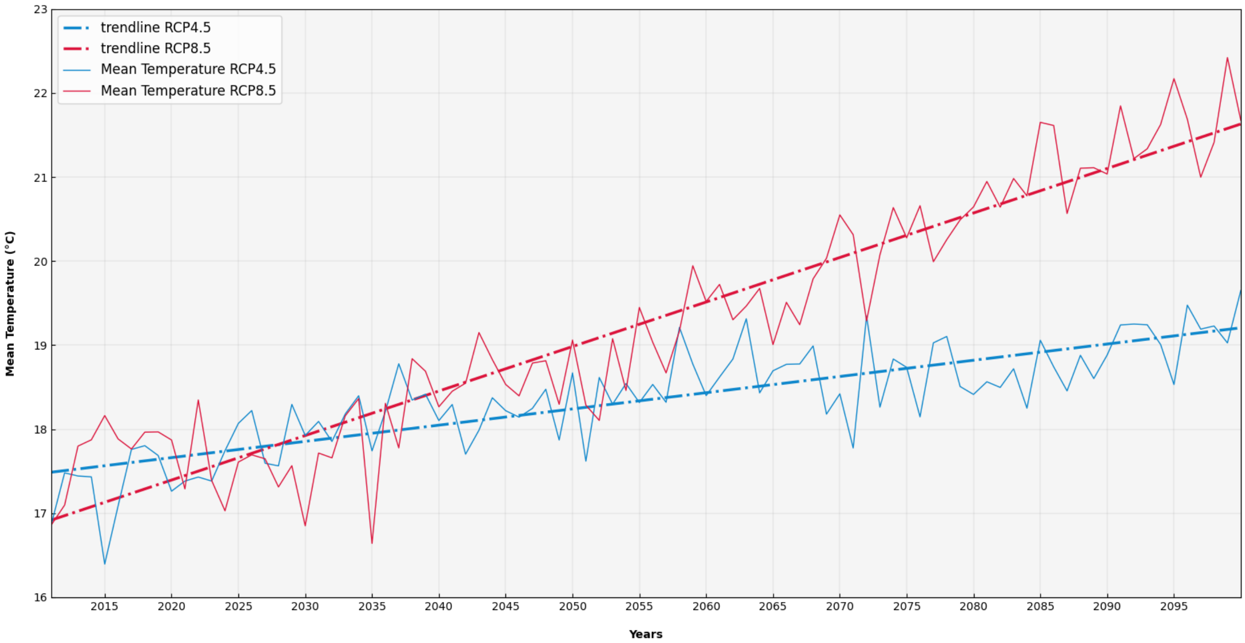

Figure 29: Ensemble mean of mean temperature of the period 2011-2100 for the RCP4.5 (blue line) and RCP8.5 (red line), Gediz pilot.

The mean temperature of the examined reference and future periods is shown in Table 14, for the Gediz pilot area. It may be seen that the absolute change of the mean temperature compared to the reference period is +1.4°C and +1.3°C for the near-term period, while in the long-term period it is expected to reach up to +2.4°C and +4.6°C, for the RCP4.5 and RCP8.5 respectively. In addition, for the near-term period (2011-2040) the absolute value of the mean temperature is expected to be around 17.8°C for both scenarios. These values gradually increase until they reach 18.8°C and 21°C in the long-term period (2071-2100), for RCP4.5 and RCP8.5 respectively.

Table 14: Ensemble mean temperature for the reference period and the future sub-periods based on the RCP4.5 and RCP8.5. Values are presented as absolute change from the reference period 1971-2000 and as absolute value in °C, Gediz pilot.

Mean Temperature	**2011-2040**		**2041-2070**		**2071-2100**	
	RCP4.5	**RCP8.5**	**RCP4.5**	**RCP8.5**	**RCP4.5**	**RCP8.5**
absolute change (°C)	+1.4	+1.3	+2.1	+2.7	+2.4	+4.6
absolute value (°C)	*17.8*	*17.7*	*18.5*	*19.1*	*18.8*	*21.0*

In Figure 30, concerning the spatial distribution of the mean temperature range, it is evident that during the reference period, the average temperature range varies from approximately 16°C to around 18°C. For the period 2041-2070, it is anticipated that the mean temperature range will extend from 18°C to 20°C for both scenarios. Furthermore, the larger region of the pilot area is projected to encounter temperatures ranging from 19°C to 20°C.

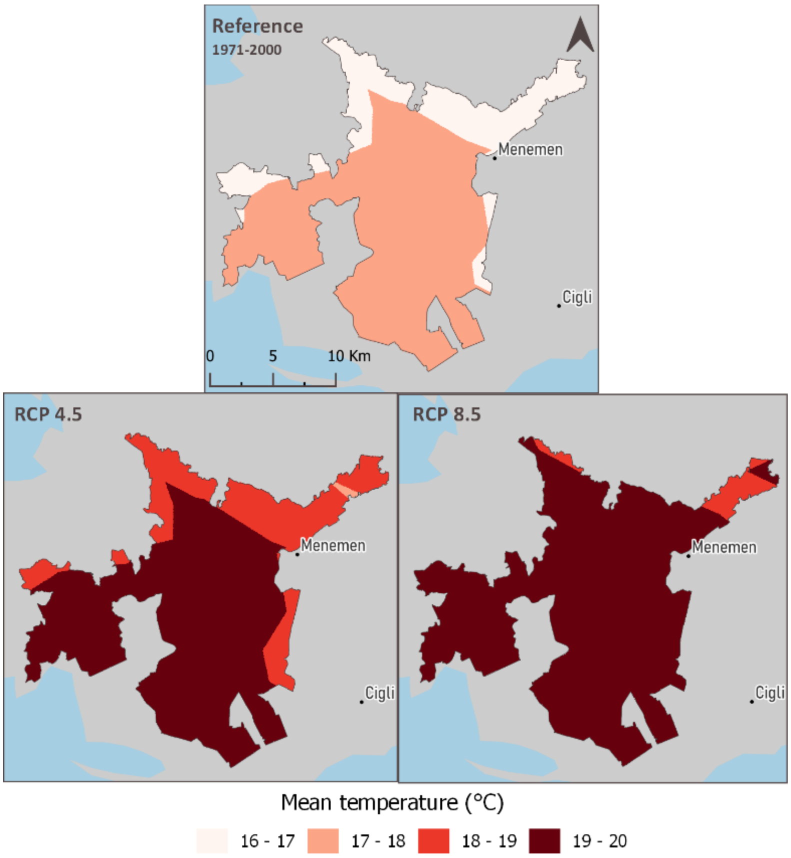

Figure 30: Spatial distribution of the mean annual temperature, for the reference period (top) and the future period 2041-2070, based on the RCP4.5 and RCP8.5 (bottom), Gediz pilot.

Total Precipitation

The projected mean annual total precipitation for the period 2011 to 2100 for the two scenarios at Gediz pilot area, is presented in the form of annual time series in Figure 31. As it may be seen, total precipitation tends to be stable over the 90-year period for both scenarios. Additionally, the minimum annual total precipitation value is expected to be around 350 mm, while the maximum value is expected around 940 mm, both values in the case of RCP8.5.

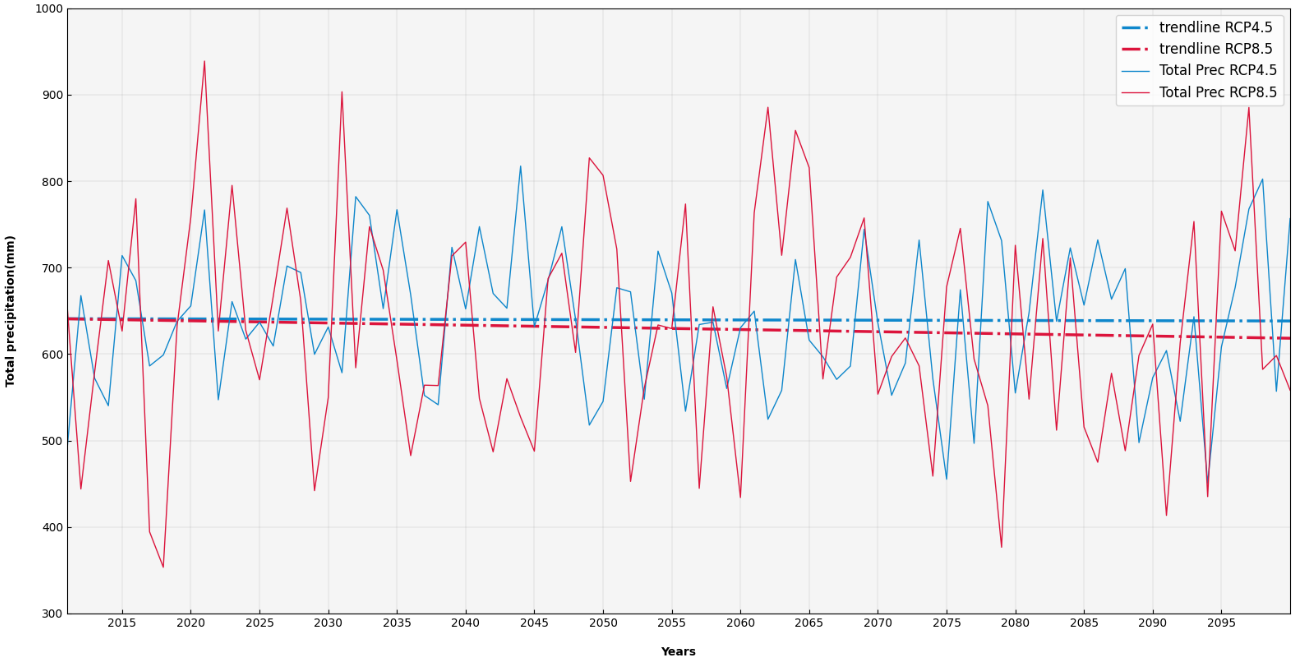

Figure 31: Ensemble mean of total precipitation of the period 2011-2100 for the RCP4.5 (blue line) and RCP8.5 (red line), Gediz pilot.

In Table 15, the projected average annual total precipitation for the examined future sub-periods is provided, divided in the dry and wet periods of the year. In the case of the Gediz pilot area, the selected dry months include the period from May to September while the selected wet period starts from October until April. It may be seen that the total precipitation is expected to show an increase for both the dry and wet periods of the year in relation to the reference period. Exceptions are the short-term period for the RCP4.5 where a small decrease of 2 mm is expected for the dry period and the long-term period for RCP8.5 (-9 mm). The highest increase is expected during the near-term period with an increase of 32 mm on average for the two scenarios.

Table 15: Ensemble mean of total precipitation for the future sub-periods based on the RCP4.5 and RCP8.5 divided in dry and wet period. Values are presented as absolute change from the reference period 1971-2000 and as absolute value in mm, Gediz pilot.

Total Precipitation		2011-2040		2041-2070		2071-2100	
		RCP4.5	RCP8.5	RCP4.5	RCP8.5	RCP4.5	RCP8.5
Dry period	absolute change (mm)	-2	7	2	14	4	3
	absolute value (mm)	*47*	*56*	*50*	*63*	*52*	*52*
Wet period	absolute change (mm)	38	25	29	28	28	-9
	absolute value (mm)	*596*	*583*	*587*	*586*	*586*	*549*

Figure 32 displays the geospatial variation in total precipitation for the periods 1971-2000 and 2041-2070, encompassing both the dry and wet seasons of the year. In the Gediz pilot area, it is evident that during the wet period, an estimated 500 to 580 mm of precipitation per year occurs within the reference period. Conversely, the dry period experiences much lower estimates, with only 30 to 60 mm projected across the entire pilot area. Noticeable changes are observed across both RCPs in comparison to the reference period, affecting both dry and wet seasons. In the forthcoming period, an increase in precipitation is anticipated during the wet season for both scenarios. Moreover, under RCP8.5, an increase in precipitation is expected for a significant extend of the Gediz pilot area during the dry season. Conversely, the amount of precipitation expected under RCP8.5 remains similar.

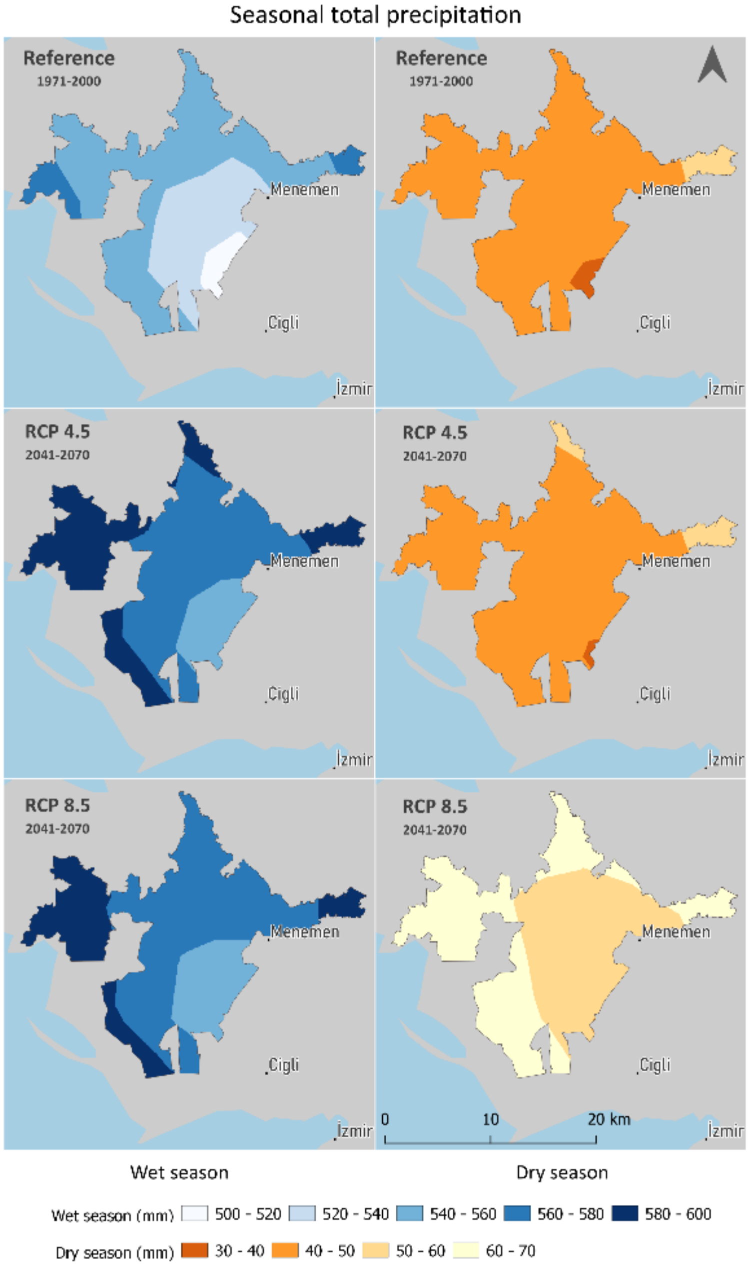

Figure 32: Spatial distribution of the mean total precipitation during the reference period (top) and the future period based on the RCP4.5 (middle) and RCP8.5 (bottom), for the dry (right) and the wet (left) periods, Gediz pilot.

Actual Evapotranspiration

The total annual actual evapotranspiration for the period 2011-2100 is presented in Figure 33 for both RCP4.5 and RCP8.5. As it may be observed, there is a tendency for the evapotranspiration to increase during the 90-year period in both scenarios. According to the results for the RCP4.5, the trend for the period 2011-2100 shows a small increase of around 20 mm, while for the RCP8.5 the increase is expected to be higher, up to

50mm. Additionally, the actual evapotranspiration for both scenarios is above 650 mm for almost all the 90-year period. The maximum value of annual actual evapotranspiration is around 870 mm, and it is observed in the case of the RCP8.5.

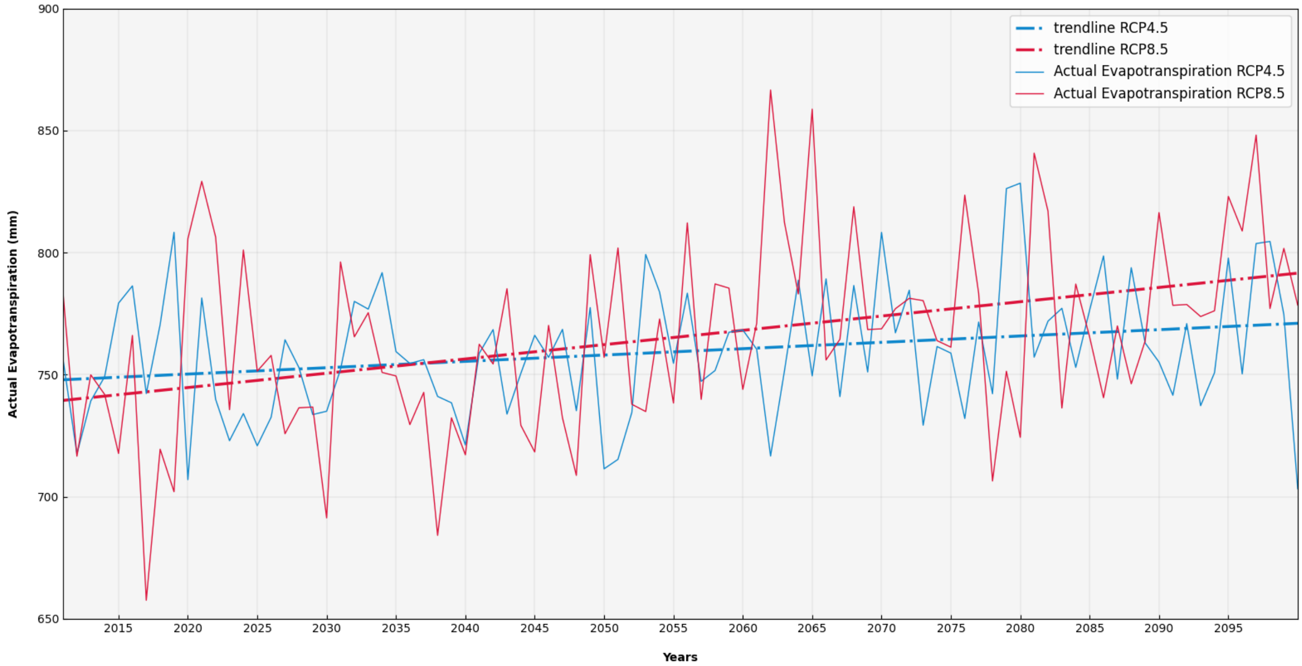

Figure 33: Ensemble mean of actual evapotranspiration of the period 2011-2100 for the RCP4.5 (blue line) and RCP8.5 (red line), Gediz pilot.

The expected total actual evapotranspiration for the examined future periods under RCP4.5 and RCP8.5 for the Gediz pilot area, is presented in Table 16. The values are presented as the absolute change from the reference period 1971-2000 and as absolute values. It may be observed that the absolute change of the evapotranspiration compared to the reference period is +29 mm on average for the near-term period for both scenarios, while in the long-term period is expected to increase even more, up to 54 mm on average for the two scenarios. In addition, for the near-term period (2011-2040) the mean evapotranspiration is expected to be 749 mm on average for the two scenarios and gradually increase up to 774 mm on average in the long-term period (2071-2100).

Table 16: Actual evapotranspiration per sub-period for RCP4.5 and RCP8.5. Values are presented as absolute change from the reference period 1971-2000 and as absolute value in mm, Gediz pilot.

Actual Evapotranspiration	**2011-2040**		**2041-2070**		**2071-2100**	
	RCP4.5	**RCP8.5**	**RCP4.5**	**RCP8.5**	**RCP4.5**	**RCP8.5**
absolute change (mm)	32	26	40	52	48	60
absolute value (mm)	*752*	*746*	*759*	*771*	*768*	*779*

Regarding the spatial distribution of the total actual evapotranspiration (Figure 34), it is observed that during the reference period the evapotranspiration ranges from 450 mm to 690 mm. As it is shown, during the future period, the actual evapotranspiration tends to remain similar for both scenarios, however it is noticed that close to the coast a small part of the pilot area will experience values of evapotranspiration up to 750 mm.

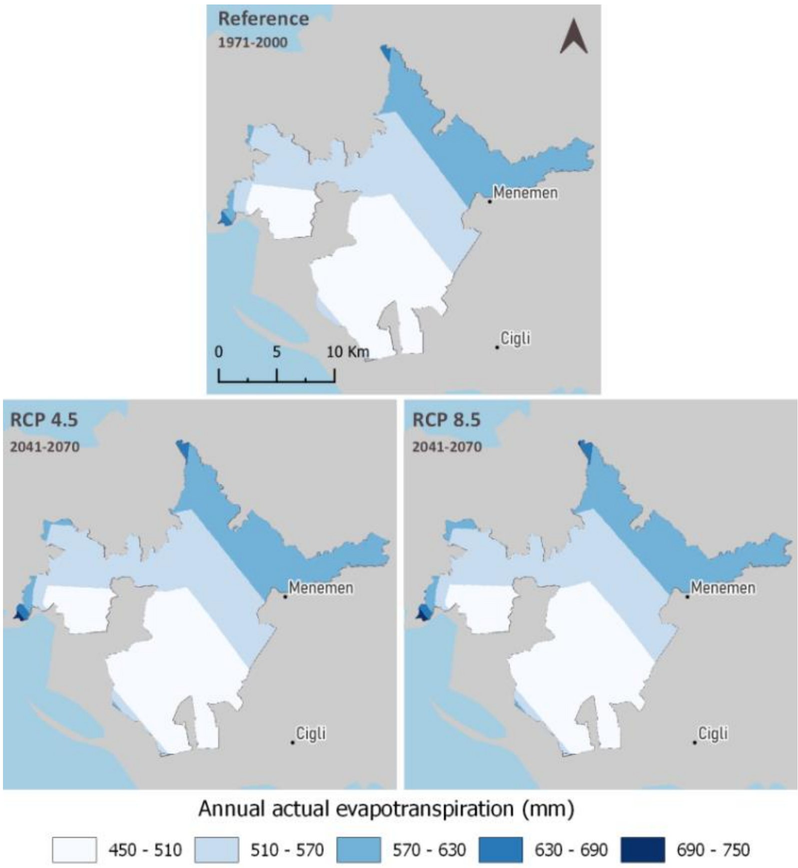

Figure 34: Spatial distribution of the mean annual actual evapotranspiration, for the reference period (top) and the future period 2041-2070, based on the RCP4.5 and RCP8.5 (bottom), Gediz pilot.

4.5 Galilee, Hula Valley (Israel)

Mean Temperature

The projected annual mean temperature for the period 2011-2100 is presented in the form of time series in Figure 35. As it may be observed, there is a clear tendency of temperature increase during the 90-year period in both scenarios. Based on the findings for the RCP4.5, the trend over the period 2011-2100 anticipates a rise of up to 2.3°C, whereas under the RCP8.5 scenario, the trend shows a significantly higher increase, reaching 5.9°C. Additionally, the mean temperature for both scenarios is above 20°C throughout the 90-year period. The maximum value of annual mean temperature is observed in the case of the RCP8.5 and in specific during the last years of the time series, when it reaches the value of almost 27°C.

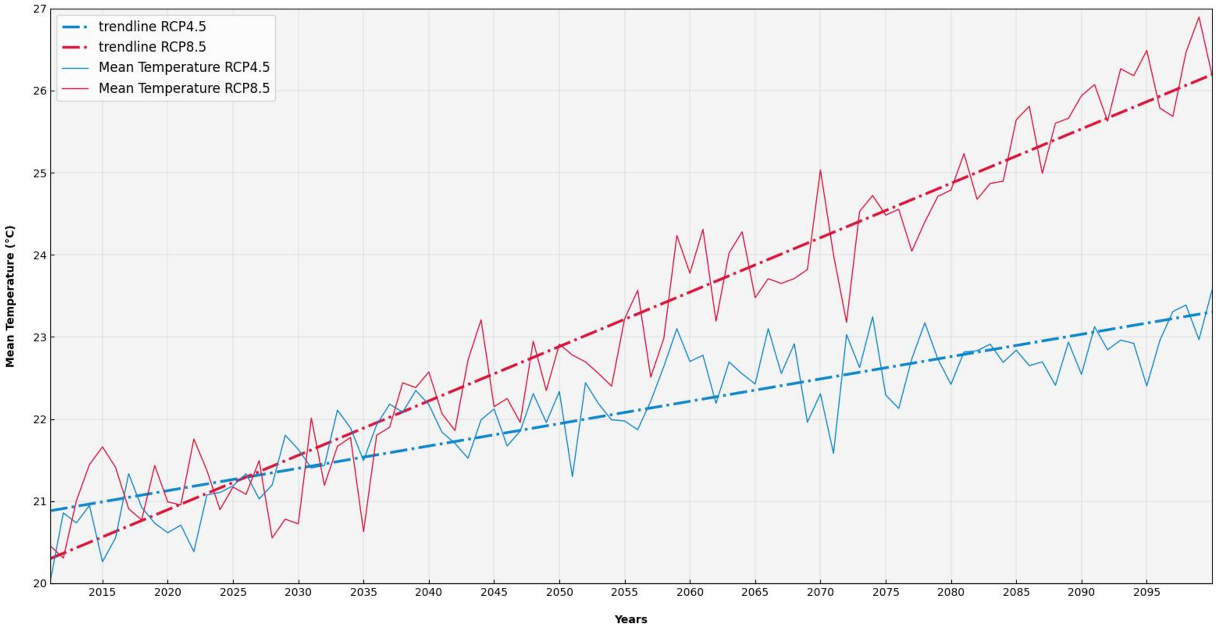

Figure 35: Ensemble mean of mean temperature of the period 2011-2100 for the RCP4.5 (blue line) and RCP8.5 (red line), Hula pilot.

The mean temperature of the examined reference and future periods is shown in Table 17, for the Hula Valley pilot area. It may be seen that the absolute change of the mean temperature compared to the reference period is +1.7°C for the near-term period, while in the long-term period it is expected to reach up to +4.5°C on average, for both scenarios. In addition, for the near-term period (2011-2040) the absolute value of the mean temperature is expected to be around 21.3°C for both scenarios. These values gradually increase until they reach 22.8°C and 25.2°C in the long-term period (2071-2100), for RCP4.5 and RCP8.5 respectively.

Table 17: Ensemble mean temperature for the reference period and the future sub-periods based on the RCP4.5 and RCP8.5. Values are presented as absolute change from the reference period 1971-2000 and as absolute value in °C, Hula pilot.

Mean Temperature	2011-2040		2041-2070		2071-2100	
	RCP4.5	RCP8.5	RCP4.5	RCP8.5	RCP4.5	RCP8.5
absolute change (°C)	+1.7	+1.7	+2.6	+3.5	+3.2	+5.7
absolute value (°C)	*21.2*	*21.3*	*22.2*	*23.1*	*22.8*	*25.2*

Total Precipitation

The projected mean annual total precipitation for the period 2011 to 2100 for the two scenarios at Hula Valley pilot area, is presented in the form of annual time series in Figure 36. As it may be seen, total precipitation tends to decrease over the 90-year period for both scenarios. Regarding RCP4.5, the trend is expected to be reduced by up to 130 mm, while for the RCP8.5 up to 300 mm. Additionally, the minimum annual total precipitation value is expected to be around 340 mm for both scenarios; values which are observed during the last years of the period under study.

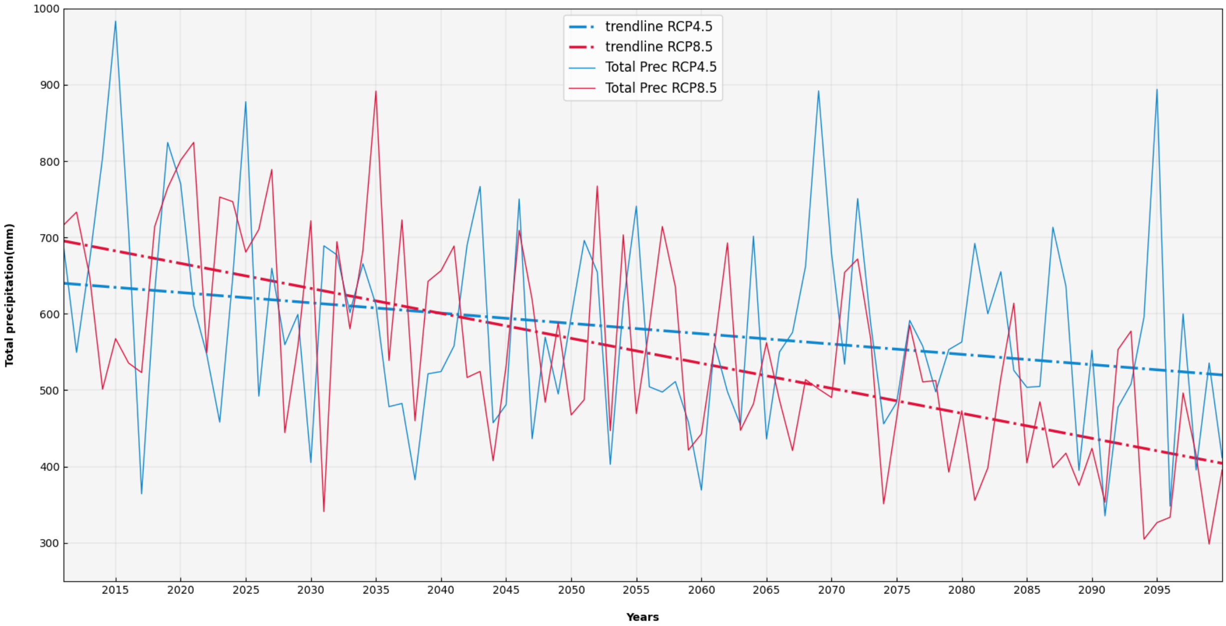

Figure 36: Ensemble mean of total precipitation of the period 2011-2100 for the RCP4.5 (blue line) and RCP8.5 (red line), Hula pilot.

In Table 18, the projected average annual total precipitation for the examined future sub-periods is provided, divided in the dry and wet periods of the year. In the case of the Hula Valley pilot area, the selected dry months include the period from April to October while the selected wet period starts from November until March. It may be seen that the total precipitation is expected to show a decrease for most subperiods, for both scenarios, in the dry and wet seasons of the year in relation to the reference period. The only exception is the period 2011-2070 for RCP8.5 in the wet period where an increase of 8 mm is observed compared to the reference period. The maximum reduction is expected in the wet season of 2071-2100, for RCP8.5, where it reaches -163 mm compared to the 1971-2000 period.

Table 18: Ensemble mean of total precipitation for the future sub-periods based on the RCP4.5 and RCP8.5 divided in dry and wet period. Values are presented as absolute change from the reference period 1971-2000 and as absolute value in mm, Hula pilot.

Total Precipitation		**2011-2040**		**2041-2070**		**2071-2100**	
		RCP4.5	**RCP8.5**	**RCP4.5**	**RCP8.5**	**RCP4.5**	**RCP8.5**
Dry period	absolute change (mm)	-23	-15	-12	-34	-27	-39
	absolute value (mm)	*62*	*70*	*72*	*51*	*57*	*45*
Wet period	absolute change (mm)	-18	8	-69	-78	-81	-163
	absolute value (mm)	*554*	*580*	*503*	*495*	*491*	*409*

Actual Evapotranspiration

The total annual actual evapotranspiration for the period 2011-2100 is presented in Figure 37 for both RCP4.5 and RCP8.5. As it may be observed, there is a tendency for the evapotranspiration to decrease during the 90-year period in both scenarios. According to the results for the RCP4.5, the trend for the period 2011-2100 shows a decrease of 50 mm, while for the RCP8.5 the decrease is expected to be higher, up to 120 mm. Additionally, the actual evapotranspiration for both scenarios is above 250 mm for almost all the 90-year period. The maximum value of annual actual evapotranspiration is around 530 mm, and it is observed in the case of the RCP4.5.

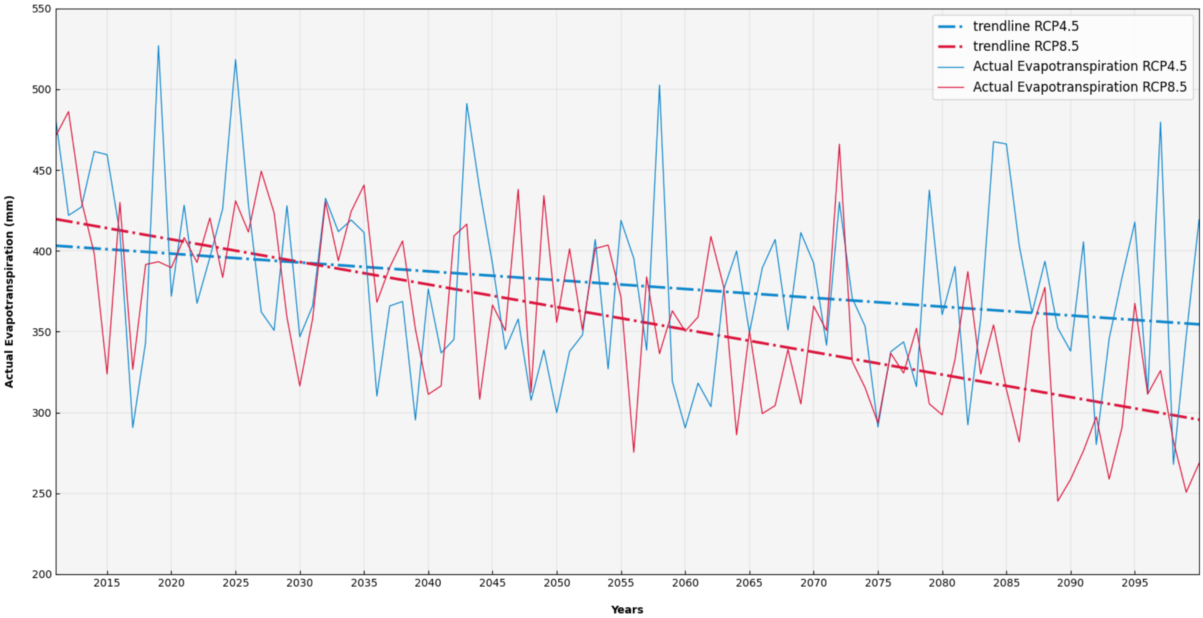

Figure 37: Ensemble mean of actual evapotranspiration of the period 2011-2100 for the RCP4.5 (blue line) and RCP8.5 (red line), Hula pilot.

The expected total actual evapotranspiration for the examined future periods under RCP4.5 and RCP8.5 for the Hula Valley pilot area, is presented in Table 19. The values are presented as the absolute change from the reference period 1971-2000 and as absolute values. It may be observed that the absolute change of the evapotranspiration compared to the reference period is -28 mm on average for the near-term period, while in the long-term period is expected to decrease even more, up to -59 mm and -110 mm, for the RCP4.5 and RCP8.5 respectively. In addition, for the near-term period (2011-2040) the mean evapotranspiration is expected to be 398 mm on average for the RCP4.5 and RCP8.5 and gradually decrease up to 343 mm on average in the long-term period.

Table 19: Actual evapotranspiration per sub-period for RCP4.5 and RCP8.5. Values are presented as absolute change from the reference period 1971-2000 and as absolute value in mm, Hula pilot.

Actual Evapotranspiration	2011-2040		2041-2070		2071-2100	
	RCP4.5	RCP8.5	RCP4.5	RCP8.5	RCP4.5	RCP8.5
absolute change (mm)	-27	-30	-60	-69	-59	-110
absolute value (mm)	*400*	*397*	*368*	*358*	*369*	*318*

4.6 Middle Jordan Valley, Deir Alla (Jordan)

Mean Temperature

The projected annual mean temperature for the period 2011-2100 is presented in the form of time series in Figure 38. As it may be observed, there is a clear tendency of temperature increase during the 90-year period in both scenarios. Based on the findings for the RCP4.5, the trend over the period 2011-2100 anticipates a

This project is part of the PRIMA programme supported by the European Union.
GA n° [2041] [LENSES] [Call 2020 Section 1 Nexus IA]

rise of up to 2.5°C, whereas under the RCP8.5 scenario, the trend shows a significantly higher increase, reaching 6°C. Additionally, the mean temperature for both scenarios is above 23°C throughout the 90-year period. The maximum value of annual mean temperature is observed in the case of the RCP8.5 and in specific during the last years of the time series, when it reaches the value of almost 30°C.

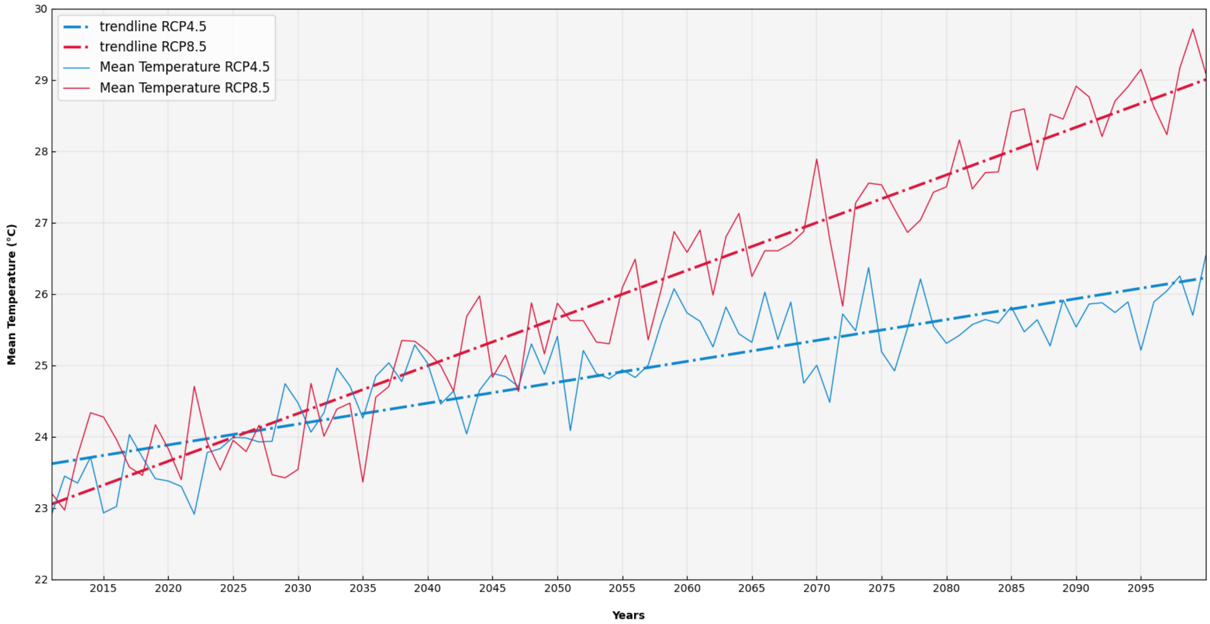

Figure 38: Ensemble mean of mean temperature of the period 2011-2100 for the RCP4.5 (blue line) and RCP8.5 (red line), Deir Alla pilot.

The mean temperature of the examined reference and future periods is shown in Table 20, for the Deir Alla pilot area. It may be seen that the absolute change of the mean temperature compared to the reference period is +1.9°C for the near-term period, while in the long-term period it is expected to reach up to +4.7°C on average, for both scenarios. In addition, for the near-term period (2011-2040) the absolute value of the mean temperature is expected to be around 24°C for both scenarios. These values gradually increase until they reach 25.6°C and 28°C in the long-term period (2071-2100), for RCP4.5 and RCP8.5 respectively.

Table 20: Ensemble mean temperature for the reference period and the future sub-periods based on the RCP4.5 and RCP8.5. Values are presented as absolute change from the reference period 1971-2000 and as absolute value in °C, Deir Alla pilot.

Mean Temperature	**2011-2040**		**2041-2070**		**2071-2100**	
	RCP4.5	**RCP8.5**	**RCP4.5**	**RCP8.5**	**RCP4.5**	**RCP8.5**
absolute change (°C)	+1.9	+1.9	+2.9	+3.8	+3.5	+5.9
absolute value (°C)	*24.0*	*24.1*	*25.1*	*26.0*	*25.6*	*28.0*

Total Precipitation

The projected mean annual total precipitation for the period 2011 to 2100 for the two scenarios at Deir Alla pilot area, is presented in the form of annual time series in Figure 39. As it may be seen, total precipitation tends to decrease over the 90-year period for both scenarios. Regarding RCP4.5, the trend is expected to be reduced by up to 90 mm, while for the RCP8.5 up to 140 mm. Additionally, the minimum annual total precipitation value is expected to be around 160 mm for both scenarios.

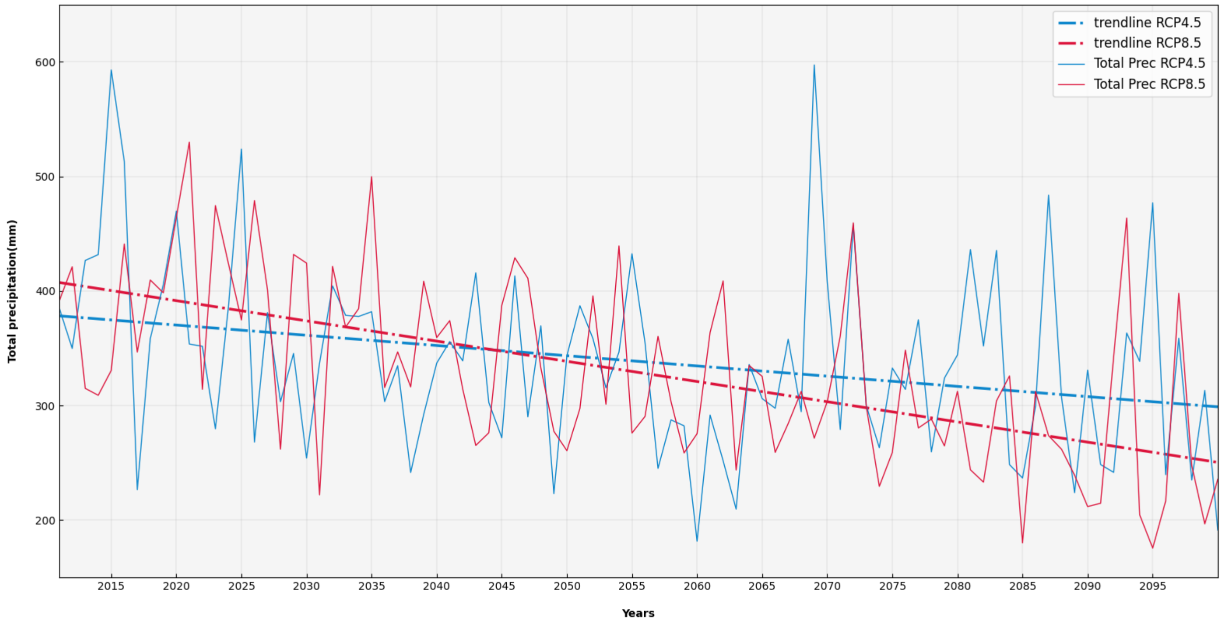

Figure 39: Ensemble mean of total precipitation of the period 2011-2100 for the RCP4.5 (blue line) and RCP8.5 (red line), Deir Alla pilot.

In Table 21, the projected average annual total precipitation for the examined future sub-periods is provided, divided in the dry and wet periods of the year. In the case of the Dair Alla pilot area, the selected dry months include the period from April to October while the selected wet period starts from November until March. It may be seen that the total precipitation is expected to present a decrease for most subperiods, for both scenarios, in the dry and wet seasons of the year in relation to the reference period. The only exception is the period 2011-2040 for RCP8.5 in the wet period where an increase of 1 mm is observed compared to the reference period, which is considered insignificant. The maximum reduction is expected in the wet season of 2071-2100, for RCP8.5, where it reaches -94 mm compared to the 1971-2000 period.

Table 21: Ensemble mean of total precipitation for the future sub-periods based on the RCP4.5 and RCP8.5 divided in dry and wet period. Values are presented as absolute change from the reference period 1971-2000 and as absolute value in mm, Deir Alla pilot.

Total Precipitation		2011-2040		2041-2070		2071-2100	
		RCP4.5	RCP8.5	RCP4.5	RCP8.5	RCP4.5	RCP8.5
Dry period	absolute change (mm)	-8	-6	-5	-17	-13	-18
	absolute value (mm)	*36*	*38*	*39*	*27*	*31*	*27*
Wet period	absolute change (mm)	-17	1	-57	-53	-57	-94
	absolute value (mm)	*330*	*348*	*290*	*294*	*289*	*253*

Actual Evapotranspiration

The total annual actual evapotranspiration for the period 2011-2100 is presented in Figure 40 for both RCP4.5 and RCP8.5. As it may be observed, there is a tendency for the evapotranspiration to decrease during the 90-year period in both scenarios. According to the results for the RCP4.5, the trend for the period 2011-2100 shows a decrease of 50 mm, while for the RCP8.5 the decrease is expected to be higher, up to 130 mm.

Additionally, the actual evapotranspiration for both scenarios is above 200 mm for almost all the 90-year period. The maximum value of annual actual evapotranspiration is around 510 mm, and it is observed in the case of the RCP4.5.

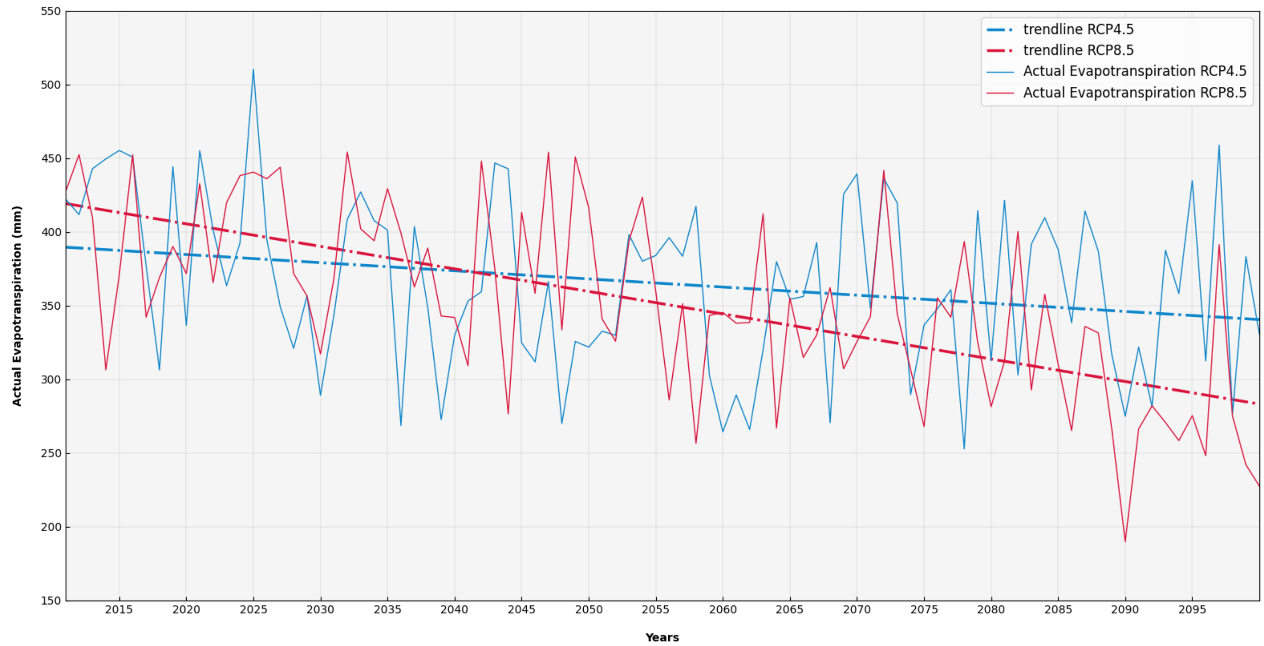

Figure 40: Ensemble mean of actual evapotranspiration of the period 2011-2100 for the RCP4.5 (blue line) and RCP8.5 (red line), Deir Alla pilot.

The expected total actual evapotranspiration for the examined future periods under RCP4.5 and RCP8.5 for the Dair Alla pilot area, is presented in Table 22

Table 22. The values are presented as the absolute change from the reference period 1971-2000 and as absolute values. It may be observed that the absolute change of the evapotranspiration compared to the reference period is -24 mm on average for the near-term period, while in the long-term period is expected to decrease even more, up to -56 mm and -106 mm, for the RCP4.5 and RCP8.5 respectively. In addition, for the near-term period (2011-2040) the mean evapotranspiration is expected to be 389 mm on average for the RCP4.5 and RCP8.5 and gradually decrease up to 332 mm on average in the long-term period.

Table 22: Actual evapotranspiration per sub-period for RCP4.5 and RCP8.5. Values are presented as absolute change from the reference period 1971-2000 and as absolute value in mm, Deir Alla pilot.

Actual Evapotranspiration	2011-2040		2041-2070		2071-2100	
	RCP4.5	RCP8.5	RCP4.5	RCP8.5	RCP4.5	RCP8.5
absolute change (mm)	-28	-20	-59	-59	-56	-106
absolute value (mm)	*385*	*393*	*354*	*354*	*357*	*307*

4.7 Tarquinia plain (Italy)

Mean Temperature

The projected annual mean temperature for the period 2011-2100 is presented in the form of time series in Figure 41. As it may be observed, there is a clear tendency of temperature increase during the 90-year period in both scenarios. Based on the findings for the RCP4.5, the trend over the period 2011-2100 anticipates a rise of up to 1.9°C, whereas under the RCP8.5 scenario, the trend shows a significantly higher increase, reaching 4.3°C. Additionally, the mean temperature for both scenarios is above 15°C throughout the 90-year period. The maximum value of annual mean temperature is observed in the case of the RCP8.5 and in specific during the last years of the time series, when it reaches the value of about 19.5°C.

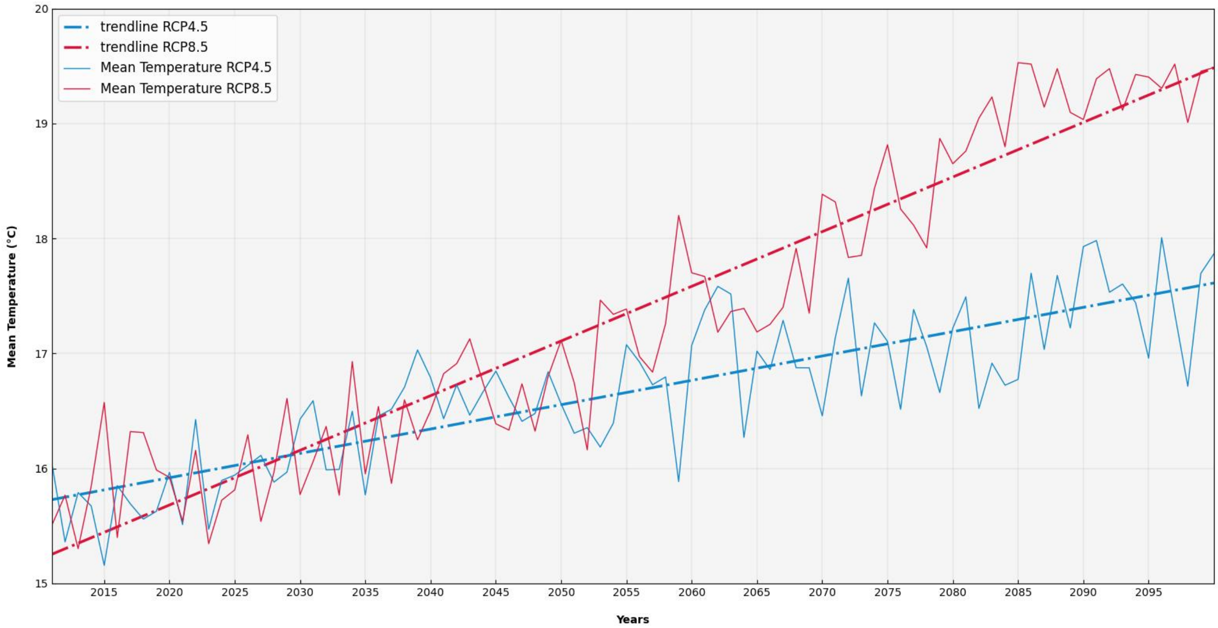

Figure 41: Ensemble mean of mean temperature of the period 2011-2100 for the RCP4.5 (blue line) and RCP8.5 (red line), Tarquinia pilot.

The mean temperature of the examined reference and future periods is shown in Table 23, for the Tarquinia pilot area. It may be seen that the absolute change of the mean temperature compared to the reference period is +1°C for the near-term period for both scenarios, while in the long-term period it is expected to reach up to +2.3°C and +4.0°C, for the RCP4.5 and RCP8.5 respectively. In addition, for the near-term period the absolute value of the mean temperature is expected to be 16°C for both scenarios. These values gradually increase until they reach 17.3°C and 18.9°C in the long-term period (2071-2100), for RCP4.5 and RCP8.5 respectively.

Table 23: Ensemble mean temperature for the reference period and the future sub-periods based on the RCP4.5 and RCP8.5. Values are presented as absolute change from the reference period 1971-2000 and as absolute value in °C, Tarquinia pilot.

Mean Temperature	2011-2040		2041-2070		2071-2100	
	RCP4.5	RCP8.5	RCP4.5	RCP8.5	RCP4.5	RCP8.5
absolute change (°C)	+1.0	+1.0	+1.7	+2.2	+2.3	+4.0
absolute value (°C)	*16.0*	*16.0*	*16.7*	*17.1*	*17.3*	*18.9*

Concerning the spatial distribution depicted in Figure 42, the observations pertain to the mean temperature range. In the reference period, this range spans from around 14°C in the more mountainous region of the pilot (northern part) and extends up to 17°C in the northern part. In the 2041-2070 timeframe, divergent outcomes are anticipated based on the different scenarios. Specifically, under both scenarios, a notable increase in mean temperature is expected throughout the entire pilot area. This increase will range from 16°C to nearly 19°C.

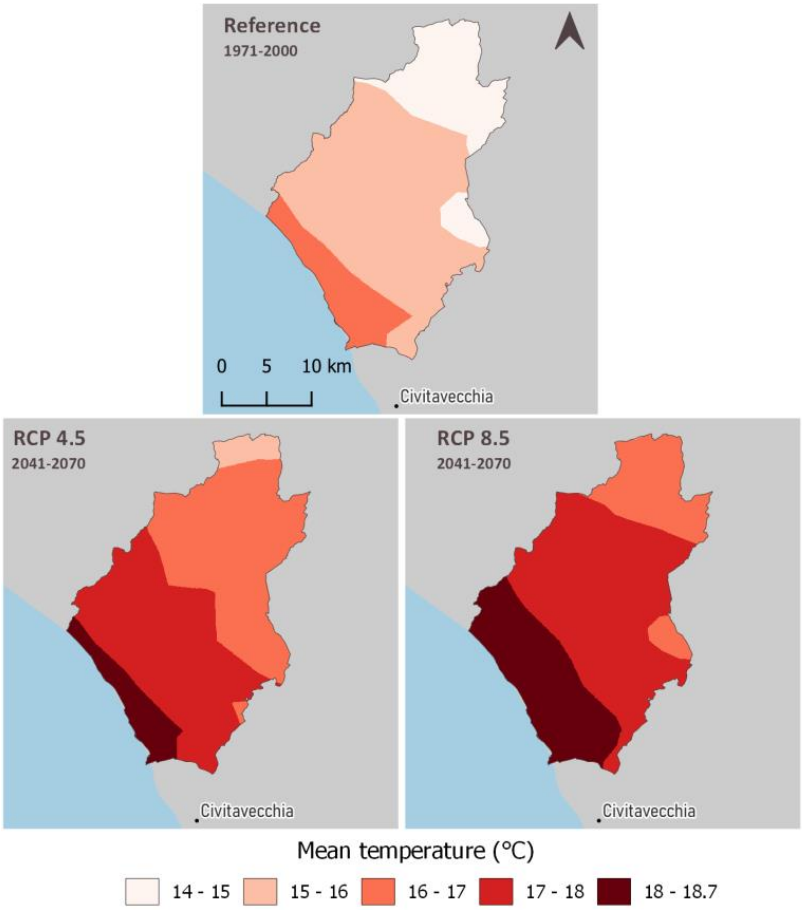

Figure 42: Spatial distribution of the mean annual temperature, for the reference period (top) and the future period 2041-2070, based on the RCP4.5 and RCP8.5 (bottom), Tarquinia pilot.

Total Precipitation

The projected mean annual total precipitation for the period 2011 to 2100 for the two scenarios at Tarquinia pilot area, is presented in the form of annual time series in Figure 43. As it may be seen, total precipitation tends to decrease over the 90-year period for both scenarios. According to the results for both RCPs, the trend for the period 2011-2100 shows a decrease of around 60 mm, with the values of RCP4.5 expected to be slightly higher. Additionally, the total precipitation for both scenarios is above 400 mm for almost all the 90-year period. The maximum value of annual actual evapotranspiration is around 1000 mm, and it is observed in the case of the RCP4.5.

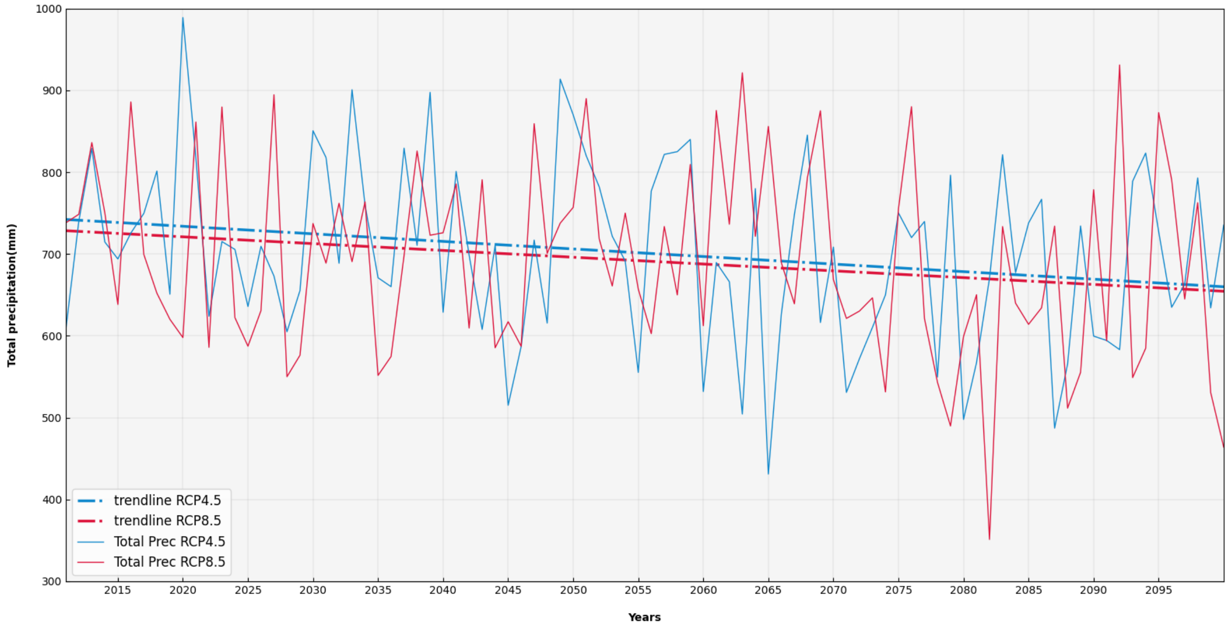

Figure 43: Ensemble mean of total precipitation of the period 2011-2100 for the RCP4.5 (blue line) and RCP8.5 (red line), Tarquinia pilot.

In Table 24, the projected average annual total precipitation for the examined future sub-periods is provided, divided in the dry and wet periods of the year. In the case of the Tarquinia pilot area, the selected dry months include the period from April to October while the selected wet period starts from November until March. It may be seen that the total precipitation is expected to show an increase for the period 2011-2070 for both scenarios, apart from RCP4.5 during the dry period of 2041-2070, where a decrease of 10 mm is expected. For the long-term period, 2071-2100, a decrease is expected for both scenarios and seasons, with a maximum reduction of -27 mm for RCP8.5 during the dry season.

Table 24: Ensemble mean of total precipitation for the future sub-periods based on the RCP4.5 and RCP8.5 divided in dry and wet period. Values are presented as absolute change from the reference period 1971-2000 and as absolute value in mm, Tarquinia pilot.

Total Precipitation		2011-2040		2041-2070		2071-2100	
		RCP4.5	RCP8.5	RCP4.5	RCP8.5	RCP4.5	RCP8.5
Dry period	absolute change (mm)	4	14	-10	20	-4	-27
	absolute value (mm)	*197*	*206*	*182*	*213*	*188*	*166*
Wet period	absolute change (mm)	57	15	37	35	-3	-6
	absolute value (mm)	*539*	*497*	*518*	*517*	*479*	*476*

Figure 44 displays the geospatial variation in total precipitation for the periods 1971-2000 and 2041-2070, encompassing both the dry and wet seasons of the year. In the Tarquinia pilot area, it is evident that during the wet period, an estimated 320 to 350 mm of precipitation per year occurs within the reference period. Additionally, the dry period experiences around 325 to 360 mm projected across the entire pilot area. Noticeable changes are observed across both RCPs in comparison to the reference period, affecting both dry and wet seasons. In the forthcoming period, an increase in precipitation is anticipated during the wet season for both scenarios. Moreover, under both scenarios, an increase in precipitation is expected for a significant extend of the Tarquinia pilot area during the dry season.

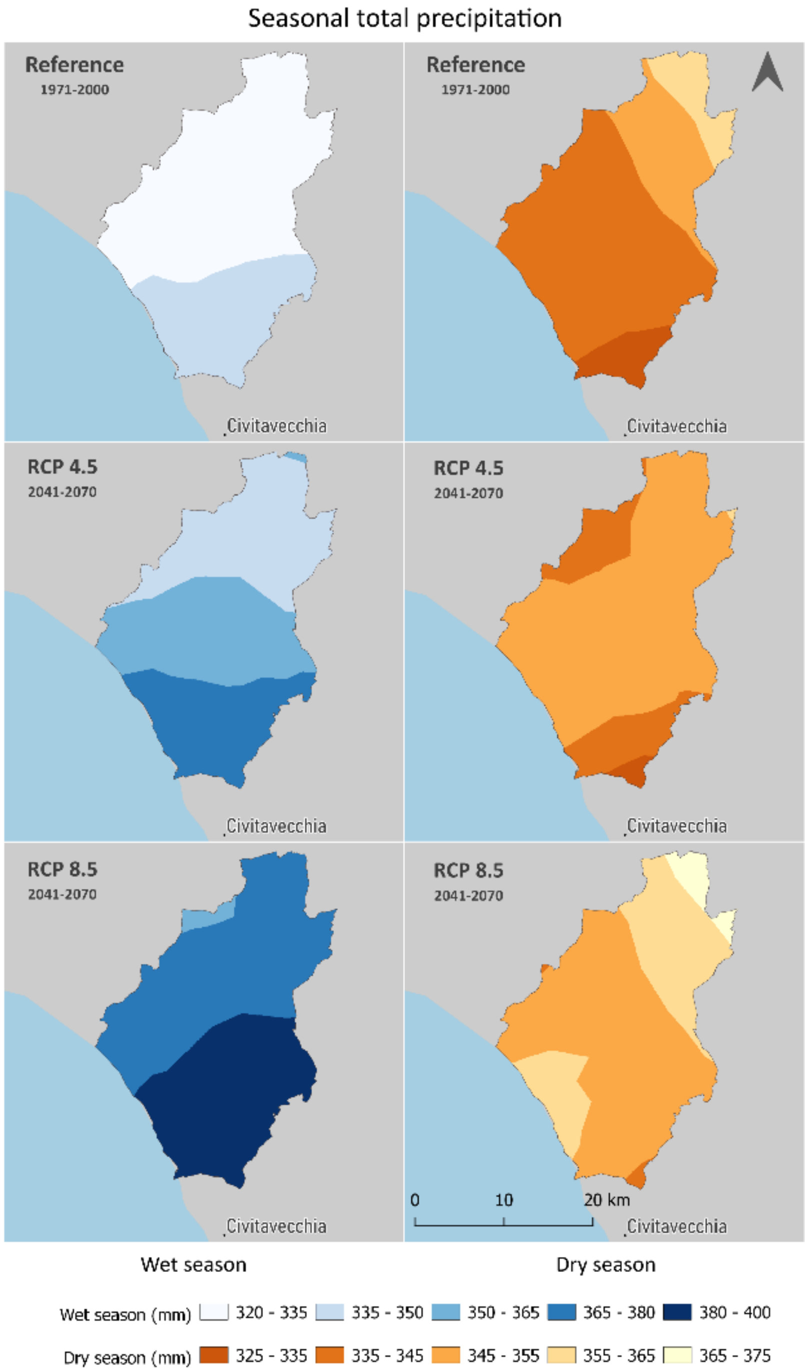

Figure 44: Spatial distribution of the mean total precipitation during the reference period (top) and the future period based on the RCP4.5 (middle) and RCP8.5 (bottom), for the dry (right) and the wet (left) periods, Tarquinia pilot.

Actual Evapotranspiration

The total annual actual evapotranspiration for the period 2011-2100 is presented in Figure 45 for both RCP4.5 and RCP8.5. As it may be observed, there is a tendency for the evapotranspiration to slightly decrease during the 90-year period based on RCP8.5 and to slightly increase in the case of RCP4.5. According to the results for the RCP4.5, the trend for the period 2011-2100 shows an increase of less than 10 mm, while for the

RCP8.5 the decrease is expected to be up to 10 mm. Additionally, the actual evapotranspiration for both scenarios is above 650 mm for almost all the 90-year period. The maximum value of annual actual evapotranspiration is around 780 mm, and it is observed in the case of the RCP8.5.

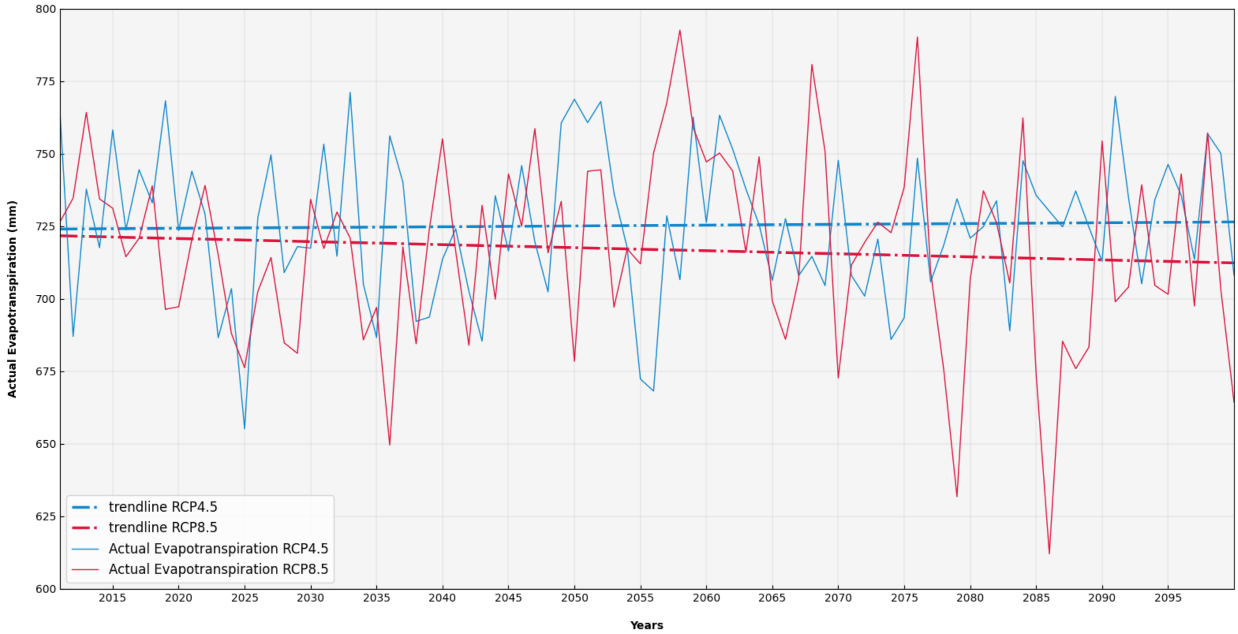

Figure 45: Ensemble mean of actual evapotranspiration of the period 2011-2100 for the RCP4.5 (blue line) and RCP8.5 (red line), Tarquinia pilot.

The expected total actual evapotranspiration for the examined future periods under RCP4.5 and RCP8.5 for the Tarquinia pilot area, is presented in Table 25. The values are presented as the absolute change from the reference period 1971-2000 and as absolute values. It may be observed that the absolute change of the evapotranspiration compared to the reference period is +12 mm for the near-term period, while in the long-term period is expected to increase even more, up to +21 mm on average for both scenarios. In addition, for the near-term period the value of the evapotranspiration is expected to be 719 mm and gradually decrease up to 717 mm on average in the long-term period for the two scenarios.

Table 25: Actual evapotranspiration per sub-period for RCP4.5 and RCP8.5. Values are presented as absolute change from the reference period 1971-2000 and as absolute value in mm, Tarquinia pilot.

Actual Evapotranspiration	2011-2040		2041-2070		2071-2100	
	RCP4.5	RCP8.5	RCP4.5	RCP8.5	RCP4.5	RCP8.5
absolute change (mm)	17	6	20	22	18	2
absolute value (mm)	*724*	*713*	*727*	*729*	*725*	*709*

Regarding the spatial distribution of the total actual evapotranspiration (Figure 46), it is observed that during the reference period the evapotranspiration ranges from 600 mm to 840 mm. As it is shown, during the future period, the actual evapotranspiration tends to increase similarly for the two scenarios, in the range from 600 up to 900 mm.

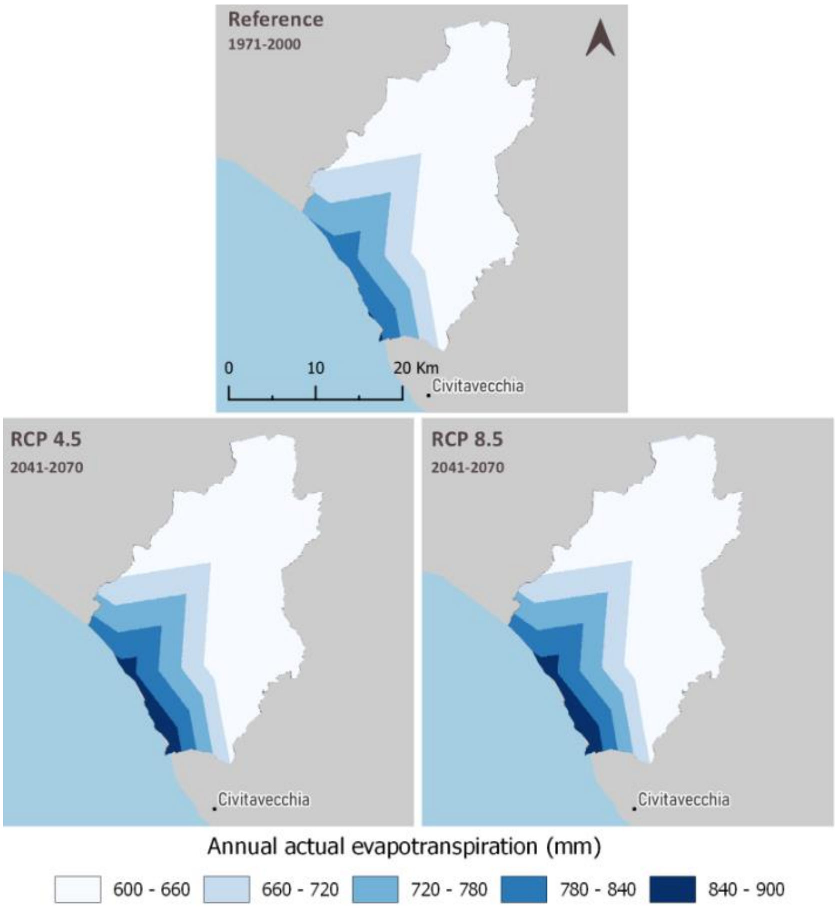

Figure 46: Spatial distribution of the mean annual actual evapotranspiration, for the reference period (top) and the future period 2041-2070, based on the RCP4.5 and RCP8.5 (bottom), Tarquinia pilot.

4.8 Discussion

In this section, the results of a published research article of *Cos J. et al.* (2022) comparing the climate projections of CMIP5 and CMIP6 scenarios (i.e., the RCPs and SSPs respectively) for the Mediterranean region are presented in order to explore their similarities and differences.

In particular, the paper studies the climatic variables of surface-air temperature and precipitation. The selected SSP scenarios were SSP1-2.6, SSP2-4.5, and SSP5-8.5 and compared with the respective RCP scenarios, i.e., the RCP2.6, RCP4.5, and RCP8.5. The results are presented as changes from the reference period 1986-2005, for the future periods 2041-2060 and 2081-2100. The results are also assessed at intra-annual seasonal level, to highlight potential variations between seasons.

As it can be seen in Figure 47 where the mean temperature changes are presented seasonally and annually for the high emissions scenario, the projections of CMIP5 (RCP8.5) and CMIP6 (SSP5-8.5) agree in general on the regions showing the highest amplified warming, with the latter projecting larger amplification magnitudes. Higher increase is also depicted for CMIP6 compared to CMIP5 during the winter season in the eastern part of the Mediterranean, where most of the LENSES pilots are located, while during the summer season, the increase is evident throughout the Mediterranean.

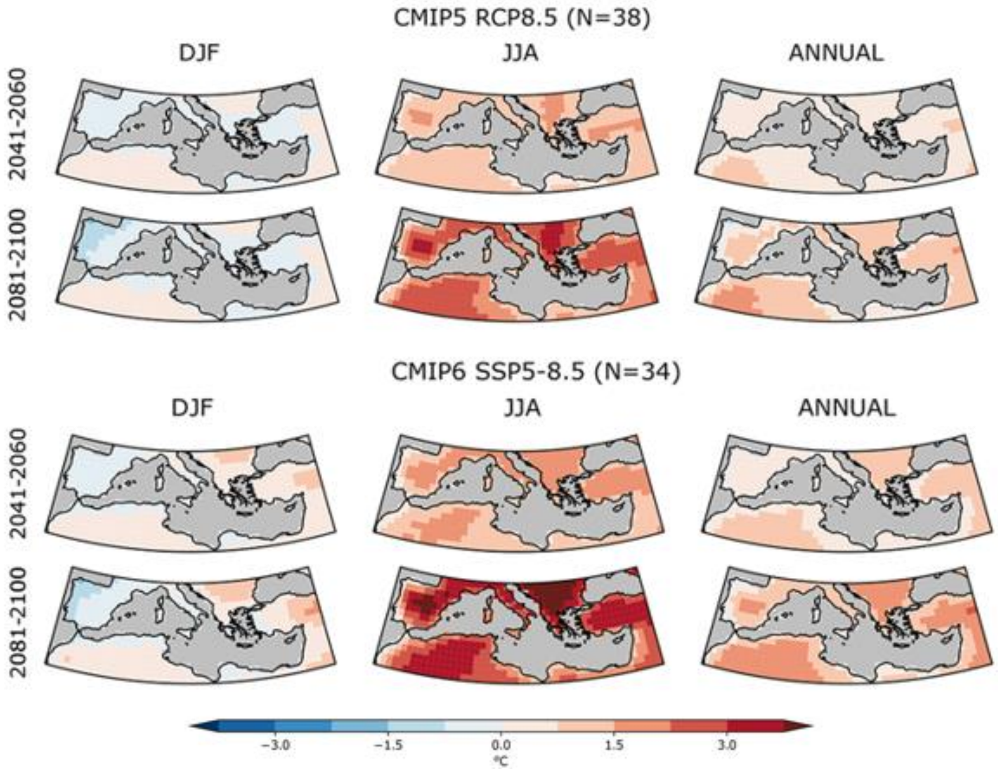

Figure 47: Temperature change in the Mediterranean region for the CMIP5 RCP8.5 (top) and the CMIP6 SSP-8.5 (bottom) scenarios, baseline period: 1986-2005. DJF: December–January–February, JJA: June– July–August. Source: Cos et al. (2022)

With respect to the projected changes in precipitation for the high emissions scenario, there is less disagreement between CMIP5 and CMIP6, with the latter showing larger precipitation decrease in some regions. The largest amplified drying shifts latitudinally from the south of the Mediterranean region in winter months to the north in summer months. The most affected region in summer is projected to be the south-west of the Iberian Peninsula, where the Doñana LENSES pilot is located. Both CMIPs agree on the precipitation patterns of change, but CMIP6 dries more and faster in the amplified drying regions, and projects larger precipitation increases in south-east of the domain. However, there is no increasing trend where the LENSES pilots, Hula and Deir Alla, are located and this is in agreement with our findings presented in the previous sections.

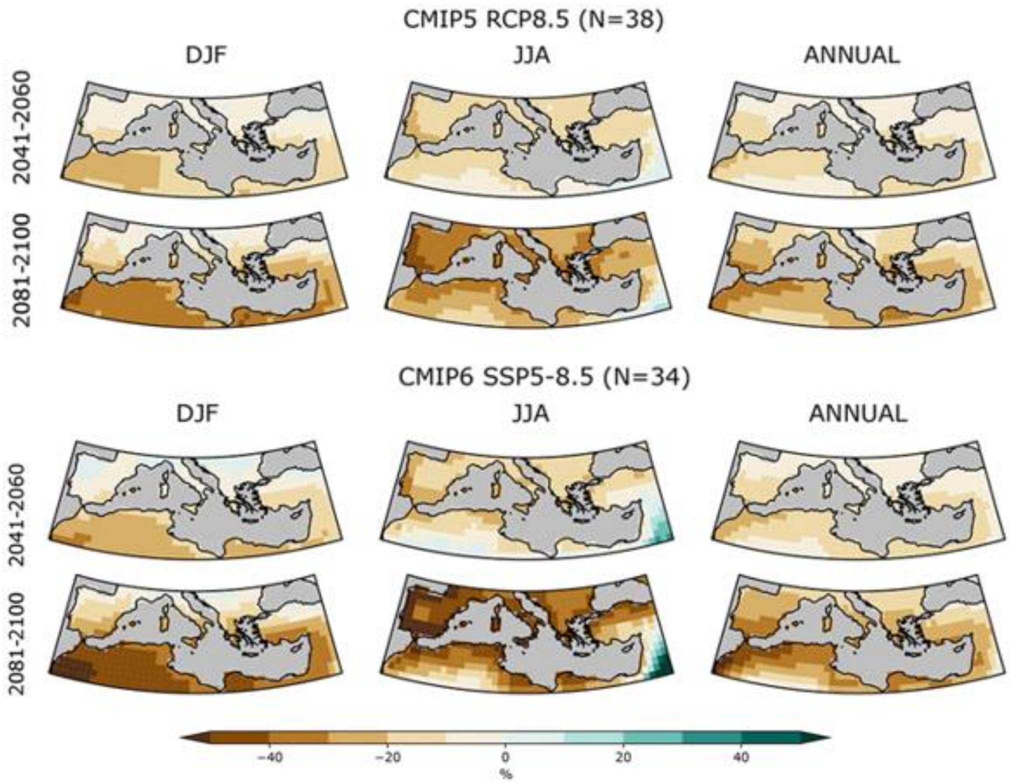

Figure 48: Precipitation change in the Mediterranean region for the CMIP5 RCP8.5 (top) and the CMIP6 SSP-8.5 (bottom) scenarios, baseline period: 1986-2005. DJF: December–January–February, JJA: June– July–August. Source: Cos et al. (2022)

Overall, it is observed that temperature and precipitation differences increase in magnitude from the mid- to the long term, while the spatial pattern remains the same, according to the high emission scenario (RCP8.5, SSP5-8.5). The low emission scenario (RCP2.6, SSP1-2.6), instead, shows a hotspot weakening from the mid- to the long term as the warming amplification is reduced and the precipitation differences are maintained. The intermediate emission scenario (RCP4.5, SSP2-4.5) lies in between, a little closer though to the low emission scenario.

As it may be seen in Figure 49, the difference in temperature between CMIP5 and CMIP6 in the intermediate emission scenario is smaller compared to the high emission scenario and is more pronounced again in the long-term period.

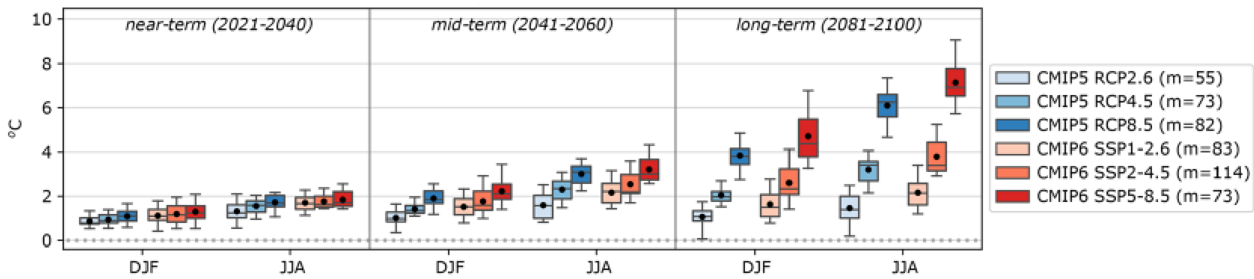

Figure 49: Temperature: CMIP5 and CMIP6 JJA and DJF projections for the near-, mid- and long-term periods with respect to the baseline period considering the 2.6, 4.5 and 8.5 W m−2 RCP and SSP radiative forcing scenarios. The black horizontal line in the boxes represents the median and the black dot is the mean. The number of members in the boxplot distributions is represented by m in the legend.

Regarding precipitation, as it is depicted in Figure 50, for the near-term period the projections are close between the scenarios for both CMIP5 and CMIP6 datasets. During the mid-term period, it may be seen that although the results for the two phases of the CMIP are similar, there is a slight overestimation in the case of CMIP6, compared to CMIP5 projections. Lastly, during the long-term period the results are very similar for both the winter and summer seasons.

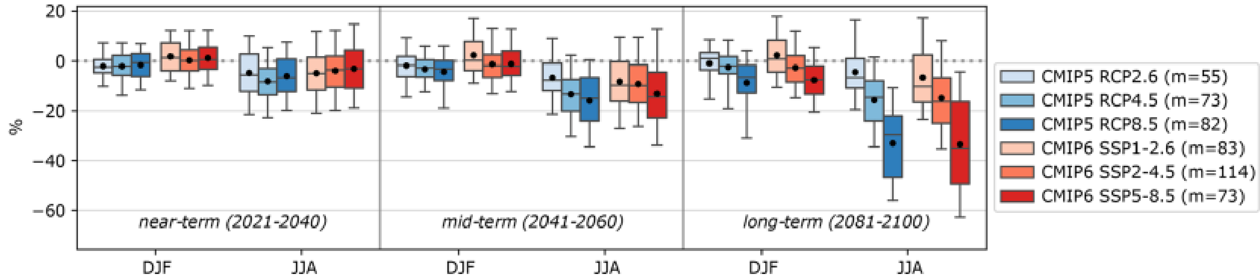

Figure 50: Precipitation: CMIP5 and CMIP6 JJA and DJF projections for the near-, mid- and long-term periods with respect to the baseline period considering the 2.6, 4.5 and 8.5 W m−2 RCP and SSP radiative forcing scenarios. The black horizontal line in the boxes represents the median and the black dot is the mean. The number of members in the boxplot distributions is represented by m in the legend.

To conclude with, we have to bear in mind these differences in climate projections when trying to translate the CMIP5 projections presented in this deliverable into the CMIP6.

5 Climate Risk Assessment for the LENSES pilots

In this section, the results of the climate risk assessment are provided for the pilot areas of the LENSES project. Specifically, the section is broken down into individual sub-sections for each pilot area, where in each sub-section are presented:

- The results of the climate-related hazard indicators in the form of tables and maps.
- The results of the exposure indicators in the form of tables.
- The results of the vulnerability indicators in the form of tables.
- The results of the adaptive capacity in the form of tables.
- The results of the overall climate risk assessment in the form of tables.

5.1 Pinios River Basin Hydrologic Observatory (Greece)

In this section the results of the hazard, exposure and vulnerability assessment, as well as of the adaptive capacity and the overall climate risk assessment are provided, for the Pinios River Basin Hydrologic Observatory (Greece).

5.1.1 Climate Related Hazard Indicators

In the following paragraphs, the results for the hazard indicators are presented, for the food, water, and ecosystems sectors.

Actual Aridity

The relative change (%) of the actual aridity in the future compared to the reference period for both scenarios, is presented in Table 26. It can be observed that there is an increase of aridity for all the three future sub-periods for both scenarios. The highest increase (+61%) is expected for the long-term period and the lowest increase (+9%) for the short-term period both in case of RCP8.5.

Table 26: Relative change (%) of the mean annual aridity (actual evapotranspiration/precipitation), for the future sub-periods based on the RCP4.5 and RCP8.5, compared to the reference period, Pinios pilot.

Actual Aridity	2011-2040		2041-2070		2071-2100	
	RCP4.5	RCP8.5	RCP4.5	RCP8.5	RCP4.5	RCP8.5
relative change (%)	32	9	51	54	37	61

Biologically Effective Degree Days over 10-days (BEDD)

The projected relative change (%) of the BEDD over 10-days, for the future sub-periods based on the RCP4.5 and RCP8.5, compared to the reference period, is summarized in Table 27. In general, an increase of the BEDD indicator is expected in the future for both scenarios. In particular, it may be concluded that for the short-term and mid-term period, there is no significant difference between the scenarios, with an average 7.5% and 17.5% increase from the reference period respectively. For the long-term period the increase is more noticeable, up to 19% for RCP4.5 and 35% for RCP8.5.

Table 27: Relative change (%) of the Biologically Effective Degree Days over 10-days, for the future sub-periods based on the RCP4.5 and RCP8.5, compared to the reference period, Pinios pilot.

BEDD	2011-2040		2041-2070		2071-2100	
	RCP4.5	RCP8.5	RCP4.5	RCP8.5	RCP4.5	RCP8.5
relative change (%)	6	9	14	21	19	35

Fire Danger

The relative change (%) of the FWI in the future compared to the reference period for both scenarios, is shown in Table 28. It can be observed that there is an increase of FWI in the future for both scenarios. Specifically, for the short-term period the increase from the reference period is 7% on average while in the long-term period this increasing trend reaches up to 16% for RCP4.5 and to 33% for RCP8.5.

Table 28: Relative change (%) of the FWI, for the future sub-periods based on the RCP4.5 and RCP8.5, compared to the reference period, Pinios pilot.

Fire Weather Index	2011-2040		2041-2070		2071-2100	
	RCP4.5	RCP8.5	RCP4.5	RCP8.5	RCP4.5	RCP8.5
relative change (%)	6	8	11	19	16	33

Frost days

The relative change (%) of the frost days indicator in the future compared to the reference period for both scenarios, is shown in Table 29. It can be observed that there is a decrease in the future for both scenarios. Specifically, for the short-term period the increase from the reference period is 41.5% on average while in the long-term period this decreasing trend reaches up to 74% for RCP4.5 and to 95% for RCP8.5.

Table 29: Relative change (%) of the Frost Days, for the future sub-periods based on the RCP4.5 and RCP8.5, compared to the reference period, Pinios pilot.

Frost days	2011-2040		2041-2070		2071-2100	
	RCP4.5	RCP8.5	RCP4.5	RCP8.5	RCP4.5	RCP8.5
relative change (%)	-44	-39	-61	-71	-74	-95

Heat Stress days over 30°C

The relative change (%) of the projected number of heat stress days (>30°C) in the future, is summarized in Table 30. As it can be observed, the difference between the two scenarios is noticeable, with the RCP8.5 presenting the highest increase. Specifically, for the near-term period (2011-2040) an increase of 43% is projected on average for the two scenarios. For the mid-term period (2041-2070), an increase of 77% is projected based on RCP4.5 and 109% for the RCP8.5. Finally, for the long-term period (2071-2090), the increase is expected to reach 86% for the RCP4.5 and 218% for the RCP8.5.

Table 30: Relative change (%) of the Heat Stress days over 30°C, for the future sub-periods based on the RCP4.5 and RCP8.5, compared to the reference period, Pinios pilot.

Heat Stress days over 30°C	2011-2040		2041-2070		2071-2100	
	RCP4.5	RCP8.5	RCP4.5	RCP8.5	RCP4.5	RCP8.5
relative change (%)	41	45	77	109	86	218

Soil Moisture

The projected relative change (%) of soil moisture in the future based on the RCP4.5 and RCP8.5, is summarized in Table 31. In general, a decreasing trend is observed under both scenarios. In particular, it may be concluded that for the short-term period, there is no significant difference in the projected decrease between the scenarios (around -5%). For the mid-term period there is a reduction of 6.5% on average for the two scenarios, while for the long-term period the reduction is similar to the mid-term for the RCP4.5 and higher for the RCP8.5 (-8%).

Table 31: Relative change (%) of soil moisture in the future compared to the reference period, based on the RCP4.5 and RCP8.5, Pinios pilot.

Soil Moisture	2011-2040		2041-2070		2071-2100	
	RCP4.5	RCP8.5	RCP4.5	RCP8.5	RCP4.5	RCP8.5
relative change (%)	-8	-2	-8	-5	-5	-11

Following, the hazard indicators are presented through maps for the reference period (1971-2000) and the future period (2041-2070), under the RCP4.5 and RCP8.5.

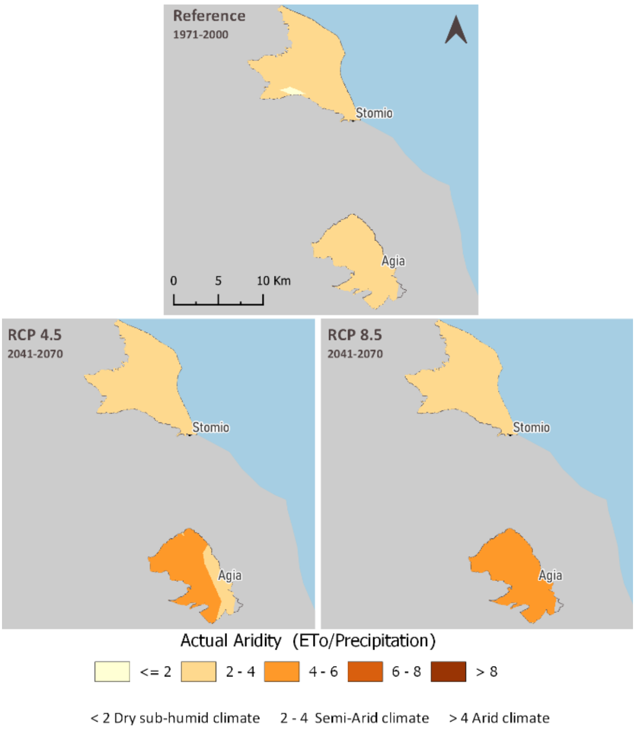

Figure 51: Spatial distribution of actual aridity, for the reference period (top) and the future period (2041-2070) based on the RCP4.5 and RCP8.5 (bottom)

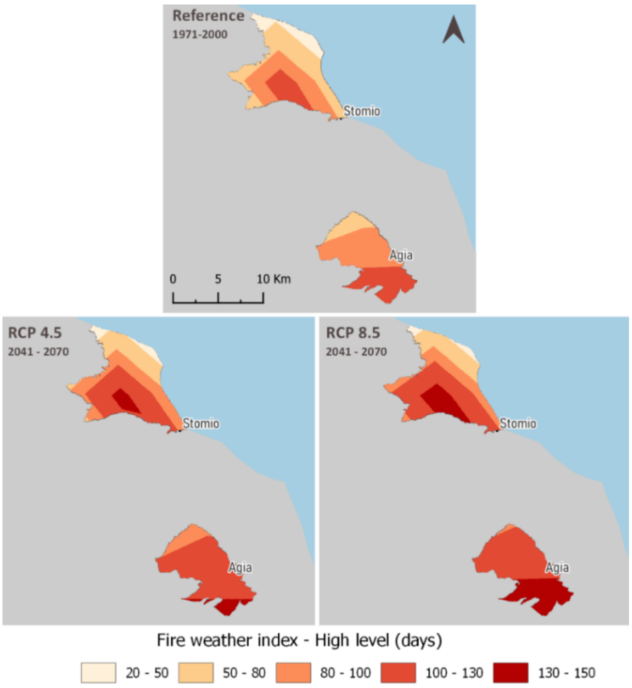

Figure 52: Spatial distribution of the FWI, for the reference period (top) and the future period (bottom)based on the RCP4.5 and RCP8.5

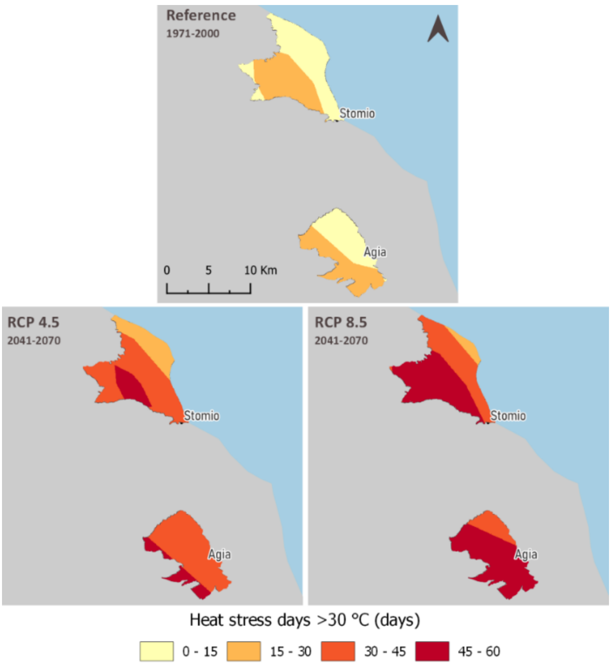

Figure 53: Spatial distribution of the mean annual number of days when maximum daily temperature is > 35°C, for the reference period (top) and the future period (2041-2070) based on the RCP4.5 and RCP8.5 (bottom)

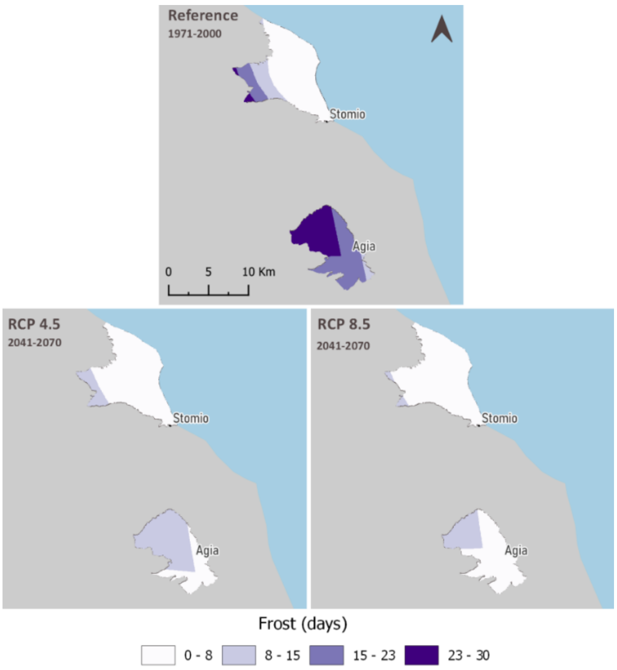

Figure 54: Spatial distribution of frost days, for the reference period (top) and the future period (2041-2070) based on the RCP4.5 and RCP8.5 (bottom)

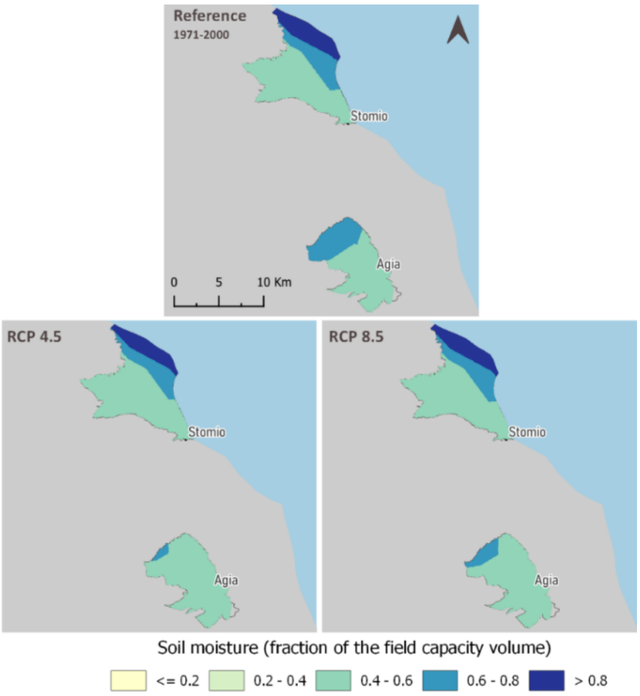

Figure 55: Spatial distribution of soil moisture, for the reference period (top) and the future period (2041-2070) based on the RCP4.5 and RCP8.5 (bottom)

5.1.2 Exposure Indicators

In the following paragraphs, the results for the exposure indicators are presented, for the food, water, and ecosystems sectors.

Share of area cultivated with crops

The share of areas cultivated with crops in each part of the Pinios area, is presented in Table 32. As it can be observed, the cultivated area is significant (51%) at the Delta region, while at the Agia region the cultivated area is much less (25%). Therefore, the exposure of agriculture is estimated to be high for the Delta region and medium-high for the Agia region.

Table 32: Share of crops under study in Pinios pilot area.

Pinios pilot	Total area (hectares)	Cultivated area (hectares)	Share of area cultivated with crops
Delta	7,420	3,749	51%
Agia	5,250	1,311	25%

Share of area covered with forests and natural areas

The share of natural areas (land covered by forests, natural grasslands, shrubs, marshes etc.) compared to the total area of the pilot is presented in Table 33. As it can be observed, the Delta region where the agricultural activity is more intensive, the share is 17%, while the Agia region the share of natural areas is

56%. Therefore, the ecosystems are considered to be moderately exposed in the Delt region and highly exposed in the Agia region.

Table 33: Share of natural areas in Pinios pilot area.

Pinios pilot	Area (hectares)	Natural area (hectares)	Share of natural area
Delta	7,420	1,227	17%
Agia	5,250	2,955	56%

5.1.3 Vulnerability Indicators

In the following paragraphs, the results for the vulnerability indicators are presented, for the food, water, and ecosystems sectors.

Water Exploitation Index

The water exploitation index (WEI) of the River Basin District of Thessaly which is located in the Pinios pilot, is presented in Table 34. Specifically, the WEI is estimated to be 40% which is above the threshold under which water stress can begin to be a limiting factor on economic development for the region. Thus, the vulnerability related to this indicator is considered to be medium-high.

Table 34: Water vulnerability index expressed as Water Exploitation Index, Thessaly River Basin District.

River Basin District	Water Exploitation Index
Thessaly	40%

Share of agricultural water consumption

The share of agricultural water consumption in River Basin District of Thessaly is shown in Table 35. Specifically, the share of agricultural water consumption is very high, up to 93%, therefore a potential reduction in water availability due to climate change, would be critical for the agricultural sector. Thus, the vulnerability related to this indicator is considered to be high.

Table 35: Water vulnerability index expressed as share of agricultural water consumption, Thessaly River Basin District.

River Basin District	Share of agricultural water consumption
Thessaly	93%

Agricultural Income

The agricultural income of Thessaly region where the Pinios pilot is located, compared to the average national agricultural income of Greece, is presented in Table 36. It is observed that the region of Thessaly, has 210% higher agricultural income compared to the national average. This indicates a high dependency of the country to the agricultural income of the region. Thus, the vulnerability related to this indicator is considered to be high.

Table 36: Food vulnerability index expressed as agriculture income, Thessaly Region.

	Million Euro	% of national average
National Average	596	100%
Thessaly Region	1250	210%

Share of protected areas

As it may be seen in Table 37, the share of protected areas over the total area of each region of the pilot, is estimated to be 56% in the Delta region where agricultural activity is more intensive and 79% in the Agia region of the pilot. Therefore, the share of protected areas is considered medium-high for the Delta and high for the Agia region.

Table 37: Share of protected areas, Pinios pilot area.

Pinios pilot	Total area (hectares)	Protected area (hectares)	Share of protected area
Delta	7,420	4,168	56%
Agia	5,250	4,160	79%

5.1.4 Adaptive capacity

In this section, the results of the assessment of the adaptive capacity of the Pinios pilot are presented. Specifically, the results refer to the assessment of the GDP index for the pilot at national level.

The economic capacity expressed as the GDP of the country in relation to the EU average is presented in the table that follows. As it can be observed, the GDP of Greece is 16,570 Euros per capita which is close to half of the EU average (54%), thus reflecting a low-medium economic capacity of the country and subsequently of the Pinios pilot.

Table 38: Relative Economic capacity of the Pinios pilot.

Pinios pilot	GDP per capita (Euro)	in % of EU average
EU average (27 countries)	30,632	100%
Greece	16,570	54%

5.1.5 Overall Risk

In this section, the results of the climate risk assessment for the food and ecosystems Nexus systems of the Pinios national park area are presented for the period 2041-2070, based on the RCP4.5 and RCP8.5. The results are presented separately for the Delta and Agia region of the Pinios pilot. Specifically, the overall risk is presented both qualitatively and quantitatively per risk component at indicator level.

As it can be observed in Table 39, the estimated overall risk for the food sector is considered to be "Medium-High". This is a result of a "Medium" to "Medium-High" hazard, in combination with a "High" vulnerability, and a "High" and "Medium-High" exposure.

Table 39: Qualitative climate risk assessment per risk component of the food sector for the period 2041-2070, Pinios pilot area.

Indicators	Delta		Agia	
	RCP 4.5	RCP 8.5	RCP 4.5	RCP 8.5
Heat stress >35 °C	Medium	Medium-High	Medium-High	High
Frost	Low	Low	Low-Medium	Low
BEDD	Low	Low-Medium	Low	Low-Medium
Actual aridity	Medium-High	Medium-High	Medium-High	Medium-High
Fire weather index WFI>30	Medium	Medium-High	Medium-High	Medium-High
Soil moisture	Medium	Medium	Medium	Medium
Hazard composite indicator	**Medium**	**Medium**	**Medium-High**	**Medium-High**
Exposure indicator	**Medium-High**	**Medium-High**	**High**	**High**
Agricultural income	High	High	High	High
Water exploitation	Medium-High	Medium-High	Medium-High	Medium-High
Agricultural water consumption	High	High	High	High
Vulnerability composite indicator	**High**	**High**	**High**	**High**
Food System Risk	**Medium-High**	**Medium-High**	**Medium-High**	**Medium-High**

The detailed results of the climate risk assessment for the food sector are presented quantitatively at normalized scale [0, 5] in Table 40. The negative values of the hazard indicators are assigned to reflect a beneficial effect and thus compensate risk.

Table 40: Quantitative climate risk assessment per risk component of the food sector for the period 2041-2070, Pinios pilot area.

Indicators	Delta		Agia	
	Delta	Agia	Delta	RCP 8.5
Heat stress >35 °C	3.00	3.67	3.33	4.08
Frost	0.50	0.33	1.50	1.00
BEDD	-0.93	-1.41	-0.93	-1.41
Actual aridity	3.23	3.20	3.80	3.87
Fire weather index WFI>30	2.94	3.13	3.56	3.88
Soil moisture	2.56	2.44	3.00	2.88
Hazard composite indicator	**2.79**	**2.97**	**3.27**	**3.51**
Exposure indicator	**3.25**	**3.25**	**4.26**	**4.26**
Agricultural income	5.00	5.00	5.00	5.00
Water exploitation	4.00	4.00	4.00	4.00
Agricultural water consumption	4.82	4.82	4.82	4.82
Vulnerability composite indicator	**4.61**	**4.61**	**4.61**	**4.61**
Food System Risk	**3.24**	**3.35**	**3.73**	**3.88**

As it can be observed in Table 41for the ecosystem sector, the risk levels are the result of a “Medium” to “High” range of exposure, in combination with a “Medium-High” to “High” vulnerability, for both regions, while the hazard indicator is considered “Medium” to “Medium-High” for the Delta region and “Medium-

High" for the Agia region of the Pinios pilot. Thus, the overall risk for the ecosystem sector is considered "Medium-High" at scenario RCP4.5 and "High" at RCP8.5 for both regions of the pilot.

Table 41: Qualitative climate risk assessment per risk component of the ecosystem sector for the period 2041-2070, Pinios pilot area.

Indicators	Delta		Agia	
	RCP 4.5	RCP 8.5	RCP 4.5	RCP 8.5
Heat stress >35 °C	Medium-High	Medium-High	Medium-High	High
Actual aridity	Medium-High	Medium-High	Medium-High	Medium-High
Fire weather index WFI>30	Medium	Medium-High	Medium-High	Medium-High
Soil moisture	Medium	Medium	Medium-High	Medium
Hazard composite indicator	**Medium**	**Medium-High**	**Medium-High**	**Medium-High**
Exposure indicator	**Medium**	**Medium**	**High**	**High**
Vulnerability indicator	**Medium-High**	**Medium-High**	**High**	**High**
Ecosystems Risk	**Medium-High**	**High**	**Medium-High**	**High**

The detailed results of the climate risk assessment for the ecosystem sector are presented quantitatively at normalized scale [0, 5] in Table 42.

Table 42: Quantitative climate risk assessment per risk component of the ecosystem sector for the period 2041-2070, Pinios pilot area.

Indicators	Delta		Agia	
	RCP 4.5	RCP 8.5	RCP 4.5	RCP 8.5
Heat stress >35 °C	3.00	3.67	3.33	4.08
Actual aridity	3.23	3.20	3.80	3.87
Fire weather index WFI>30	2.94	3.13	3.56	3.88
Soil moisture	2.56	2.44	3.00	2.88
Hazard composite indicator	**2.90**	**3.04**	**3.40**	**3.62**
Exposure Indicator	**2.65**	**2.65**	**4.41**	**4.41**
Vulnerability Indicator	**3.19**	**3.19**	**4.86**	**4.86**
Ecosystems Risk	**3.47**	**4.10**	**3.45**	**4.33**

Following, the results of the climate risk assessment for the period 2041-2070 are summarized for Ecosystem-Food sectors.

As it may be seen in Table 43 where the results for the Pinios pilot are presented, the level of risk for Food sector is expected to be at "Medium-High" level for both RCP scenarios at Delta and Agia region of the pilot. Additionally, for the ecosystem sector and according to the RCP4.5 the level of risk is expected to be "Medium-High" for both regions of the pilot, while the level of risk under RCP8.5 increase to the "High" level. This is mostly explained by the increase of temperature under RCP8.5 and subsequently to the increase of Heat Stress indicator for Agia region and Fire Weather Index for Delta region.

Furthermore, the adaptive capacity is characterized as "Low-Medium" for the pilot, which is not considered sufficient to offset the expected risk for the WEF Nexus sectors.

Table 43: Overall risk of the WEF Nexus sectors, Pinios pilot.

	Delta		Agia		Adaptive Capacity
	RCP 4.5	RCP 8.5	RCP 4.5	RCP 8.5	
Food	Medium-High	Medium-High	Medium-High	Medium-High	Low-Medium
Ecosystem	Medium-High	High	Medium-High	High	

5.2 Doñana national park area (Spain)

In this section the results of the hazard, exposure and vulnerability assessment, as well as of the adaptive capacity and the overall climate risk assessment are provided, for the Doñana national park area (Spain).

5.2.1 Climate Related Hazard Indicators

In the following paragraphs, the results for the hazard indicators are presented, for the food, water, and ecosystems sectors.

Actual Aridity

The relative change (%) of the actual aridity in the future compared to the reference period for both scenarios, is presented in Table 44. It can be observed that there is a decrease of aridity for all the three future sub-periods for the intermediate scenario RCP4.5 compared to the reference period, while for the RCP8.5, an increase is expected. The highest decrease (-13%) is expected for the short-term period and the highest increase (12%) for the mid-term period.

Table 44: Relative change (%) of the mean annual aridity (actual evapotranspiration/precipitation), for the future sub-periods based on the RCP4.5 and RCP8.5, compared to the reference period, Doñana pilot.

Actual Aridity	2011-2040		2041-2070		2071-2100	
	RCP4.5	RCP8.5	RCP4.5	RCP8.5	RCP4.5	RCP8.5
relative change (%)	-13	2	-9	12	-8	5

Biologically Effective Degree Days over 10-days (BEDD)

The projected relative change (%) of the BEDD indicator over 10-days, for the future sub-periods based on the RCP4.5 and RCP8.5, compared to the reference period, is summarized in Table 45. In general, an increase of the BEDD indicator is expected in the future for both scenarios, which is positive for crop growth. In particular, it may be concluded that for the short-term and mid-term period, there is no significant difference between the scenarios, with an average 3.5% and 9% increase from the reference period respectively. The highest increase (20%) is expected for the long-term period under the RCP8.5.

Table 45: Relative change (%) of the Biologically Effective Degree Days over 10-days, for the future sub-periods based on the RCP4.5 and RCP8.5, compared to the reference period, Doñana pilot.

BEDD	2011-2040		2041-2070		2071-2100	
	RCP4.5	RCP8.5	RCP4.5	RCP8.5	RCP4.5	RCP8.5

This project is part of the PRIMA programme supported by the European Union.
GA n° [2041] [LENSES] [Call 2020 Section 1 Nexus IA]

relative change (%)	4	3	8	10	10	20

Fire Weather Index

The relative change (%) of the FWI in the future compared to the reference period for both scenarios, is shown in Table 46. It can be observed that there is an increase of FWI in the future for both scenarios. Specifically, for the short-term period the increase from the reference period is 8% on average, while in the long-term period this increasing trend reaches up to 16% for RCP4.5 and to 30% for RCP8.5.

Table 46: Relative change (%) of the FWI, for the future sub-periods based on the RCP4.5 and RCP8.5, compared to the reference period, Doñana pilot.

Fire Weather Index	2011-2040		2041-2070		2071-2100	
	RCP4.5	RCP8.5	RCP4.5	RCP8.5	RCP4.5	RCP8.5
relative change (%)	6	10	13	19	16	30

Heat Stress days over 35°C

The relative change (%) of the projected number of heat stress days (>35°C) in the future, is summarized in Table 47. As it can be observed, the difference between the two scenarios for all three future periods is noticeable, with the RCP8.5 presenting the highest increase. Specifically, for the near-term period an increase of 58% is projected for the RCP4.5, while the respective change for the RCP8.5 is 74%. For the mid-term period, an increase of 100% is projected based on RCP4.5 and 153% for the RCP8.5. Finally, for the long-term period, the increase is expected to reach 132% for the RCP4.5 and 258% for the RCP8.5.

Table 47: Relative change (%) of the Heat Stress days over 35°C, for the future sub-periods based on the RCP4.5 and RCP8.5, compared to the reference period, Doñana pilot.

Heat Stress days over 35°C	2011-2040		2041-2070		2071-2100	
	RCP4.5	RCP8.5	RCP4.5	RCP8.5	RCP4.5	RCP8.5
relative change (%)	58	74	100	153	132	258

River Discharge

The projected relative change (%) of river discharge in the future based on the RCP4.5 and RCP8.5, is summarized in Table 48. It may be noticed that for the short-term period, there is a slight increase of 6% for the RCP4.5 and a 9% decrease for the RCP8.5. For both mid-term and long-term periods, the trend is decreasing under both scenarios. Specifically, the decrease is higher for the RCP8.5(-20% to -39%), while for the RCP4.5 the decreasing trend is lower (-3% to -12%).

Table 48: Relative change (%) of river discharge in the future compared to the reference period, based on the RCP4.5 and RCP8.5, Doñana pilot.

River Discharge	2011-2040		2041-2070		2071-2100	
	RCP4.5	RCP8.5	RCP4.5	RCP8.5	RCP4.5	RCP8.5
relative change (%)	6	-9	-3	-20	-12	-39

Soil Moisture

The projected relative change (%) of soil moisture in the future based on the RCP4.5 and RCP8.5, is summarized in Table 49. In general, a decreasing trend is observed under both scenarios. In particular, it may be concluded that for the short-term period, there is no significant difference in the projected decrease between the scenarios (around -10%).For the mid-term period there is a reduction of 25% on average for the two scenarios, while for the long-term period the reduction is similar to the mid-term for the RCP4.5 and higher for the RCP8.5 (-39%).

Table 49: Relative change (%) of soil moisture in the future compared to the reference period, based on the RCP4.5 and RCP8.5, Doñana pilot.

Soil Moisture	2011-2040		2041-2070		2071-2100	
	RCP4.5	RCP8.5	RCP4.5	RCP8.5	RCP4.5	RCP8.5
relative change (%)	-10	-11	-23	-28	-25	-39

Following, the hazard indicators are presented through maps for the reference period (1971-2000) and the future period (2041-2070), under the RCP4.5 and RCP8.5.

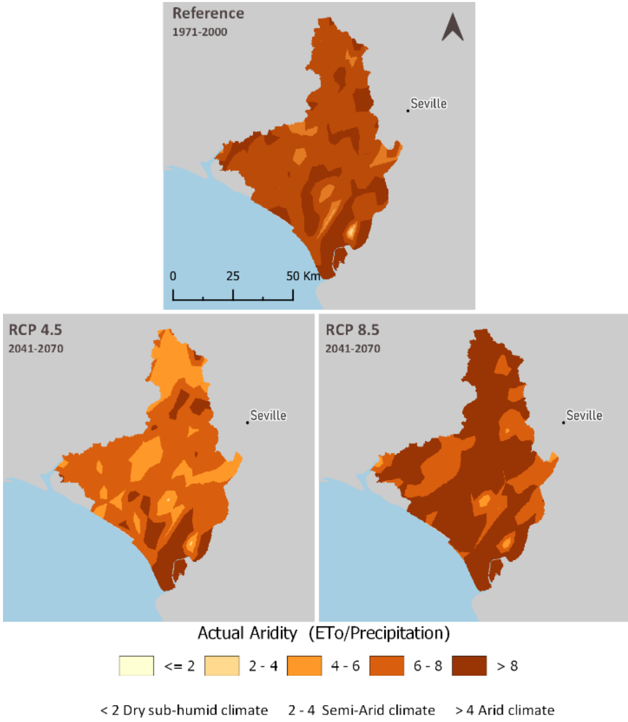

Figure 56: Spatial distribution of actual aridity, for the reference period (top) and the future period (2041-2070) based on the RCP4.5 and RCP8.5 (bottom)

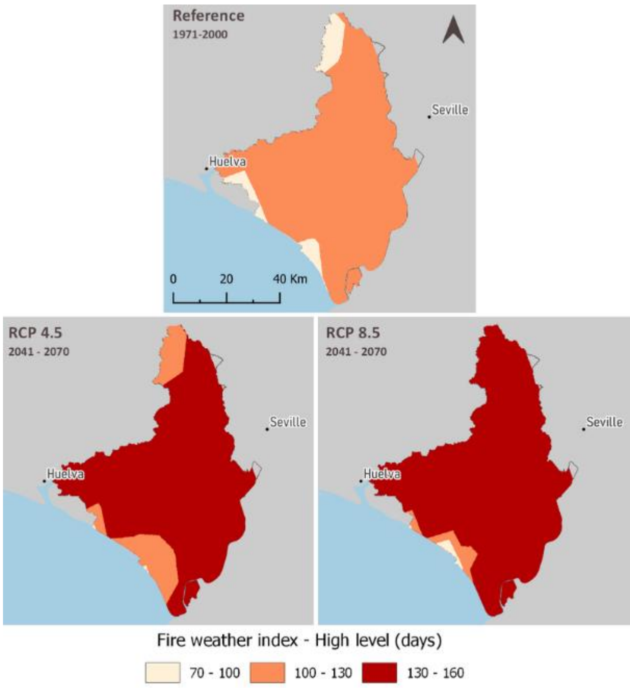

Figure 57: Spatial distribution of the FWI, for the reference period (top) and the future period (bottom)based on the RCP4.5 and RCP8.5

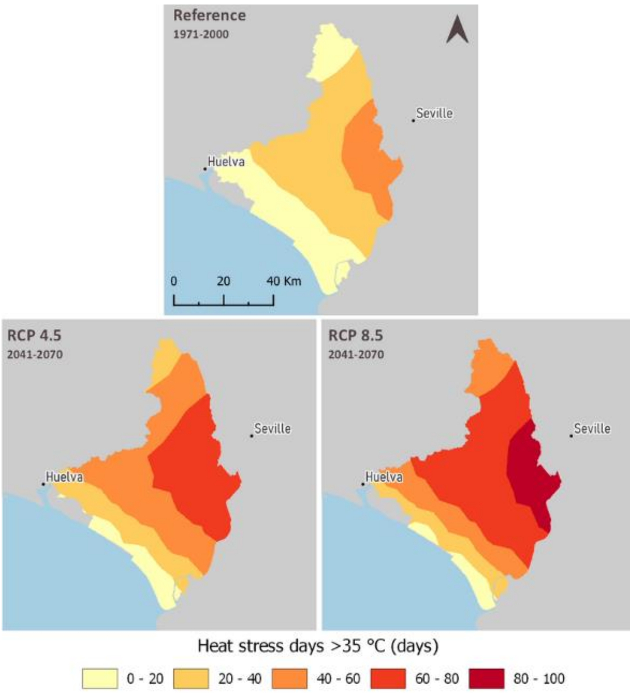

Figure 58: Spatial distribution of the mean annual number of days when maximum daily temperature is > 35°C, for the reference period (top) and the future period (2041-2070) based on the RCP4.5 and RCP8.5 (bottom)

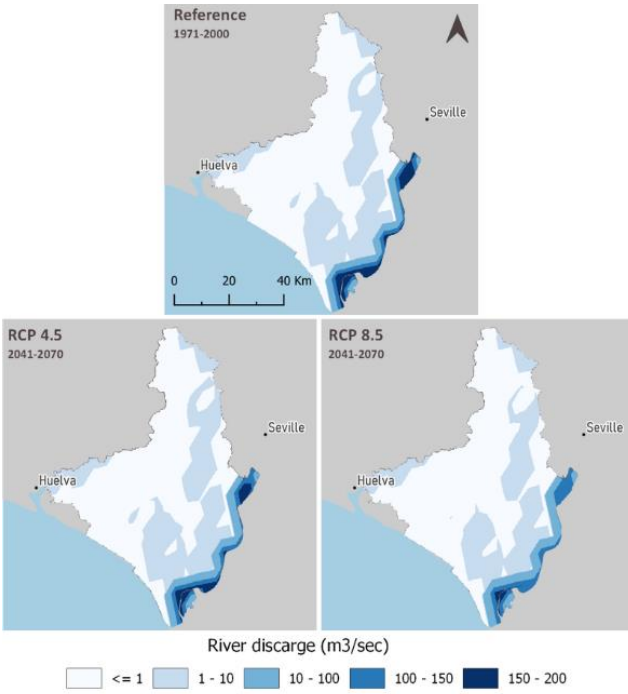

Figure 59: Spatial distribution of river discharge, for the reference period (top) and the future period (2041-2070) based on the RCP4.5 and RCP8.5 (bottom)

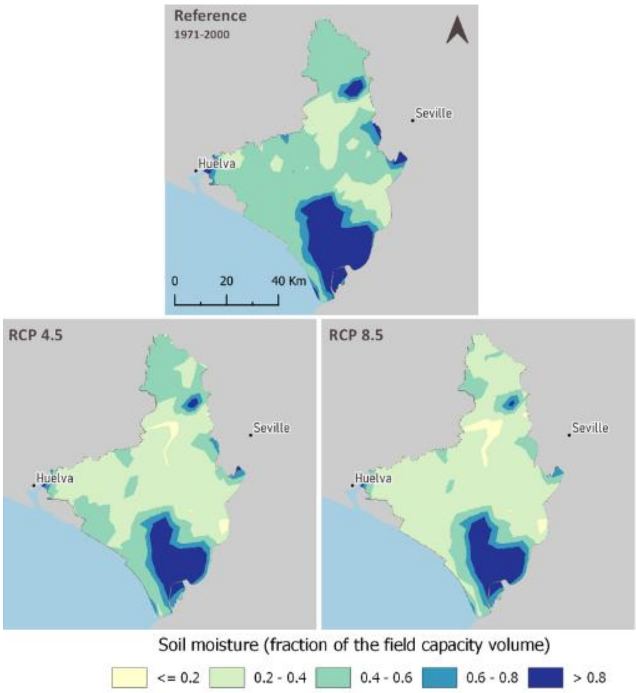

Figure 60: Spatial distribution of soil moisture, for the reference period (top) and the future period (2041-2070) based on the RCP4.5 and RCP8.5 (bottom)

5.2.2 Exposure Indicators

In the following paragraphs, the results for the exposure indicators are presented, for the food, water, and ecosystems sectors.

Share of area cultivated with crops

The share of areas cultivated with crops in each part of the Doñana area, is presented in Table 50. As it can be observed, the cultivated area is significant (55%) at the Northern part of the pilot, while at the Southern part the cultivated area is less (16%). Therefore, the exposure of agriculture is estimated to be high for the Northern area and low-medium for the Southern.

Table 50: Share of crops under study in North and South Doñana pilot area.

Doñana pilot	Total area (hectares)	Cultivated area (hectares)	Share of area cultivated with crops
Northern part	219,173	121,538	55%
Southern part	153,122	24,444	16%

Share of area covered with forests and natural areas

The share of natural areas (land covered by forests, natural grasslands, shrubs, marshes etc.) compared to the total area of the pilot is presented in Table 51. As it can be observed, the Northern part where the agricultural activity is more intensive, the share is 29%, while the Southern part where the Natural Park is located, the share of natural areas is 73%. Therefore, the ecosystems are considered to be moderately exposed in the Northern part and highly exposed in the Southern part.

Table 51: Share of natural areas in North and South Doñana pilot area.

Doñana pilot	Area (hectares)	Natural area (hectares)	Share of natural area
North part	219,173	63,154	29%
South part	153,122	112,065	73%

5.2.3 Vulnerability Indicators

In the following paragraphs, the results for the vulnerability indicators are presented, for the food, water, and ecosystems sectors.

Water Exploitation Index

The water exploitation index (WEI) of the Guadalquivir River Basin which is located in the Doñana pilot, is presented in Table 52. Specifically, the WEI is estimated to be 74%, which is above the threshold under which water stress can begin to be a limiting factor on economic development for the region. Thus, the vulnerability related to this indicator is considered to be high.

Table 52: Water vulnerability index expressed as Water Exploitation Index, Guadalquivir River Basin.

River Basin District	Water Exploitation Index
Guadalquivir	74%

Share of agricultural water consumption

The share of agricultural water consumption in Guadalquivir River Basin is shown in Table 53. Specifically, the share of agricultural water consumption is very high, up to 90%, therefore a potential reduction in water availability due to climate change, would be critical for the agricultural sector. Thus, the vulnerability related to this indicator is considered to be high.

Table 53: Water vulnerability index expressed as share of agricultural water consumption, Guadalquivir River Basin.

River Basin District	Share of agricultural water consumption
Guadalquivir	90%

Agricultural Income

The agricultural income of Andalusia region where the Doñana pilot is located, compared to the average national agricultural income of Spain, is presented in Table 54. It is observed that the region of Andalusia, has 586% higher agricultural income compared to the national average. This indicates an extremely high dependency of the country to the agricultural income of the region. Thus, the vulnerability related to this indicator is considered to be high.

Table 54: Food vulnerability index expressed as agriculture income, Andalusia Region.

	Million Euro	% of national average
National Average	1850	100%
Andalusia Region	10846	586%

Share of protected areas

As it may be seen in Table 55, the share of protected areas over the total area of the pilot, is estimated to be 24% in the Northern part where agricultural activity is more intensive and 74% in the Southern part of the pilot, where the National Park of Doñana is located. Therefore, the share of protected areas is considered medium for the Northern part and high for the Southern part.

Table 55: Share of protected areas, Northern and Southern Doñana pilot area.

Doñana pilot	Total area (hectares)	Protected area (hectares)	Share of protected area
North part	219,173	52,111	24%
South part	153,122	113,644	74%

5.2.4 Adaptive capacity

In this section, the results of the assessment of the adaptive capacity of the Doñana pilot are presented. Specifically, the results refer to the assessment of the GDP index for the pilot at national level.

The economic capacity expressed as the GDP of the country in relation to the EU average is presented in the table that follows. As it can be observed, the GDP of Spain is 25,260 Euros per capita which is close to the EU average (82%), thus reflecting a medium economic capacity of the country and subsequently of the Doñana pilot.

Table 56: Relative Economic capacity of the Doñana pilot.

Doñana pilot	GDP per capita (Euro)	in % of EU average
EU average (27 countries)	30,632	100%
Spain	25,260	82%

5.2.5 Overall Risk

In this section, the results of the climate risk assessment for the food and ecosystems Nexus system of the Doñana national park area are presented for the period 2041-2070, based on the RCP4.5 and RCP8.5. The results are presented separately for the northern and the southern part of Doñana pilot. Specifically, the overall risk is presented both qualitatively and quantitatively per risk component at indicator level.

As it can be observed in Table 57, the estimated overall risk for the food sector is considered to be “Medium-High” to “High”. This is a result of a “Medium” to “Medium-High” hazard, in combination with a “High” vulnerability, and a “High” and “Low-Medium” exposure.

This project is part of the PRIMA programme supported by the European Union.
GA n° [2041] [LENSES] [Call 2020 Section 1 Nexus IA]

Table 57: Qualitative climate risk assessment per risk component of the food sector for the period 2041-2070, Doñana pilot area.

Indicators	**Northern Area**		**Southern Area**	
	RCP 4.5	**RCP 8.5**	**RCP 4.5**	**RCP 8.5**
Heat stress >35 °C	High	High	Medium	Medium-High
BEDD	Low	Low	Low	Low
Actual aridity	High	High	High	High
Fire Weather Index	Medium-High	High	Medium-High	Medium-High
River discharge	Low	Medium	Low	High
Soil moisture	Medium-High	High	Medium	Medium
Hazard composite indicator	**Medium-High**	**Medium-High**	**Medium**	**Medium-High**
Agricultural income	High	High	High	High
Water exploitation	High	High	High	High
Agricultural water consumption	High	High	High	High
Vulnerability composite indicator	**High**	**High**	**High**	**High**
Exposure indicator	**High**	**High**	**Low-Medium**	**Low-Medium**
Food System Risk	**Medium-High**	**High**	**Medium-High**	**Medium-High**

The detailed results of the climate risk assessment for the food sector are presented quantitatively at normalized scale [0, 5] in Table 58. The negative values of the hazard indicators are assigned to reflect a beneficial effect and thus compensate risk.

Table 58: Quantitative climate risk assessment per risk component of the food sector for the period 2041-2070, Doñana pilot area.

Indicators	**Northern Area**		**Southern Area**	
	RCP 4.5	**RCP 8.5**	**RCP 4.5**	**RCP 8.5**
Heat stress >35 °C	4.21	5.00	2.43	3.14
BEDD	-0.51	-0.69	-0.51	-0.69
Actual aridity	4.10	4.23	4.16	4.24
Fire Weather Index	3.94	4.14	3.72	3.86
River discharge	0.00	3.00	0.00	4.60
Soil moisture	3.94	4.06	2.75	2.94
Hazard composite indicator	**3.47**	**3.97**	**2.83**	**3.40**
Agricultural income	5.00	5.00	5.00	5.00
Water exploitation	4.57	4.57	4.57	4.57
Agricultural water consumption	4.75	4.75	4.75	4.75
Vulnerability composite indicator	**4.77**	**4.77**	**4.77**	**4.77**
Exposure indicator	**4.39**	**4.39**	**1.60**	**1.60**
Food System Risk	**3.91**	**4.22**	**3.17**	**3.51**

PRIMA
This project is part of the PRIMA programme supported by the European Union.
GA n° [2041] [LENSES] [Call 2020 Section 1 Nexus IA]

As it can be observed in Table 59 for the ecosystem sector, the risk levels are the result of a “Medium-High” to “High” range hazard, in combination with a “Medium” to “High” vulnerability, for both areas, while the exposure is considered “High” for the Southern area and “Medium” for the Northern area of the pilot. Thus, the overall risk for the ecosystem sector is considered “Medium-High” for both areas and scenarios, except from the RCP8.5 where the risk was calculated as “High” for the Southern area.

Table 59: Qualitative climate risk assessment per risk component of the ecosystem sector for the period 2041-2070, Doñana pilot area.

Indicators	Northern Area		Southern Area	
	RCP 4.5	RCP 8.5	RCP 4.5	RCP 8.5
Heat stress >35 °C	High	High	Medium	Medium-High
Actual aridity	High	High	High	High
Fire weather index WFI>30	Medium-High	High	Medium-High	Medium-High
River discharge	Low	Medium	Low	High
Soil moisture	Medium-High	High	Medium	Medium
Hazard composite indicator	**Medium-High**	**High**	**Medium-High**	**High**
Exposure Indicator	**Medium**	**Medium**	**High**	**High**
Vulnerability Indicator	**Medium**	**Medium**	**High**	**High**
Ecosystems Risk	**Medium-High**	**Medium-High**	**Medium-High**	**High**

The detailed results of the climate risk assessment for the ecosystem sector are presented quantitatively at normalized scale [0, 5] in Table 60.

Table 60: Quantitative climate risk assessment per risk component of the ecosystem sector for the period 2041-2070, Doñana pilot area.

Indicators	Northern Area		Southern Area	
	RCP 4.5	RCP 8.5	RCP 4.5	RCP 8.5
Heat stress >35 °C	4.21	5.00	2.43	3.14
Actual aridity	4.10	4.23	4.16	4.24
Fire weather index WFI>30	3.94	4.14	3.72	3.86
River discharge	0.00	3.00	0.00	4.60
Soil moisture	3.94	4.06	2.75	2.94
Hazard composite indicator	**3.74**	**4.80**	**3.03**	**4.49**
Exposure indicator	**2.88**	**2.88**	**4.83**	**4.83**
Vulnerability indicator	**2.38**	**2.38**	**4.86**	**4.86**
Ecosystems Risk	**3.30**	**3.94**	**3.45**	**4.33**

Following, the results of the climate risk assessment for the period 2041-2070 are summarized for Ecosystem-Food sectors.

As it may be seen in Table 61 where the results for the Doñana pilot are presented, according to RCP4.5, the risk for the WEF systems, is expected to be “Medium-High” in both Northern and Southern parts of the pilot.

According to RCP8.5 the risk for the food system will be higher than RCP4.5 for the Northern area of the pilot, where there is greatest exposure due to the concentration of agricultural activities. In addition, a high level of risk is expected under RCP8.5 for ecosystems in the Southern part of the pilot, where the National Park is located and therefore there is greater exposure of ecosystems. Furthermore, the adaptive capacity is characterized as "Medium" for the pilot, which is not considered sufficient to offset the expected risk for the WEF Nexus sectors.

Table 61: Overall risk of the WEF Nexus sectors, Doñana pilot.

	Northern Area		Southern Area		Adaptive Capacity
	RCP 4.5	RCP 8.5	RCP 4.5	RCP 8.5	
Food	Medium-High	High	Medium-High	Medium-High	Medium
Ecosystem	Medium-High	Medium-High	Medium-High	High	

5.3 Koiliaris Critical Zone Observatory (Greece)

In this section the results of the hazard, exposure and vulnerability assessment, as well as of the adaptive capacity and the overall climate risk assessment are provided, for the Koiliaris Critical Zone Observatory (Greece).

5.3.1 Climate Related Hazard Indicators

In the following paragraphs, the results for the hazard indicators are presented, for the food, water, and ecosystems sectors.

Actual Aridity

Table 62 displays the percentage change in aridity compared to the reference period for both scenarios in the future. It is evident that there is an aridity increase in all three future sub-periods for both scenarios, except for a slight 6% decrease in the mid-term period under RCP4.5. The most significant increase (+15%) is anticipated in the long-term period, while the smallest increase (+3%) occurs in the short-term period, specifically for RCP4.5.

Table 62: Relative change (%) of the mean annual aridity (actual evapotranspiration/precipitation), for the future sub-periods based on the RCP4.5 and RCP8.5, compared to the reference period, Koiliaris pilot.

Actual Aridity	2011-2040		2041-2070		2071-2100	
	RCP4.5	RCP8.5	RCP4.5	RCP8.5	RCP4.5	RCP8.5
relative change (%)	3	11	-6	13	15	13

Biologically Effective Degree Days over 10-days (BEDD)

Table 63 provides an overview of the projected percentage change in the BEDD (Biologically Effective Degree Days) over 10 days for future sub-periods under the RCP4.5 and RCP8.5 scenarios compared to the reference period. Generally, an increase in the BEDD indicator is anticipated for both scenarios in the future. Specifically, it can be concluded that for the short-term and mid-term periods, there is little differentiation between the scenarios, with an average increase of 5.5% and 12.5%, respectively, compared to the reference period. However, in the long-term period, the increase becomes more pronounced, reaching up to 13% for RCP4.5 and 24% for RCP8.5.

Table 63: Relative change (%) of the Biologically Effective Degree Days over 10-days, for the future sub-periods based on the RCP4.5 and RCP8.5, compared to the reference period, Koiliaris pilot.

BEDD	2011-2040		2041-2070		2071-2100	
	RCP4.5	RCP8.5	RCP4.5	RCP8.5	RCP4.5	RCP8.5
relative change (%)	5	6	10	15	13	24

Fire Weather index

Table 64 illustrates the percentage change in the FWI (Fire Weather Index) for the future compared to the reference period under both scenarios. It is evident that there is a consistent increase in FWI for both scenarios in the future. To be specific, during the short-term period, there is an average increase of 8.5% compared to the reference period. In contrast, this upward trend becomes more pronounced in the long-term period, with an increase of up to 19% for RCP4.5 and a substantial 39% for RCP8.5.

Table 64: Relative change (%) of the FWI, for the future sub-periods based on the RCP4.5 and RCP8.5, compared to the reference period, Koiliaris pilot.

Fire Weather Index	2011-2040		2041-2070		2071-2100	
	RCP4.5	RCP8.5	RCP4.5	RCP8.5	RCP4.5	RCP8.5
relative change (%)	8	9	12	21	19	39

Heat Stress days over 30°C

Table 65 provides an overview of the percentage change in the projected number of heat stress days (>30°C) in the future. It's evident that there are notable differences between the two scenarios across all three future periods, with RCP8.5 showing the most significant increase. Specifically, for the near-term period, there is an average projected increase of 150% for both scenarios. In the mid-term period, the increase is projected to be 325% for RCP4.5 and 525% for RCP8.5. Lastly, in the long-term period, we anticipate an increase of 350% for RCP4.5 and a remarkable 1175% for RCP8.5.

Table 65: Relative change (%) of the Heat Stress days over 30°C, for the future sub-periods based on the RCP4.5 and RCP8.5, compared to the reference period, Koiliaris pilot.

Heat Stress days over 30°C	2011-2040		2041-2070		2071-2100	
	RCP4.5	RCP8.5	RCP4.5	RCP8.5	RCP4.5	RCP8.5
relative change (%)	125	175	325	525	350	1175

Soil Moisture

Table 66 provides a summary of the projected percentage change in soil moisture for the future, based on the RCP4.5 and RCP8.5 scenarios. In general, both scenarios indicate a decreasing trend. Specifically, it can be concluded that during the short-term period, there is no significant difference in the projected decrease between the scenarios, with a reduction of approximately -6.5%. In the mid-term period, there is a consistent 10% reduction for both scenarios. Finally, in the long-term period, the reduction is similar to the mid-term for both scenarios, averaging around 12%.

Table 66: Relative change (%) of soil moisture in the future compared to the reference period, based on the RCP4.5 and RCP8.5, Koiliaris pilot.

Soil Moisture	2011-2040		2041-2070		2071-2100	
	RCP4.5	RCP8.5	RCP4.5	RCP8.5	RCP4.5	RCP8.5
relative change (%)	-5	-8	-10	-10	-8	-16

Following, the hazard indicators are presented through maps for the reference period (1971-2000) and the future period (2041-2070), under the RCP4.5 and RCP8.5.

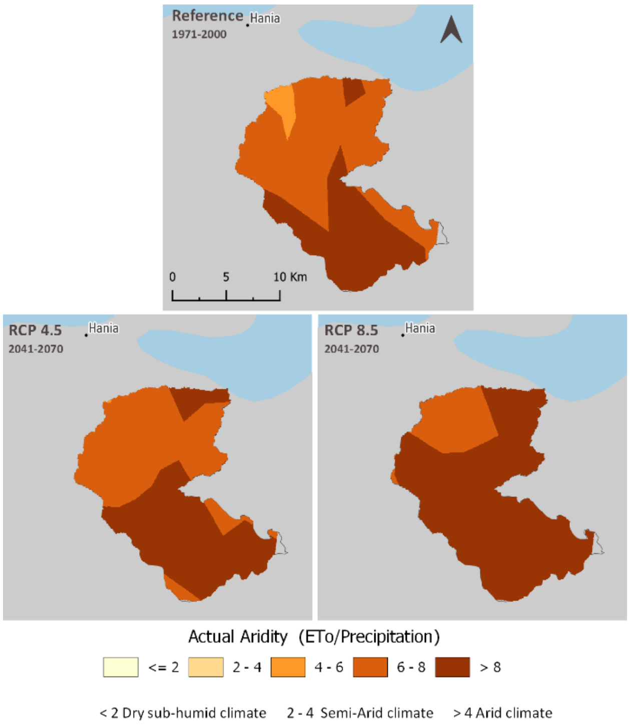

Figure 61: Spatial distribution of actual aridity, for the reference period (top) and the future period (2041-2070) based on the RCP4.5 and RCP8.5 (bottom)

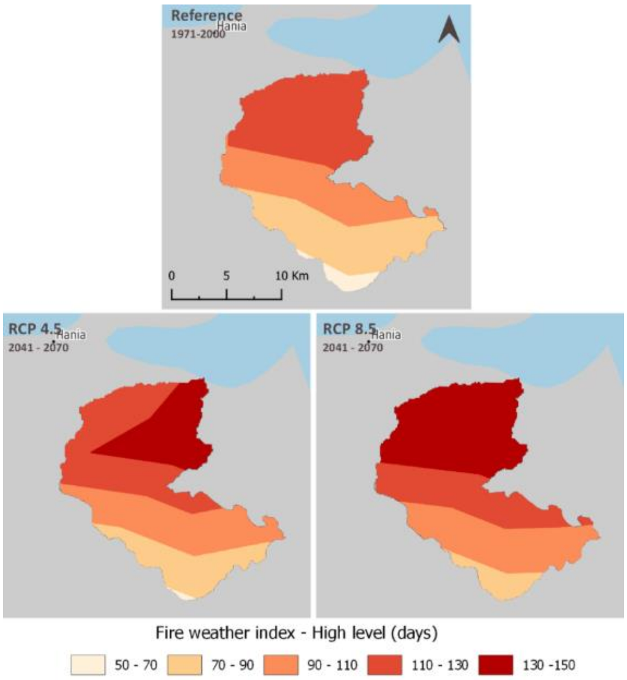

Figure 62: Spatial distribution of the FWI, for the reference period (top) and the future period (bottom)based on the RCP4.5 and RCP8.5

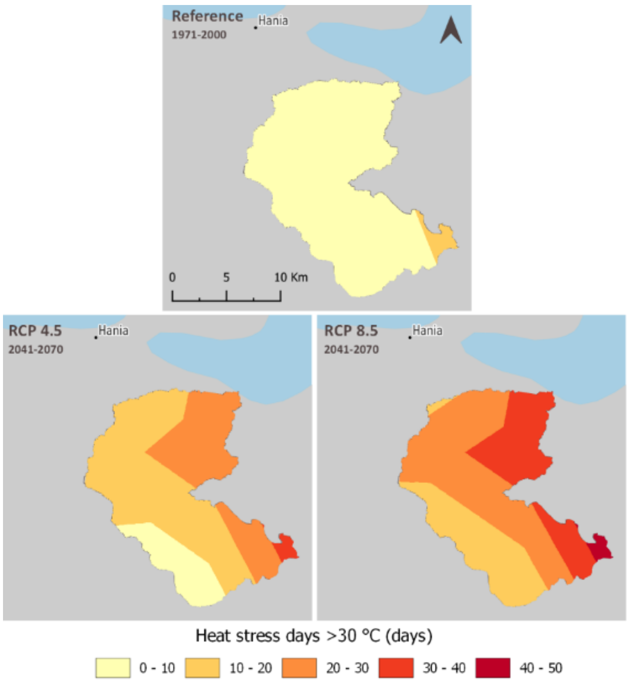

Figure 63: Spatial distribution of the mean annual number of days when maximum daily temperature is > 35°C, for the reference period (top) and the future period (2041-2070) based on the RCP4.5 and RCP8.5 (bottom)

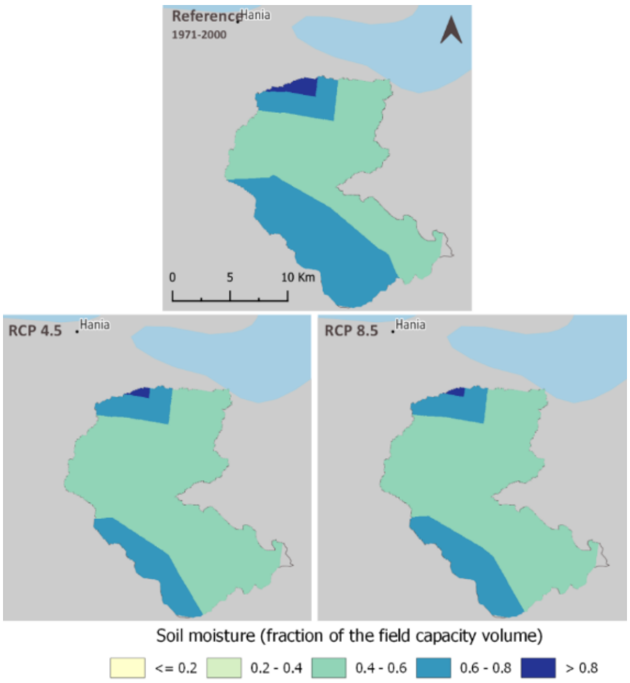

Figure 64: Spatial distribution of soil moisture, for the reference period (top) and the future period (2041-2070) based on the RCP4.5 and RCP8.5 (bottom)

5.3.2 Exposure Indicators

In the following paragraphs, the results for the exposure indicators are presented, for the food, water, and ecosystems sectors.

Share of area cultivated with crops

The share of areas cultivated with crops in Koiliaris area, is presented in Table 67. As it can be observed, the cultivated area captures the 26% of the pilot area, thus the exposure of agriculture is estimated to be medium-high.

Table 67: Share of crops under study in Koiliaris pilot area.

	Total area (hectares)	Cultivated area (hectares)	Share of area cultivated with crops
Koiliaris pilot	21,286	5,615	26%

Share of area covered with forests and natural areas

The share of natural areas (land covered by forests, natural grasslands, shrubs, marshes etc.) compared to the total area of the pilot is presented in Table 68. As it can be observed, the 73% of the pilot area is covered by natural areas and therefore the ecosystems are considered to be highly exposed in the Koiliaris pilot.

Table 68: Share of natural areas in Koiliaris pilot area

	Area (hectares)	Natural area (hectares)	Share of natural area
Koiliaris pilot	21,286	15,610	73%

5.3.3 Vulnerability Indicators

In the following paragraphs, the results for the vulnerability indicators are presented, for the food, water, and ecosystems sectors.

Water Exploitation Index

The water exploitation index (WEI) of the Northern part of Chania-Rethymno-Heraklio River Basin District, which is located in the Koiliaris pilot, is presented in Table 69. Specifically, the WEI is estimated to be 25% which is above the threshold under which water stress can begin to be a limiting factor on economic development for the region. Thus, the vulnerability related to this indicator is considered to be medium.

Table 69: Water vulnerability index expressed as Water Exploitation Index, Northern part of Chania-Rethymno-Heraklio River Basin.

River Basin District	Water Exploitation Index
Northern part of Chania-Rethymno-Heraklio	25%

Share of agricultural water consumption

The share of agricultural water consumption in Northern part of Chania-Rethymno-Heraklio River Basin District is shown in Table 70. Specifically, the share of agricultural water consumption is very high, up to 72%, therefore a potential reduction in water availability due to climate change, would be critical for the agricultural sector. Thus, the vulnerability related to this indicator is considered to be high.

Table 70: Water vulnerability index expressed as share of agricultural water consumption, Northern part of Chania-Rethymno-Heraklio River Basin.

River Basin District	Share of agricultural water consumption
Northern part of Chania-Rethymno-Heraklio	72%

Agricultural Income

The agricultural income of Creta region where the Koiliaris pilot is located, compared to the average national agricultural income of Greece, is presented in Table 71. It is observed that the region of Creta, has 124% higher agricultural income compared to the national average. This indicates dependency of the country to the agricultural income of the region. Thus, the vulnerability related to this indicator is considered to be medium-high.

Table 71: Food vulnerability index expressed as agriculture income, Creta Region.

	Million Euro	% of national average
National Average	596	100%
Creta Region	740	124%

Share of protected areas

As it may be seen in Table 72, the share of protected areas over the total area of the pilot, is estimated to be 47% and therefore, the share of protected areas is considered high.

Table 72: Share of protected areas, Koiliaris pilot area.

	Total area (hectares)	Protected area (hectares)	Share of protected area
Koiliaris pilot	21,286	10,056	47%

5.3.4 Adaptive capacity

In this section, the results of the assessment of the adaptive capacity of the Koiliaris pilot are presented. Specifically, the results refer to the assessment of the GDP index for the pilot at national level.

The economic capacity expressed as the GDP of the country in relation to the EU average is presented in the table that follows. As it can be observed, the GDP of Greece is 16,570 Euros per capita which is close to half of the EU average (54%), thus reflecting a low-medium economic capacity of the country and subsequently of the Koiliaris pilot.

Table 73: Relative Economic capacity of the Koiliaris pilot area.

Koiliaris pilot	GDP per capita (Euro)	in % of EU average

EU average (27 countries)	30,632	100%
Greece	16,570	54%

5.3.5 Overall Risk

In this section, the results of the climate risk assessment for the food and ecosystems Nexus sectors of the Koiliaris pilot area are presented for the period 2041-2070, based on the RCP4.5 and RCP8.5. Specifically, the overall risk is presented both qualitatively and quantitatively per risk component at indicator level.

As it can be observed in Table 74, the overall risk for the food sector is considered to be "Medium-High". This is a result of a "Medium" to "Medium-High" hazard, in combination with a "Medium-High" vulnerability and "Medium-High" exposure.

Table 74: Qualitative climate risk assessment per risk component of the food sector for the period 2041-2070, Koiliaris pilot area.

Indicators	**RCP 4.5**	**RCP 8.5**
Heat stress >35 °C	Medium	Medium-High
BEDD	Low	Low-Medium
Actual aridity	High	High
Fire weather index WFI>30	Medium-High	Medium-High
Soil moisture	Medium	Medium
Hazard composite indicator	**Medium**	**Medium-High**
Exposure indicator	**Medium-High**	**Medium-High**
Agricultural income	Medium-High	Medium-High
Water exploitation	Medium	Medium
Agricultural water consumption	High	High
Vulnerability composite indicator	**Medium-High**	**Medium-High**
Food System Risk	**Medium-High**	**Medium-High**

The detailed results of the climate risk assessment for the food sector are presented quantitatively at normalized scale [0, 5] in Table 75. The negative values of the hazard indicators are assigned to reflect a beneficial effect and thus compensate risk.

Table 75: Quantitative climate risk assessment per risk component of the food sector for the period 2041-2070, Koiliaris pilot area.

Indicators	RCP 4.5	RCP 8.5
Heat stress >30 °C	2.13	3.13
BEDD	-0.68	-1.00
Actual aridity	4.19	4.27
Fire weather index WFI>30	3.47	3.75
Soil moisture	2.88	2.81
Hazard composite indicator	**2.94**	**3.28**
Exposure indicator	**3.32**	**3.32**
Agricultural income	3.10	3.10
Water exploitation	2.40	2.40
Agricultural water consumption	4.30	4.30
Vulnerability composite indicator	**3.27**	**3.27**
Food System Risk	**3.08**	**3.29**

As it can be observed in Table 76 for the ecosystem sector, the risk levels are expected to be “Medium-High”, which is the result of a “Medium-High” hazard, in combination with a “High” vulnerability, and exposure of the pilot area.

Table 76: Qualitative climate risk assessment per risk component of the ecosystem sector for the period 2041-2070, Koiliaris pilot area.

Indicators	RCP 4.5	RCP 8.5
Heat stress >35 °C	Medium	Medium-High
Actual aridity	High	High
Fire weather index WFI>30	Medium-High	Medium-High
Soil moisture	Medium	Medium
Hazard composite indicator	**Medium-High**	**Medium-High**
Exposure indicator	**High**	**High**
Vulnerability indicator	**High**	**High**
Ecosystems Risk	**Medium-High**	**Medium-High**

The detailed results of the climate risk assessment for the ecosystem sector are presented quantitatively at normalized scale [0, 5] in Table 77.

Table 77: Quantitative climate risk assessment per risk component of the ecosystem sector for the period 2041-2070, Koiliaris pilot area.

Indicators	RCP 4.5	RCP 8.5
Heat stress >35 °C	2.13	3.13
Actual aridity	4.19	4.27
Fire weather index WFI>30	3.47	3.75
Soil moisture	2.88	2.81
Hazard composite indicator	**3.17**	**3.45**
Exposure indicator	**4.83**	**4.83**
Vulnerability indicator	**4.18**	**4.18**
Ecosystems Risk	**3.70**	**3.87**

Following, the results of the climate risk assessment for the period 2041-2070 are summarized for Ecosystem-Food sectors.

As it may be seen in Table 78 where the results for the Koiliaris pilot are presented, the level of risk for all sectors is expected to be "Medium-High" according to both RCP scenarios. The risk of the food sector is the result of a "Medium" to "Medium-High" hazard, as well as a "Medium-High" exposure and vulnerability. In addition, the risk of the ecosystem sector is the result of a "Medium-High" hazard, combined with a "High" exposure and vulnerability. Furthermore, the adaptive capacity is characterized as "Low-Medium" for the pilot, which is not considered sufficient to offset the expected risk for the WEF Nexus sectors.

Table 78: Overall risk of the WEF Nexus sectors, Koiliaris pilot area.

	RCP 4.5	RCP 8.5	Adaptive Capacity
Food	Medium-High	Medium-High	Low-Medium
Ecosystem	Medium-High	Medium-High	

5.4 Gediz Basin & Delta (Turkey)

In this section the results of the hazard, exposure and vulnerability assessment, as well as of the adaptive capacity and the overall climate risk assessment are provided, for the Gediz Basin & Delta (Turkey).

5.4.1 Climate Related Hazard Indicators

In the following paragraphs, the results for the hazard indicators are presented, for the food, water, and ecosystems sectors.

Actual Aridity

Table 79 presents the relative change (%) in actual aridity compared to the reference period for both scenarios in the future. It is evident that aridity increases in all three future sub-periods for both scenarios. The highest increase (+16%) is anticipated during the mid-term period, while the lowest increase (+3%)

occurs in the short-term period for both scenarios. On average, a 10.5% increase is expected during the long-term period.

Table 79: Relative change (%) of the mean annual aridity (actual evapotranspiration/precipitation), for the future sub-periods based on the RCP4.5 and RCP8.5, compared to the reference period, Gediz pilot.

Actual Aridity	2011-2040		2041-2070		2071-2100	
	RCP4.5	RCP8.5	RCP4.5	RCP8.5	RCP4.5	RCP8.5
relative change (%)	3	4	16	16	7	12

Biologically Effective Degree Days over 10-days (BEDD)

The projected relative change (%) of the BEDD over 10-days, for the future sub-periods based on the RCP4.5 and RCP8.5, compared to the reference period, is summarized in Table 80. In general, an increase of the BEDD indicator is expected in the future for both scenarios. In particular, it may be concluded that for the short-term and mid-term period, there is no significant difference between the scenarios, with an average 6.5% and 14.5% increase from the reference period respectively. For the long-term period the increase is more noticeable, up to 16% for RCP4.5 and 28% for RCP8.5.

Table 80: Relative change (%) of the Biologically Effective Degree Days over 10-days, for the future sub-periods based on the RCP4.5 and RCP8.5, compared to the reference period, Gediz pilot.

BEDD	2011-2040		2041-2070		2071-2100	
	RCP4.5	RCP8.5	RCP4.5	RCP8.5	RCP4.5	RCP8.5
relative change (%)	5	8	12	17	16	28

Fire Weather index

The relative change (%) of the FWI in the future compared to the reference period for both scenarios, is shown in Table 81. The data shows a noticeable increase in FWI (Fire Weather Index) for both scenarios in the future. Specifically, during the short-term period, there is an average increase of 2.5% compared to the reference period. In the long-term period, this upward trend becomes more pronounced, with an increase of up to 9% for RCP4.5 and up to 18% for RCP8.5.

Table 81: Relative change (%) of the FWI, for the future sub-periods based on the RCP4.5 and RCP8.5, compared to the reference period, Gediz pilot.

Fire Weather Index	2011-2040		2041-2070		2071-2100	
	RCP4.5	RCP8.5	RCP4.5	RCP8.5	RCP4.5	RCP8.5
relative change (%)	1	4	5	10	9	18

Heat Stress days over 35°C

The relative change (%) of the projected number of heat stress days (>35°C) in the future, is summarized in Table 82. As it can be observed, there is a clear increasing trend and the difference between the two scenarios for all three future periods is noticeable, with the RCP8.5 presenting the highest increase. Specifically, for the near-term period an increase of 37.5% on average is projected, while for the mid-term period, an increase of

65% is projected on average for the two scenarios. Finally, for the long-term period, the increase is expected to reach 65% for the RCP4.5 and 135% for the RCP8.5.

Table 82: Relative change (%) of the Heat Stress days over 35°C, for the future sub-periods based on the RCP4.5 and RCP8.5, compared to the reference period, Gediz pilot.

Heat Stress days over 35°C	2011-2040		2041-2070		2071-2100	
	RCP4.5	RCP8.5	RCP4.5	RCP8.5	RCP4.5	RCP8.5
relative change (%)	35	40	55	75	65	135

Soil Moisture

The projected relative change (%) of soil moisture in the future based on the RCP4.5 and RCP8.5, is summarized in Table 83. In general, a decreasing trend is observed under both scenarios. In particular, it may be concluded that for the short-term period, there is no significant difference in the projected decrease between the scenarios. For the mid-term period there is a reduction of 5% on average for the two scenarios, while for the long-term period the reduction is similar to the mid-term for both scenarios.

Table 83: Relative change (%) of soil moisture in the future compared to the reference period, based on the RCP4.5 and RCP8.5, Gediz pilot.

Soil Moisture	2011-2040		2041-2070		2071-2100	
	RCP4.5	RCP8.5	RCP4.5	RCP8.5	RCP4.5	RCP8.5
relative change (%)	1	-2	-7	-3	-3	-8

Following, the hazard indicators are presented through maps for the reference period (1971-2000) and the future period (2041-2070), under the RCP4.5 and RCP8.5.

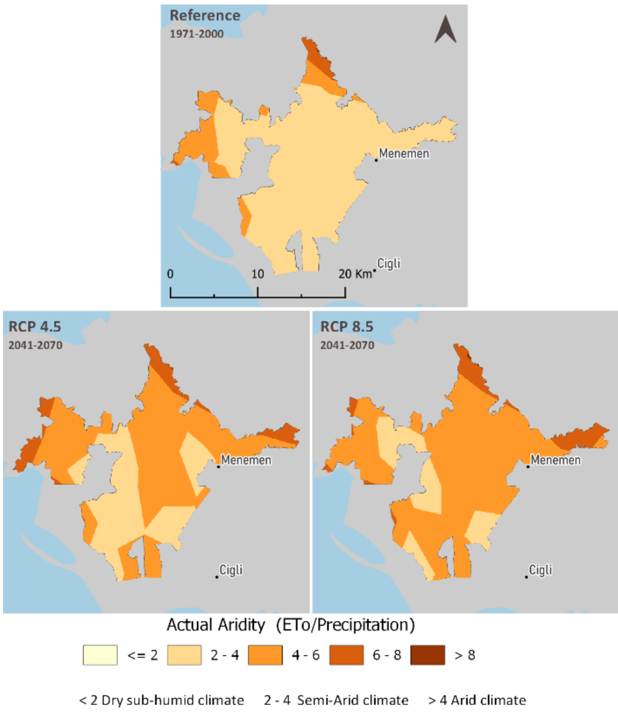

Figure 65: Spatial distribution of actual aridity, for the reference period (top) and the future period (2041-2070) based on the RCP4.5 and RCP8.5 (bottom)

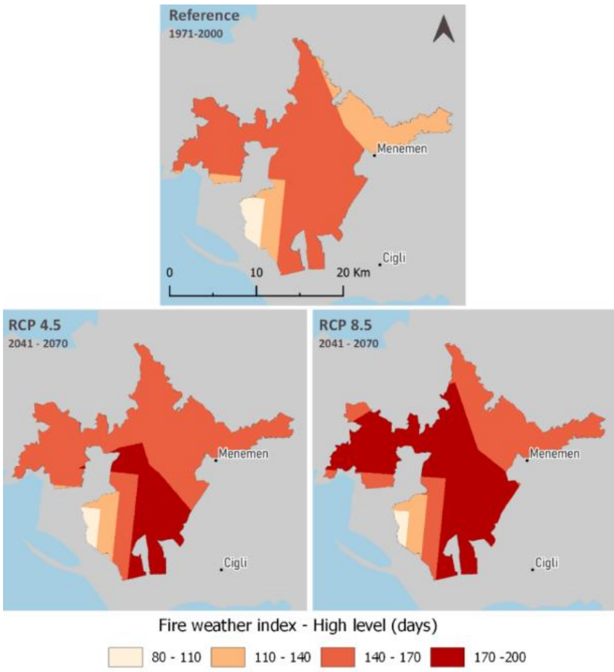

Figure 66: Spatial distribution of the FWI, for the reference period (top) and the future period (bottom)based on the RCP4.5 and RCP8.5

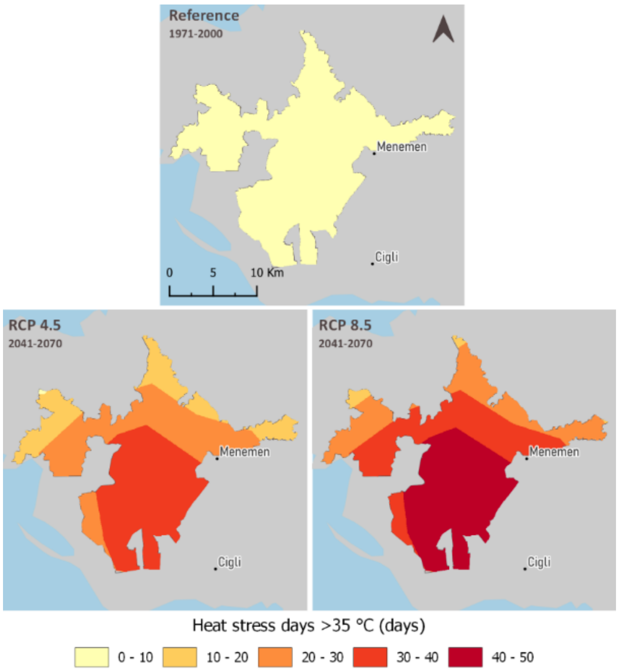

Figure 67: Spatial distribution of the mean annual number of days when maximum daily temperature is > 35°C, for the reference period (top) and the future period (2041-2070) based on the RCP4.5 and RCP8.5 (bottom)

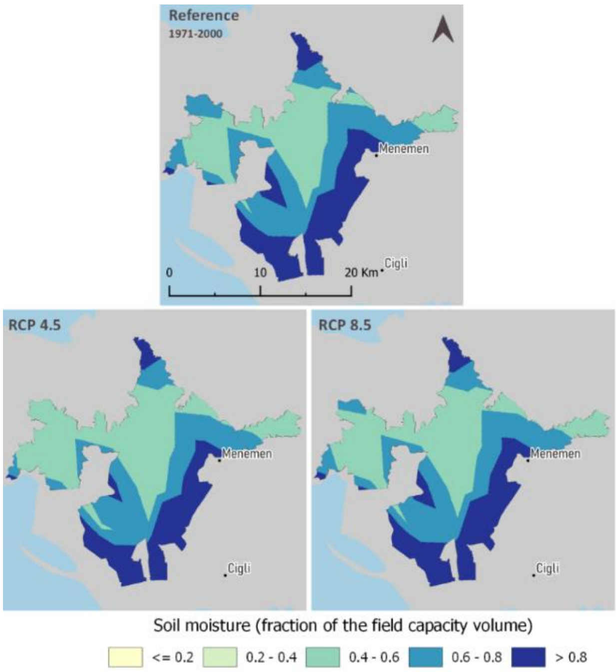

Figure 68: Spatial distribution of soil moisture, for the reference period (top) and the future period (2041-2070) based on the RCP4.5 and RCP8.5 (bottom)

This project is part of the PRIMA programme supported by the European Union.
GA n° [2041] [LENSES] [Call 2020 Section 1 Nexus IA]

5.4.2 Exposure Indicators

In the following paragraphs, the results for the exposure indicators are presented, for the food, water, and ecosystems sectors.

Share of area cultivated with crops

The share of areas cultivated with crops in the Gediz pilot area, is presented in Table 84. As it can be observed, the cultivated area captures almost the whole pilot area (96%). Therefore, the exposure of agriculture is estimated to be at high level.

Table 84: Share of crops under study in Gediz pilot area.

	Total area (hectares)	**Cultivated area (hectares)**	**Share of area cultivated with crops**
Gediz pilot	29,540	28,270	96%

Share of area covered with forests and natural areas

The share of natural areas (land covered by forests, natural grasslands, shrubs, marshes etc.) compared to the total area of the pilot is presented in Table 85. As it can be observed, only 1% it is covered by natural areas and therefore, the ecosystems are considered to be low exposed.

Table 85: Share of natural areas in Gediz pilot area.

	Area (hectares)	**Natural area (hectares)**	**Share of natural area**
Turkish pilot	29,540	340	1%

5.4.3 Vulnerability Indicators

In the following paragraphs, the results for the vulnerability indicators are presented, for the food, water, and ecosystems sectors.

Water Exploitation Index

The water exploitation index (WEI) of Turkey where the Gediz pilot is located, is presented in Table 86. Specifically, the WEI is estimated to be 22% which is above the threshold under which water stress can begin to be a limiting factor on economic development for the region. Thus, the vulnerability related to this indicator is considered to be medium.

Table 86: Water vulnerability index expressed as Water Exploitation Index, Gediz pilot area.

Turkey	**Water Exploitation Index**
National level	22%

Share of agricultural water consumption

The share of agricultural water consumption in Turkey is shown in Table 87. Specifically, the share of agricultural water consumption is very high, up to 74%, therefore a potential reduction in water availability due to climate change, would be critical for the agricultural sector. Thus, the vulnerability related to this indicator is considered to be high.

Table 87: Water vulnerability index expressed as share of agricultural water consumption, Gediz pilot area.

Turkey	Share of agricultural water consumption
National level	74%

Agricultural Income

The agricultural income of Turkey, compared to the Mediterranean average agricultural income, is presented in Table 88. It is observed that Turkish agricultural income compared to the Mediterranean average is close (87%). This indicates that the dependency of the country to the agricultural income is close to the other Mediterranean countries. The vulnerability related to this indicator is considered to be high.

Table 88: Food vulnerability index expressed as agriculture income, Turkey.

	Value added of agriculture as percent of the national GDP
Mediterranean Average	7%
Turkey	6%
Turkey compared to Mediterranean average	87%

Share of protected areas

As it may be seen in Table 89, the share of protected areas over the total area of the pilot, is estimated to be 2%. Therefore, the share of protected areas is considered low for the Gediz pilot.

Table 89: Share of protected areas, Gediz pilot area

	Total area (hectares)	Protected area (hectares)	Share of protected area
Gediz pilot	29,540	630	2%

5.4.4 Adaptive capacity

In this section, the results of the assessment of the adaptive capacity of the Gediz pilot are presented. Specifically, the results refer to the assessment of the GDP index for the pilot at national level.

The economic capacity expressed as the GDP of the country in relation to the Mediterranean average is presented in the table that follows. As it can be observed, the GDP of Turkey is 796,745 million US dollars which is above (191%) the Mediterranean average. This reflecting a low-medium economic capacity of the country and subsequently of the Gediz pilot.

This project is part of the PRIMA programme supported by the European Union.
GA n° [2041] [LENSES] [Call 2020 Section 1 Nexus IA]

Table 90: Relative Economic capacity of the Gediz pilot area.

	GDP (million US dollars)	in % of Mediterranean average
Mediterranean average (21 countries)	415,200	100%
Turkey	796,745	191%

5.4.5 Overall Risk

In this section, the results of the climate risk assessment for the food and ecosystems Nexus sectors of the Gediz pilot area are presented for the period 2041-2070, based on the RCP4.5 and RCP8.5. Specifically, the overall risk is presented both qualitatively and quantitatively per risk component at indicator level.

Food Risk

As it can be observed in Table 91, the overall risk for the food sector is considered to be "Medium-High. This is a result of a "Medium" to "Medium-High" hazard, in combination with a "Medium-High" vulnerability, and a "High" exposure.

Table 91: Qualitative climate risk assessment per risk component of the food sector for the period 2041-2070, Gediz pilot area

Indicators	**RCP 4.5**	**RCP 8.5**
Heat stress >35 °C	Medium	Medium-High
BEDD	Low	Low-Medium
Actual aridity	Medium-High	Medium-High
Fire weather index WFI>30	Medium-High	High
Soil moisture	Medium	Medium
Hazard composite indicator	**Medium**	**Medium-High**
Exposure indicator	**High**	**High**
Agricultural income	High	High
Water exploitation	Medium	Medium
Agricultural water consumption	High	High
Vulnerability composite indicator	**Medium-High**	**Medium-High**
Food System Risk	**Medium-High**	**Medium-High**

The detailed results of the climate risk assessment for the food sector are presented quantitatively at normalized scale [0, 5] in Table 92. The negative values of the hazard indicators are assigned to reflect a beneficial effect and thus compensate risk.

Table 92: Quantitative climate risk assessment per risk component of the food sector for the period 2041-2070, Gediz pilot area

Indicators	RCP 4.5	RCP 8.5
Heat stress >35 °C	2.57	3.36
BEDD	-0.77	-1.16
Actual aridity	3.84	3.88
Fire weather index WFI>30	3.96	4.13
Soil moisture	2.50	2.25
Hazard composite indicator	**2.94**	**3.17**
Exposure indicator	**5.00**	**5.00**
Agricultural income	4.36	4.36
Water exploitation	2.15	2.15
Agricultural water consumption	4.35	4.35
Vulnerability composite indicator	**3.62**	**3.62**
Food System Risk	**3.49**	**3.63**

As it can be observed in Table 93 for the ecosystem sector, the risk levels are the result of a "Medium-High" hazard, in combination with a "Low" vulnerability and exposure. Thus, the overall risk for the ecosystem sector is considered "Low-Medium" for both RCP's scenarios.

Table 93: Qualitative climate risk assessment per risk component of the ecosystem sector for the period 2041-2070, Gediz pilot area.

Indicators	RCP 4.5	RCP 8.5
Heat stress >35 °C	Medium	Medium-High
Actual aridity	Medium-High	Medium-High
Fire weather index WFI>30	Medium-High	High
Soil moisture	Medium	Medium
Hazard composite indicator	**Medium-High**	**Medium-High**
Exposure indicator	**Low**	**Low**
Vulnerability indicator	**Low**	**Low**
Ecosystems Risk	**Low-Medium**	**Low-Medium**

The detailed results of the climate risk assessment for the ecosystem sector are presented quantitatively at normalized scale [0, 5] in Table 94.

Table 94: Quantitative climate risk assessment per risk component of the ecosystem sector for the period 2041-2070, Gediz pilot area.

Indicators	RCP 4.5	RCP 8.5
Heat stress >35 °C	2.57	3.36
Actual aridity	3.84	3.88
Fire weather index WFI>30	3.96	4.13
Soil moisture	2.50	2.25
Hazard composite indicator	**3.22**	**3.36**
Exposure indicator	**0.23**	**0.23**
Vulnerability indicator	**0.42**	**0.42**
Ecosystems Risk	**1.27**	**1.30**

Following, the results of the climate risk assessment for the period 2041-2070 are summarized for Ecosystem-Food sectors.

As it may be seen in Table 95 where he results for the Gediz pilot are presented, the level of risk for the food sectors is expected to be at “Medium-High” level for both RCP scenarios, due to the high exposure of the pilot area, that is highly cultivated and the “Medium” to “Medium-High” level of the composite Hazard indicator. In addition, a “Low-Medium” level of risk is expected under both RCP scenarios for the ecosystem sector, which is the result of the “Low” exposure and vulnerability indicators. Furthermore, the adaptive capacity is characterized as “Low-Medium” for the pilot, which is not considered sufficient to offset the expected risk for the food sector.

Table 95: Overall risk of the WEF Nexus sectors, Gediz pilot area.

	RCP 4.5	RCP 8.5	Adaptive Capacity
Food	Medium-High	Medium-High	Low-Medium
Ecosystem	Low-Medium	Low-Medium	

5.5 Galilee, Hula Valley (Israel)

In this section the results of the hazard, exposure and vulnerability assessment, as well as of the adaptive capacity and the overall climate risk assessment are provided, for the Galilee, Hula Valley (Israel).

5.5.1 Climate Related Hazard Indicators

In the following paragraphs, the results for the hazard indicators are presented, for the food, water, and ecosystems sectors.

Actual Aridity

Due to the limited extend of the pilot area the model couldn't project correct the actual aridity indicator, thus no change from the reference period is predicted for the area.

Biologically Effective Degree Days over 10-days (BEDD)

The projected relative change (%) of the BEDD over 10-days, for the future sub-periods based on the RCP4.5 and RCP8.5, compared to the reference period, is summarized in Table 96. In general, an increase of the BEDD indicator is expected in the future for both scenarios. In particular, it may be concluded that for the short-term and mid-term period, there is no significant difference between the scenarios, with an average 5% and 11.5% increase from the reference period respectively. For the long-term period the increase is more noticeable, up to 12% for RCP4.5 and double for RCP8.5.

Table 96: Relative change (%) of the Biologically Effective Degree Days over 10-days, for the future sub-periods based on the RCP4.5 and RCP8.5, compared to the reference period, Hula pilot.

BEDD	2011-2040		2041-2070		2071-2100	
	RCP4.5	RCP8.5	RCP4.5	RCP8.5	RCP4.5	RCP8.5
relative change (%)	4	6	9	14	12	24

Fire Weather index

The relative change (%) of the FWI in the future compared to the reference period for both scenarios, is shown in Table 97. It can be observed that there is an increase of FWI in the future for both scenarios. Specifically, for the short-term period the increase from the reference period is 5% for both scenarios while in the long-term period this increasing trend reaches up to 9% for RCP4.5 and to 16% for RCP8.5.

Table 97: Relative change (%) of the FWI, for the future sub-periods based on the RCP4.5 and RCP8.5, compared to the reference period, Hula pilot.

Fire Weather Index	2011-2040		2041-2070		2071-2100	
	RCP4.5	RCP8.5	RCP4.5	RCP8.5	RCP4.5	RCP8.5
relative change (%)	5	5	7	9	9	16

Heat Stress days over 35°C

The relative change (%) of the projected number of heat stress days (>35°C) in the future, is summarized in Table 47. As it can be observed, the difference between the two scenarios for all three future periods is noticeable, with the RCP8.5 presenting the highest increase. Specifically, for the near-term period, an increase of 40% on average is projected for the two scenarios. For the mid-term period, an increase of 65% is projected based on RCP4.5 and 93% for the RCP8.5. Finally, for the long-term period, the increase is expected to reach 72% for the RCP4.5 and 131% for the RCP8.5.

Table 98: Relative change (%) of the Heat Stress days over 35°C, for the future sub-periods based on the RCP4.5 and RCP8.5, compared to the reference period, Hula pilot.

Heat Stress days over 30°C	2011-2040		2041-2070		2071-2100	
	RCP4.5	RCP8.5	RCP4.5	RCP8.5	RCP4.5	RCP8.5
relative change (%)	38	42	65	93	75	131

This project is part of the PRIMA programme supported by the European Union.
GA n° [2041] [LENSES] [Call 2020 Section 1 Nexus IA]

Soil Moisture

The projected relative change (%) of soil moisture in the future based on the RCP4.5 and RCP8.5, is summarized in Table 99. In general, a decreasing trend is observed under both scenarios. In particular, it may be concluded that for the short-term period, there is no significant difference in the projected decrease between the scenarios (-9%). For the mid-term period there is a reduction of 23.5% on average for the two scenarios, while for the long-term period the reduction is similar to the mid-term for the RCP4.5 and higher for the RCP8.5 (-35%).

Table 99: Relative change (%) of soil moisture in the future compared to the reference period, based on the RCP4.5 and RCP8.5, Hula pilot.

Soil Moisture	2011-2040		2041-2070		2071-2100	
	RCP4.5	RCP8.5	RCP4.5	RCP8.5	RCP4.5	RCP8.5
relative change (%)	-9	-9	-21	-26	-28	-35

5.5.2 Exposure Indicators

Share of area cultivated with crops

The share of areas cultivated with crops is 100% and therefore the exposure of agriculture is high for the Hula Valley pilot area.

5.5.3 Vulnerability Indicators

In the following paragraphs, the results for the vulnerability indicators are presented, for the food and water sectors.

Water Exploitation Index

The water exploitation index (WEI) of Israel which is located in the Hula Valley pilot area, is presented in Table 100. Specifically, the WEI is estimated to be 93% which is high above the threshold under which water stress can begin to be a limiting factor on economic development for the region. Thus, the vulnerability related to this indicator is considered to be high.

Table 100: Water vulnerability index expressed as Water Exploitation Index, Hula Valley pilot.

Israel	Water Exploitation Index
National level	93%

Agricultural Income

The agricultural income of Israel, compared to the Mediterranean average agricultural income, is presented in Table 101. It is observed that the agricultural income of Israel compared to the Mediterranean average is 21%. This indicates that the dependency of the country to the agricultural income is significantly lower than the other Mediterranean countries dependency. Thus, the vulnerability related to this indicator is considered to be low.

Table 101: Food vulnerability index expressed as agriculture income, Hula Valley pilot.

	Value added of agriculture as percent of the national GDP
Mediterranean Average	7%
Israel	1.5%
Israel compared to Mediterranean average	21%

5.5.4 Adaptive capacity

In this section, the results of the assessment of the adaptive capacity of the Hula Valley pilot are presented. Specifically, the results refer to the assessment of the GDP index for the pilot at national level.

The economic capacity expressed as the GDP of the country in relation to the Mediterranean average is presented in the table that follows. As it can be observed, the GDP of Israel is 440,600 million US dollars, which is almost equal (106%) to the Mediterranean average. This reflecting a low-medium economic capacity of the country and subsequently of the Hula Valley pilot.

Table 102: Relative Economic capacity of the Hula Valley pilot.

	GDP (million US dollars)	in % of Mediterranean average
Mediterranean average (21 countries)	415,200	100%
Israel	440,600	106%

5.5.5 Overall Risk

In this section, the results of the climate risk assessment for the food sector of the Hula Valley pilot area are presented for the period 2041-2070, based on the RCP4.5 and RCP8.5. Specifically, the overall risk is presented both qualitatively and quantitatively per risk component at indicator level.

As it can be observed in Table 103, the overall risk for the food sector is considered to be “High” for the Hula Valley pilot area. This is a result of a “High” level of hazard indicator, in combination with a “Medium-High” vulnerability, and a “High” exposure of the pilot to climate change.

Table 103: Qualitative climate risk assessment per risk component of the food sector for the period 2041-2070, Hula Valley pilot.

Indicators	**RCP 4.5**	**RCP 8.5**
Heat stress >35 °C	High	High
BEDD	Low	Low
Actual aridity	High	High
Fire weather index WFI>30	High	High
Soil moisture	High	High
Hazard composite indicator	**High**	**High**
Exposure indicator	**High**	**High**
Agricultural income	Low	Low
Water exploitation	High	High
Vulnerability composite indicator	**Medium-High**	**Medium-High**
Food System Risk	**High**	**High**

This project is part of the PRIMA programme supported by the European Union.
GA n° [2041] [LENSES] [Call 2020 Section 1 Nexus IA]

The detailed results of the climate risk assessment for the food sector are presented quantitatively at normalized scale [0, 5] in Table 104. The negative values of the hazard indicators are assigned to reflect a beneficial effect and thus compensate risk.

Table 104: Quantitative climate risk assessment per risk component of the food sector for the period 2041-2070, Hula Valley pilot.

Indicators	RCP 4.5	RCP 8.5
Heat stress >35 °C	5.00	5.00
BEDD	-0.60	-0.95
Actual aridity	4.33	4.33
Fire weather index WFI>30	5.00	5.00
Soil moisture	4.13	4.25
Hazard composite indicator	**4.20**	**4.20**
Exposure indicator	**5.00**	**5.00**
Agricultural income	0.95	0.95
Water exploitation	4.88	4.88
Vulnerability composite indicator	2.92	2.92
Food System Risk	4.10	4.09

Following, the results of the climate risk assessment for the period 2041-2070 are summarized for the Food sector.

As it may be seen in Table 105 where the results for the Hula Valley pilot are presented, the level of risk for the food sector is expected to be at a “High” level under both RCP4.5 and RCP8.5 scenarios. This is the result of a “High” level on hazard and exposure indicator, as well as a “Medium-High” level of vulnerability. Furthermore, the adaptive capacity is characterized as “Low-Medium” for the pilot, which is not considered sufficient to offset the expected risk related to climate change.

Table 105: Overall risk of the WEF Nexus sectors, Hula Valley pilot.

	RCP 4.5	RCP 8.5	Adaptive Capacity
Food	High	High	Low-Medium

5.6 Middle Jordan Valley, Deir Alla (Jordan)

In this section the results of the hazard, exposure and vulnerability assessment, as well as of the adaptive capacity and the overall climate risk assessment are provided, for the Middle Jordan Valley, Deir Alla (Jordan).

5.6.1 Climate Related Hazard Indicators

In the following paragraphs, the results for the hazard indicators are presented, for the food, water, and ecosystems sectors.

Biologically Effective Degree Days over 10-days (BEDD)

The projected relative change (%) of the BEDD over 10-days, for the future sub-periods based on the RCP4.5 and RCP8.5, compared to the reference period, is summarized in Table 106. In general, an increase of the BEDD indicator is expected in the future for both scenarios. It may be concluded that for the short-term and mid-term period, there is no significant difference between the scenarios, with an average 5% and 11.5% increase from the reference period respectively. For the long-term period the increase is more noticeable, up to 11% for RCP4.5 and 24% for RCP8.5.

Table 106: Relative change (%) of the Biologically Effective Degree Days over 10-days, for the future sub-periods based on the RCP4.5 and RCP8.5, compared to the reference period, Deir Alla pilot.

BEDD	2011-2040		2041-2070		2071-2100	
	RCP4.5	RCP8.5	RCP4.5	RCP8.5	RCP4.5	RCP8.5
relative change (%)	4	6	9	14	11	24

Fire Weather index

The relative change (%) of the FWI in the future compared to the reference period for both scenarios, is shown in Table 107. It can be observed that there is a slight increase of FWI in the future for both scenarios. Specifically, for the short-term and mid-term periods the increase is not exceeds the 6% for both scenarios, while in the long-term period this increasing trend reaches up to 11% for RCP8.5.

Table 107: Relative change (%) of the FWI, for the future sub-periods based on the RCP4.5 and RCP8.5, compared to the reference period, Deir Alla pilot.

Fire Weather Index	2011-2040		2041-2070		2071-2100	
	RCP4.5	RCP8.5	RCP4.5	RCP8.5	RCP4.5	RCP8.5
relative change (%)	3	2	5	6	6	11

Heat Stress days over 35°C

The relative change (%) of the projected number of heat stress days (>35°C) in the future, is summarized in Table 108. As it can be observed, the difference between the two scenarios for all three future periods is noticeable, with the RCP8.5 presenting the highest increase. Specifically, for the near-term period an increase of 23.5% is projected on average for the two scenarios. For the mid-term period, an increase of 38% is projected based on RCP4.5 and 54% for the RCP8.5. Finally, for the long-term period, the increase is expected to reach 45% for the RCP4.5 and 79% for the RCP8.5.

Table 108: Relative change (%) of the Heat Stress days over 35°C, for the future sub-periods based on the RCP4.5 and RCP8.5, compared to the reference period, Deir Alla pilot.

Heat Stress days over 35°C	2011-2040		2041-2070		2071-2100	
	RCP4.5	RCP8.5	RCP4.5	RCP8.5	RCP4.5	RCP8.5
relative change (%)	22	25	38	54	45	79

5.6.2 Exposure Indicators

In the following paragraphs, the results for the exposure indicators are presented, for the food, water, and ecosystems sectors.

Share of area cultivated with crops

The share of areas cultivated with crops in the Deir Alla pilot area, is presented in Table 109. As it can be observed, the cultivated area is significant (56%) and therefore, the exposure of agriculture is estimated to be high.

Table 109: Share of crops under study in Deir Alla pilot area.

	Total area (hectares)	Cultivated area (hectares)	Share of area cultivated with crops
Deir Alla pilot	451	251	56%

Share of area covered with forests and natural areas

The share of natural areas (land covered by forests, natural grasslands, shrubs, marshes etc.) compared to the total area of the pilot is presented in Table 110. As it can be observed, the pilot is covered by natural areas by 34% and therefore, the ecosystems are considered to be exposed in a medium-high level.

Table 110: Share of natural areas in Deir Alla pilot area.

	Area (hectares)	Natural area (hectares)	Share of natural area
Deir Alla pilot	451	152	34%

5.6.3 Vulnerability Indicators

In the following paragraphs, the results for the vulnerability indicators are presented, for the food, water, and ecosystems sectors.

Water Exploitation Index

The water exploitation index (WEI) of Jordan where the Deir Alla pilot is located, is presented in Table 111. Specifically, the WEI is estimated to be 58% which is above the threshold under which water stress can begin to be a limiting factor on economic development for the region. Thus, the vulnerability related to this indicator is considered to be high.

Table 111: Water vulnerability index expressed as Water Exploitation Index, Deir Alla pilot area.

Jordan	Water Exploitation Index
National level	58%

Share of agricultural water consumption

The share of agricultural water consumption in Jordan is shown in Table 112. Specifically, the share of agricultural water consumption is up to 50%, therefore a potential reduction in water availability due to climate change, would be critical for the agricultural sector. Thus, the vulnerability related to this indicator is considered to be medium-high.

Table 112: Water vulnerability index expressed as share of agricultural water consumption, Deir Alla pilot area.

Jordan	Share of agricultural water consumption
National level	50%

Agricultural Income

The agricultural income of Jordan, compared to the Mediterranean average agricultural income, is presented in Table 113. It is observed that agricultural income of Jordan is lower (64%) compared to the Mediterranean average. This indicates that the dependency of the country to the agricultural income is lower than the average Mediterranean countries dependency. The vulnerability related to this indicator is considered to be medium-high.

Table 113: Food vulnerability index expressed as agriculture income, Deir Alla pilot area.

	Agricultural income
	Value added of agriculture as percent of the national GDP
Mediterranean Average	7%
Jordan	4.5%
Jordan compared to Mediterranean average	64%

Share of protected areas

As it may be seen in Table 114, the share of protected areas over the total area of the pilot, is estimated to be 0%. Therefore, the share of protected areas is considered low for the Deir Alla pilot.

Table 114: Share of protected areas, Deir Alla pilot area.

	Total area (hectares)	Protected area (hectares)	Share of protected area
Deir Alla pilot	451	0	0%

This project is part of the PRIMA programme supported by the European Union.
GA n° [2041] [LENSES] [Call 2020 Section 1 Nexus IA]

5.6.4 Adaptive capacity

In this section, the results of the assessment of the adaptive capacity of the Deir Alla pilot are presented. Specifically, the results refer to the assessment of the GDP index for the pilot at national level.

The economic capacity expressed as the GDP of the country in relation to the Mediterranean average is presented in the table that follows. As it can be observed, the GDP of Jordan is 44,800 million US dollars, which is significantly lower (10%) to the Mediterranean average. This reflecting a low economic capacity of the country and subsequently of the Deir Alla pilot.

Table 115: Relative Economic capacity of the Deir Alla pilot area.

	GDP (million US dollars)	in % of Mediterranean average
Mediterranean average (21 countries)	415,200	100%
Turkey	44,800	10%

5.6.5 Overall Risk

In this section, the results of the climate risk assessment for the food and ecosystems Nexus sectors of the Deir Alla pilot area are presented for the period 2041-2070, based on the RCP4.5 and RCP8.5. Specifically, the overall risk is presented both qualitatively and quantitatively per risk component at indicator level.

As it can be observed in Table 116, the overall risk for the food sector is considered to be "Medium" according to RCP4.5 and "Medium-High" according to RCP8.5. This is a result of a "Medium-High" hazard, in combination with a "Medium-High" vulnerability, and a "High" exposure. Additionally, an important role has the indicator Heat Stress, which is expected to be at "High" level under RCP8.5 affecting the overall climate risk.

Table 116: Qualitative climate risk assessment per risk component of the food sector for the period 2041-2070, Deir Alla pilot area.

Hazard indicators actual values	**RCP 4.5**	**RCP 8.5**
Heat stress >35 °C	Medium-High	High
BEDD	Low	Low
Fire weather index WFI>30	High	High
Hazard composite indicator	**Medium-High**	**Medium-High**
Exposure indicator	**High**	**High**
Agricultural income	Medium-High	Medium-High
Water exploitation	High	High
Agricultural water consumption	Medium-High	Medium-High
Vulnerability composite indicator	**Medium-High**	**Medium-High**
Food System Risk	**Medium**	**Medium-High**

The detailed results of the climate risk assessment for the food sector are presented quantitatively at normalized scale [0, 5] in Table 117. The negative values of the hazard indicators are assigned to reflect a beneficial effect and thus compensate risk.

This project is part of the PRIMA programme supported by the European Union.
GA n° [2041] [LENSES] [Call 2020 Section 1 Nexus IA]

Table 117: Quantitative climate risk assessment per risk component of the food sector for the period 2041-2070, Deir Alla pilot area.

Hazard indicators actual values	RCP 4.5	RCP 8.5
Heat stress >35 °C	3.90	4.37
BEDD	-0.57	-0.93
Fire weather index WFI>30	5.00	5.00
Hazard composite indicator	**3.40**	**3.65**
Exposure indicator	**4.40**	**4.40**
Agricultural income	3.21	3.21
Water exploitation	4.30	4.30
Agricultural water consumption	3.50	3.50
Vulnerability composite indicator	**3.67**	**3.67**
Food System Risk	**2.78**	**3.80**

Ecosystem Risk

As it can be observed in Table 118 for the ecosystem sector, the risk levels are expected to be "Medium-High" for the Deir Alla pilot area. This is the result of a "High" hazard, in combination with a "Medium-High" exposure of the ecosystems and a "Low" vulnerability, due to the absence of protected ecosystem areas in the pilot.

Table 118: Qualitative climate risk assessment per risk component of the ecosystem sector for the period 2041-2070, Deir Alla pilot area.

Hazard indicators actual values	RCP 4.5	RCP 8.5
Heat stress >35 °C **(days)**	Medium-High	High
Fire weather index WFI>30 **(days)**	High	High
Hazard composite indicator	**High**	**High**
Exposure indicator	**Medium-High**	**Medium-High**
Vulnerability indicator	**Low**	**Low**
Ecosystems Risk	**Medium-High**	**Medium-High**

The detailed results of the climate risk assessment for the ecosystem sector are presented quantitatively at normalized scale [0, 5] in Table 119.

Table 119: Quantitative climate risk assessment per risk component of the ecosystem sector for the period 2041-2070, Deir Alla pilot area.

Hazard indicators actual values	RCP 4.5	RCP 8.5
Heat stress >35 °C **(days)**	3.90	4.37
Fire weather index WFI>30 **(days)**	5.00	5.00
Hazard composite indicator	**4.12**	**4.49**
Exposure indicator	**3.69**	**3.69**
Vulnerability indicator	**0.00**	**0.00**
Ecosystems Risk	**3.21**	**3.43**

Following, the results of the climate risk assessment for the period 2041-2070 are summarized for Ecosystem-Food sectors.

As it may be seen in Table 120 where he results for the Deir Alla pilot are presented, the level of risk for the food sector is expected to be at "Medium" level for RCP4.5 and "Medium-High" for RCP8.5. This is mostly the result of the Heat stress indicator that is expected at a "High" level under RCP8.5. In addition, a "Medium-High" level of risk is expected under both RCP scenarios for the ecosystem sector, which is the result of a "High" level hazard, "Medium-High" exposure and a "Low" vulnerability.

Furthermore, the adaptive capacity is characterized as "Low" for the pilot, which is not considered sufficient to offset the expected risk for the food and ecosystem sector.

Table 120: Overall risk of the WEF Nexus sectors, Deir Alla pilot area.

	RCP 4.5	RCP 8.5	Adaptive Capacity
Food	Medium	Medium-High	Low
Ecosystem	Medium-High	Medium-High	

5.7 Tarquinia plain (Italy)

In this section the results of the hazard, exposure and vulnerability assessment, as well as of the adaptive capacity and the overall climate risk assessment are provided, for the Tarquinia plain (Italy).

5.7.1 Climate Related Hazard Indicators

In the following paragraphs, the results for the hazard indicators are presented, for the food, water, and ecosystems sectors.

Actual Aridity

The relative change (%) of the actual aridity in the future compared to the reference period for both scenarios, is presented in Table 121. It can be observed that there is an increase of aridity for all the three future sub-periods for both scenarios. The highest increase (+36%) is expected for the long-term period and the lowest increase (+10%) for the short-term period both in case of RCP8.5.

Table 121: Relative change (%) of the mean annual aridity (actual evapotranspiration/precipitation), for the future sub-periods based on the RCP4.5 and RCP8.5, compared to the reference period, Tarquinia pilot.

Actual Aridity	2011-2040		2041-2070		2071-2100	
	RCP4.5	RCP8.5	RCP4.5	RCP8.5	RCP4.5	RCP8.5
relative change (%)	20	10	17	30	16	36

Biologically Effective Degree Days over 10-days (BEDD)

The projected relative change (%) of the BEDD over 10-days, for the future sub-periods based on the RCP4.5 and RCP8.5, compared to the reference period, is summarized in Table 122. In general, an increase of the BEDD indicator is expected in the future for both scenarios. It may be concluded that for the short-term and mid-term period, there is no significant difference between the scenarios, with an average 7% and 15%

increase from the reference period respectively. For the long-term period the increase is more noticeable, up to 16% for RCP4.5 and 30% for RCP8.5.

Table 122: Relative change (%) of the Biologically Effective Degree Days over 10-days, for the future sub-periods based on the RCP4.5 and RCP8.5, compared to the reference period, Tarquinia pilot.

BEDD	2011-2040		2041-2070		2071-2100	
	RCP4.5	RCP8.5	RCP4.5	RCP8.5	RCP4.5	RCP8.5
relative change (%)	6	8	13	18	16	30

Fire Weather index

The relative change (%) of the FWI in the future compared to the reference period for both scenarios, is shown in Table 123. It can be observed that there is an increase of FWI in the future for both scenarios. Specifically, for the short-term period the increase from the reference period is 7.5% on average while in the long-term period this increasing trend reaches up to 16% for RCP4.5 and to 35% for RCP8.5.

Table 123: Relative change (%) of the FWI, for the future sub-periods based on the RCP4.5 and RCP8.5, compared to the reference period, Tarquinia pilot.

Fire Weather Index	2011-2040		2041-2070		2071-2100	
	RCP4.5	RCP8.5	RCP4.5	RCP8.5	RCP4.5	RCP8.5
relative change (%)	6	9	15	22	16	35

Heat Stress days over 30°C

The relative change (%) of the projected number of heat stress days (>30°C) in the future, is summarized in Table 124. As it can be observed, the difference between the two scenarios for all three future periods is noticeable, with the RCP8.5 presenting the highest increase. Specifically, for the near-term period increase of 100% is projected for the RCP4.5, while the respective change for the RCP8.5 is 130%. For the mid-term period, an increase of 200% is projected based on RCP4.5 and 290% for the RCP8.5. Finally, for the long-term period, the increase is expected to reach 260% for the RCP4.5 and 550% for the RCP8.5.

Table 124: Relative change (%) of the Heat Stress days over 30°C, for the future sub-periods based on the RCP4.5 and RCP8.5, compared to the reference period, Tarquinia pilot.

Heat Stress days over 30°C	2011-2040		2041-2070		2071-2100	
	RCP4.5	RCP8.5	RCP4.5	RCP8.5	RCP4.5	RCP8.5
relative change (%)	100	130	200	290	260	550

Soil Moisture

The projected relative change (%) of soil moisture in the future based on the RCP4.5 and RCP8.5, is summarized in Table 125. In general, a decreasing trend is observed under both scenarios. It may be concluded that for the short-term period, there is no trend as the relative change for both scenarios is 0%.

For the mid-term period there is a reduction of 8% on average for the two scenarios, while for the long-term period the reduction is the same to the mid-term for the RCP4.5 and higher for the RCP8.5 (-14%).

Table 125: Relative change (%) of soil moisture in the future compared to the reference period, based on the RCP4.5 and RCP8.5, Tarquinia pilot.

Soil Moisture	2011-2040		2041-2070		2071-2100	
	RCP4.5	RCP8.5	RCP4.5	RCP8.5	RCP4.5	RCP8.5
relative change (%)	0	0	-10	-6	-10	-14

Following, the hazard indicators are presented through maps for the reference period (1971-2000) and the future period (2041-2070), under the RCP4.5 and RCP8.5.

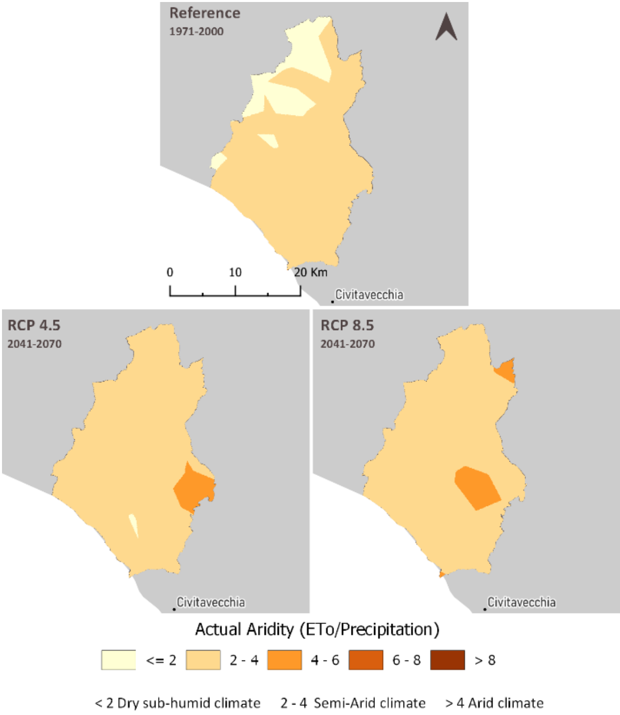

Figure 69: Spatial distribution of actual aridity, for the reference period (top) and the future period (2041-2070) based on the RCP4.5 and RCP8.5 (bottom)

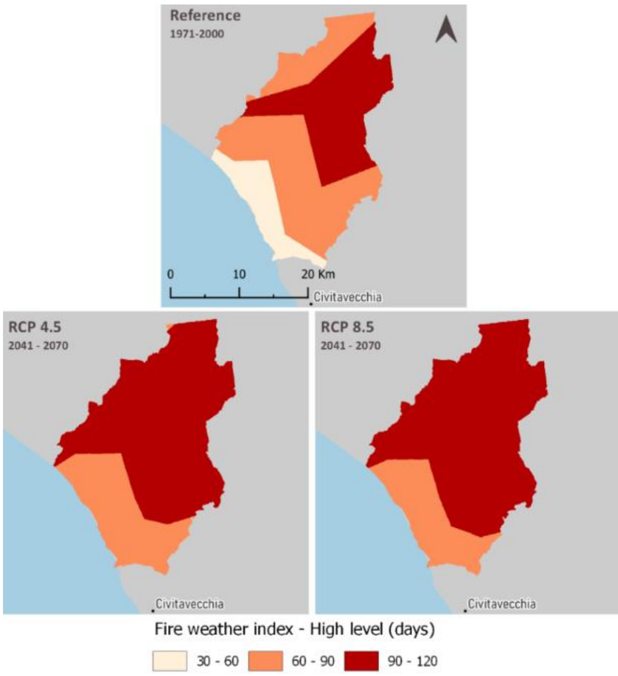

Figure 70: Spatial distribution of the FWI, for the reference period (top) and the future period (bottom)based on the RCP4.5 and RCP8.5

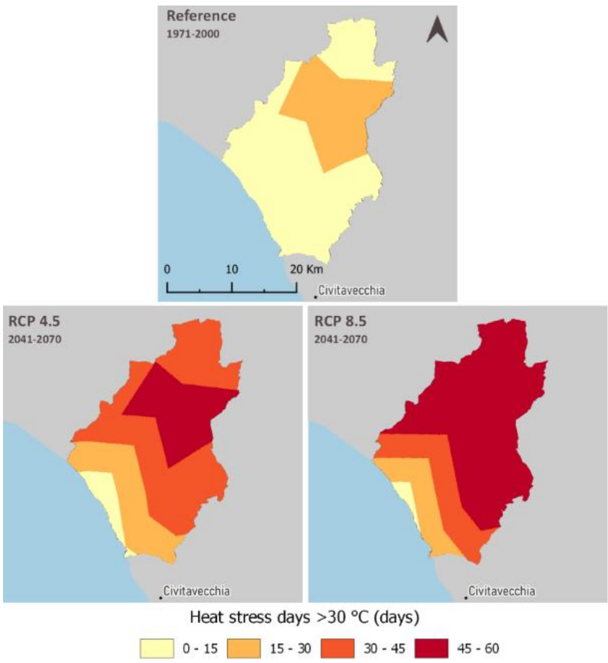

Figure 71: Spatial distribution of the mean annual number of days when maximum daily temperature is > 30°C, for the reference period (top) and the future period (2041-2070) based on the RCP4.5 and RCP8.5 (bottom)

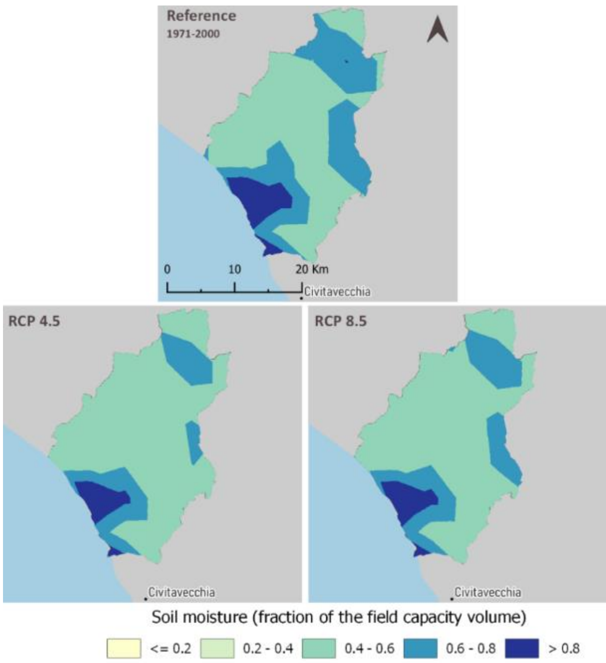

Figure 72: Spatial distribution of soil moisture, for the reference period (top) and the future period (2041-2070) based on the RCP4.5 and RCP8.5 (bottom)

5.7.2 Exposure Indicators

In the following paragraphs, the results for the exposure indicators are presented, for the food, water, and ecosystems sectors.

Share of area cultivated with crops

The share of areas cultivated with crops in Tarquinia pilot area, is presented in Table 126. As it can be observed, the cultivated area in the pilot is significant (77%) and therefore, the exposure of agriculture is estimated to be high.

Table 126: Share of crops under study in Tarquinia pilot area.

	Total area (hectares)	Cultivated area (hectares)	Share of area cultivated with crops
Tarquinia pilot	57,386	44,228	77%

Share of area covered with forests and natural areas

The share of natural areas (land covered by forests, natural grasslands, shrubs, marshes etc.) compared to the total area of the pilot is presented in Table 127. As it can be observed, the pilot is covered by natural areas by 17%. Therefore, the ecosystems are considered to be moderately exposed in the Tarquinia pilot.

Table 127: Share of natural areas in Tarquinia pilot area.

	Area (hectares)	Natural area (hectares)	Share of natural area
Tarquinia pilot	57,386	9,587	17%

5.7.3 Vulnerability Indicators

In the following paragraphs, the results for the vulnerability indicators are presented, for the food, water, and ecosystems sectors.

Water Exploitation Index

The water exploitation index (WEI) of the Middle Apennines River Basin which is located in the Tarquinia pilot, is presented in Table 128. Specifically, the WEI is estimated to be 41% which is above the threshold under which water stress can begin to be a limiting factor on economic development for the region. Thus, the vulnerability related to this indicator is considered to be high.

Table 128: Water vulnerability index expressed as Water Exploitation Index, Middle Apennines River Basin.

River Basin District	Water Exploitation Index
RBD Middle Apennines	41%

Share of agricultural water consumption

The share of agricultural water consumption is presented in Table 129 at national level. Specifically, the share of agricultural water consumption in Italy is high, up to 50%, therefore a potential reduction in water availability due to climate change, would be critical for the agricultural sector. Thus, the vulnerability related to this indicator is considered to be medium-high.

Table 129: Water vulnerability index expressed as share of agricultural water consumption, Tarquinia pilot.

Italy	Share of agricultural water consumption
National level	50%

Agricultural Income

The agricultural income of Lazio region where the Tarquinia pilot is located, compared to the average national agricultural income of Italy, is presented in Table 130. It is observed that the agricultural income of the region of Lazio is almost the same (108%) compared to the national average. This indicates a moderate dependency of the country to the agricultural income of the region. Thus, the vulnerability related to this indicator is considered to be moderate.

Table 130: Food vulnerability index expressed as agriculture income, Lazio Region

Tarquinia pilot	Agricultural income	
	Million Euro	% of national average
National Average	1,468	100%
Lazio Region	1,600	108%

Share of protected areas

As it may be seen in Table 131, the share of protected areas over the total area of the pilot, is estimated to be 22% and therefore the share of protected areas is considered as medium-high.

Table 131: Share of protected areas, Tarquinia pilot area.

	Total area (hectares)	Protected area (hectares)	Share of protected area
Tarquinia pilot	57,386	12,570	22%

5.7.4 Adaptive capacity

In this section, the results of the assessment of the adaptive capacity of the Tarquinia pilot are presented. Specifically, the results refer to the assessment of the GDP index for the pilot at national level.

The economic capacity expressed as the GDP of the country in relation to the EU average is presented in the table that follows. As it can be observed, the GDP of Italy is 29,304 Euros per capita which is close to the EU average (96%), thus reflecting a medium economic capacity of the country and subsequently of the Tarquinia pilot.

This project is part of the PRIMA programme supported by the European Union.
GA n° [2041] [LENSES] [Call 2020 Section 1 Nexus IA]

Table 132: Relative Economic capacity of the Tarquinia pilot area.

Tarquinia pilot	GDP per capita (Euro)	in % of EU average
EU average (27 countries)	30,632	100%
Italy	29,304	96%

5.7.5 Overall Risk

In this section, the results of the climate risk assessment for the food and ecosystems Nexus sectors of the Tarquinia pilot are presented for the period 2041-2070, based on the RCP4.5 and RCP8.5. Specifically, the overall risk is presented both qualitatively and quantitatively per risk component at indicator level.

As it can be observed in Table 133, the overall risk for the food sector is considered to be "Medium-High". This is a result of a "Medium" to "Medium-High" hazard, in combination with a "Medium-High" vulnerability, and a "High" exposure.

Table 133: Qualitative climate risk assessment per risk component of the food sector for the period 2041-2070, Tarquinia pilot area.

Indicators	**RCP 4.5**	**RCP 8.5**
Heat stress >35 °C	Medium	Medium-High
BEDD	Low	Low-Medium
Actual aridity	Medium-High	Medium-High
Fire weather index WFI>30	Medium-High	Medium-High
Soil moisture	Medium	Medium
Hazard composite indicator	**Medium**	**Medium-High**
Exposure indicator	**High**	**High**
Agricultural income	Medium	Medium
Water exploitation	High	High
Agricultural water consumption	Medium-High	Medium-High
Vulnerability composite indicator	**Medium-High**	**Medium-High**
Food System Risk	**Medium-High**	**Medium-High**

The detailed results of the climate risk assessment for the food sector are presented quantitatively at normalized scale [0, 5] in Table 134. The negative values of the hazard indicators are assigned to reflect a beneficial effect and thus compensate risk.

Table 134: Quantitative climate risk assessment per risk component of the food sector for the period 2041-2070, Tarquinia pilot area.

Indicators	RCP 4.5	RCP 8.5
Heat stress >30 °C	2.77	3.62
BEDD	-0.85	-1.22
Actual aridity	3.27	3.37
Fire weather index WFI>30	3.39	3.57
Soil moisture	2.75	2.63
Hazard composite indicator	**2.74**	**3.03**
Exposure indicator	**4.93**	**4.93**
Agricultural income	2.72	2.72
Water exploitation	4.02	4.02
Agricultural water consumption	3.67	3.67
Vulnerability composite indicator	**3.47**	**3.47**
Food System Risk	**3.32**	**3.49**

As it can be observed in Table 135 for the ecosystem sector, the level of risk is considered to be "Medium" according to RCP4.5 and "Medium-High" according to RCP8.5. This is a result of a "Medium-High" hazard, in combination with a "Medium-High" vulnerability, and a "Medium" exposure of the ecosystem sector. Additionally, an important role has the indicator Heat Stress, which is expected to be at a "Medium-High" level under RCP8.5 affecting the overall climate risk.

Table 135: Qualitative climate risk assessment per risk component of the ecosystem sector for the period 2041-2070, Tarquinia pilot area.

Indicators	RCP 4.5	RCP 8.5
Heat stress >30 °C	Medium	Medium-High
Actual aridity	Medium-High	Medium-High
Fire weather index WFI>30	Medium-High	Medium-High
Soil moisture	Medium	Medium
Hazard composite indicator	**Medium-High**	**Medium-High**
Exposure indicator	**Medium**	**Medium**
Vulnerability indicator	**Medium-High**	**Medium-High**
Ecosystems Risk	**Medium**	**Medium-High**

This project is part of the PRIMA programme supported by the European Union.
GA n° [2041] [LENSES] [Call 2020 Section 1 Nexus IA]

The detailed results of the climate risk assessment for the ecosystem sector are presented quantitatively at normalized scale [0, 5] in Table 136.

Table 136: Quantitative climate risk assessment per risk component of the ecosystem sector for the period 2041-2070, Tarquinia pilot area.

Indicators	RCP 4.5	RCP 8.5
Heat stress >30 °C	2.77	3.62
Actual aridity	3.27	3.37
Fire weather index WFI>30	3.39	3.57
Soil moisture	2.75	2.63
Hazard composite indicator	**3.05**	**3.26**
Exposure indicator	**2.67**	**2.67**
Vulnerability indicator	**3.10**	**3.10**
Ecosystems Risk	**2.98**	**3.11**

Following, the results of the climate risk assessment for the period 2041-2070 are summarized for Ecosystem-Food sectors.

As it may be seen in Table 137 where the results for the Tarquinia pilot are presented, the level of risk for the food sector is expected to be at a “Medium-High” level under both RCP scenarios. This is the result of a “High” exposure and “Medium-High” vulnerability and hazard indicator at “Medium” level for RCP4.5 and “Medium-High” for RCP8. In addition, the level of risk for the ecosystem sector is expected to be at “Medium” level for RCP4.5 and “Medium-High” for RCP8.5. This is mostly the result of the Heat stress indicator that is expected at a higher level under RCP8.5.

Furthermore, the adaptive capacity is characterized as “Medium” for the pilot, which is not considered sufficient to offset the expected risk for the food and ecosystem sector.

Table 137: Overall risk of the WEF Nexus sectors, Tarquinia pilot area.

	RCP 4.5	RCP 8.5	Adaptive Capacity
Food	Medium-High	Medium-High	Medium
Ecosystem	Medium	Medium-High	

This project is part of the PRIMA programme supported by the European Union.
GA n° [2041] [LENSES] [Call 2020 Section 1 Nexus IA]

6 Conclusions

In this final section, an overview of the results is given for each pilot, for both Climate Projections and Climate Risk Assessment.

Doñana

Regarding the results of the climate projections for the pilot, the trend is increasing for the temperature, and is expected to reach up to +4.3°C under the RCP8.5 scenario during the long-term period. As for the precipitation the trend is decreasing up to -62 mm for both dry and wet periods. Regarding actual evapotranspiration, a decrease is expected for the future period up to -73 mm.

The results of the climate risk assessment for the period 2041-2070 shows that according to RCP4.5, the risk for the WEF systems, is expected to be “Medium-High” in both Northern and Southern parts of the pilot. According to RCP8.5 the risk for the food system will be higher than RCP4.5 for the Northern area of the pilot where there is greatest exposure due to the concentration of agricultural activities. In addition, a high level of risk is expected under RCP8.5 for ecosystems in the Southern part of the pilot, where the National Park is located and therefore there is greater exposure of ecosystems. In addition, the adaptive capacity is characterized as “Medium” for the pilot, which is not considered sufficient to offset the expected risk for the WEF Nexus sectors.

Pinios

Regarding the results of the climate projections for the pilot, the trend is increasing for the temperature, and is expected to reach up to +4.3°C under the RCP8.5 scenario during the long-term period. As for the precipitation, the signal is not clear for the whole study period. In fact, there is 10 mm decrease during the short-term dry period in case of RCP4.5 and an increase in both dry and wet seasons during the mid-term period up to 23 mm. Actual evapotranspiration is anticipated to have the maximum increase during the mid- and long-term periods in the case of RCP8.5, up to around 50 mm.

The results of the climate risk assessment for the period 2041-2070 shows that the level of risk for Food sector is expected to be “Medium-High” for both RCP scenarios at Delta and Agia region of the pilot. In addition, for the ecosystem sector, according to the RCP 4.5 the level of risk is expected to be “Medium-High” for both regions of the pilot, while the level of risk under RCP 8.5 increase to the “High” level. This is mostly explained by the increase of temperature under RCP8.5 and subsequently to the increase of Heat Stress indicator for Agia region and Fire Weather Index for Delta region. Furthermore, the adaptive capacity is characterized as “Low-Medium” for the pilot, which is not considered sufficient to offset the expected risk for the WEF Nexus sectors.

Koiliaris

Regarding the results of the climate projections for the pilot, the trend is increasing for the temperature, and is expected to reach up to +4°C under the RCP8.5 scenario during the long-term period. As for the precipitation, there is a strong decreasing signal for the whole study period and especially for the wet season where the decrease is expected to be around -110 mm. Actual evapotranspiration is anticipated to have the maximum increase during the mid- and long-term periods in the case of RCP8.5, up to 46 mm on average.

The results of the climate risk assessment for the period 2041-2070 shows that the level of risk for all WEF NEXUS sectors is expected to be “Medium-High” according to both RCP scenarios. The risk of the food sector is the result of a “Medium” to “Medium-High” hazard, as well as a “Medium-High” exposure and vulnerability. In addition, the risk of the ecosystem sector is the result of a “Medium-High” hazard, combined with a “High” exposure and vulnerability. Furthermore, the adaptive capacity is characterized as “Low-Medium” for the pilot, which is not considered sufficient to offset the expected risk for the WEF Nexus sectors.

Gediz

Regarding the results of the climate projections for the pilot, the trend is increasing for the mean temperature, and is expected to reach up to +4.6°C under the RCP8.5 scenario during the long-term period. As for the precipitation, there is an increasing trend for the whole study period and especially for the wet period where the increase is expected to have a maximum value (up to +38 mm) in the case of RCP4.5 during the short-term period. Actual evapotranspiration is anticipated to have the maximum increase during the long-term period in the case of RCP8.5, up to 60 mm.

The results of the climate risk assessment for the period 2041-2070 shows that the level of risk for the food sectors is expected to be “Medium-High” for both RCP scenarios, due to the high exposure of the pilot area, that is highly cultivated and the “Medium” to “Medium-High” level of the composite Hazard indicator. In addition, a “Low-Medium” level of risk is expected under both RCP scenarios for the ecosystem sector, which is the result of the “Low” exposure and vulnerability indicators. Furthermore, the adaptive capacity is characterized as “Low-Medium” for the pilot, which is not considered sufficient to offset the expected risk for the food sector.

Hula Valley

Regarding the results of the climate projections for the pilot, the trend is increasing for the mean temperature, and is expected to reach up to +5.7°C under the RCP8.5 scenario during the long-term period. As for the precipitation, there is a strong decreasing signal for the whole study period and especially for the wet season where the decrease is expected to be up to -163 mm during the wet period, based on RCP8.5. Actual evapotranspiration is expected to be reduced for the whole study period, with the maximum reduction during the long-term period in the case of RCP8.5, up to -110 mm.

The results of the climate risk assessment for the period 2041-2070 shows that the level of risk for the food sector is expected to be “High” under both RCP4.5 and RCP8.5 scenarios. This is the result of a “High” level on hazard and exposure indicator, as well as a “Medium-High” level of vulnerability. Furthermore, the adaptive capacity is characterized as “Low-Medium” for the pilot, which is not considered sufficient to offset the expected risk related to climate change.

Deir Alla

Regarding the results of the climate projections for the pilot, the trend is increasing for the mean temperature, and is expected to reach up to +5.9°C under the RCP8.5 scenario during the long-term period. As for the precipitation, there is a strong decreasing signal for the whole study period and especially for the wet season where the decrease is expected to be up to -94 mm during the wet period, based on RCP8.5. Actual evapotranspiration is expected to be reduced for the whole study period, with the maximum reduction during the long-term period in the case of RCP8.5, up to -106 mm.

This project is part of the PRIMA programme supported by the European Union.
GA n° [2041] [LENSES] [Call 2020 Section 1 Nexus IA]

The results of the climate risk assessment for the period 2041-2070 shows that the level of risk for the food sector is expected to be “Medium” for RCP4.5 and rise on the “Medium-High” level for RCP8.5. The rise of temperature under RCP8.5 affect the Heat stress indicator that is expected to be at a “High” level for this scenario. In addition, a “Medium-High” level of risk is expected under both RCP scenarios for the ecosystem sector, which is the result of a “High” level hazard, “Medium-High” exposure and a “Low” vulnerability. Furthermore, the adaptive capacity is characterized as “Low” for the pilot, which is not considered sufficient to offset the expected risk for the food and ecosystem sector.

Tarquinia

Regarding the results of the climate projections for the pilot, the trend is increasing for the mean temperature, and is expected to reach up to +4°C under the RCP8.5 scenario during the long-term period. As for the precipitation, there is a decreasing trend for the dry period up to -27 mm, while the trend is increasing for the wet period where the increase is expected to have a maximum value up to +36 mm on average for both scenarios. Actual evapotranspiration is anticipated to have the maximum increase during the long-term period in the case of RCP8.5, up to 21 mm.

The results of the climate risk assessment for the period 2041-2070 shows that the risk for the food sector is expected to be at a “Medium-High” level under both RCP scenarios. This is the result of a “High” exposure and “Medium-High” vulnerability and hazard indicator at “Medium” level for RCP4.5 and “Medium-High” for RCP8. In addition, the level of risk for the ecosystem sector is expected to be at “Medium” level for RCP4.5 and “Medium-High” for RCP8.5. This is mostly the result of the Heat stress indicator that is expected at a higher level under RCP8.5 due to the rise of temperature. Furthermore, the adaptive capacity is characterized as “Medium” for the pilot, which is not considered sufficient to offset the expected risk for the food and ecosystem sector.

References

Berg, P., Photiadou, C., Nauta, L., Ludwig, F. (2021). Product User Guide, Specification and Workflow. Dataset: Hydrology related climate impact indicators from 1970 to 2100 derived from bias adjusted European climate projections. C3S_424_SMHI Operational Water Service. Copernicus Climate Change Service.

Bervoets, J., Eveillé, F., & Thulstrup, A. (2018). Strengthening the Water-Food-Energy-Ecosystems (WFEE) Nexus. Food and Agriculture Organization of the United Nations (FAO), Rome, Italy.

Cardona, O.D., van Aalst, M. K., Birkmann, J., Fordham, M., McGregor, G., Perez, R., Pulwarty, R.S., Schipper, E.L.F., Sinh, B.T. (2012). Determinants of risk: exposure and vulnerability. In: Managing the Risks of Extreme Events and Disasters to Advance Climate Change Adaptation [Field, C.B., V. Barros, T.F. Stocker, D. Qin, D.J. Dokken, K.L. Ebi, M.D. Mastrandrea, K.J. Mach, G.-K. Plattner, S.K. Allen, M. Tignor, and P.M. Midgley (eds.)]. A Special Report of Working Groups I and II of the Intergovernmental Panel on Climate Change (IPCC). Cambridge University Press, Cambridge, UK, and New York, NY, USA, pp. 65-108.

Coordinated Regional Climate Downscaling Experiment. (2021). Retrieved from https://cordex.org/about/. Accessed 4 September 2021.

Copernicus Climate Change Service (C3S). Retrieved from https://cds.climate.copernicus.eu/cdsapp#!/dataset/projections-cordex-domains-single-levels?tab=overview. Accessed 20 September 2021.

Cos, J., Doblas-Reyes, F., Jury, M., Marcos, R., Bretonnière, P. A., & Samsó, M. (2022). The Mediterranean climate change hotspot in the CMIP5 and CMIP6 projections. Earth System Dynamics, 13(1), 321-340. https://doi.org/10.5194/esd-13-321-2022

European Environmental Agency (EEA). 2017. Climate change, impacts and vulnerability in Europe 2016 An indicator-based report EEA Report No 1/2017.

European Environmental Agency (EEA). (2015). Water Exploitation Index for natural renewable freshwater resources in the Mediterranean countries. Water Exploitation Index for natural renewable freshwater resources in the Mediterranean countries — European Environment Agency (europa.eu)

European Environmental Agency (EEA). (2019). Water exploitation index plus (WEI+) in European river sub-basins. Water exploitation index plus (WEI+) for river basin districts (1990-2015) — European Environment Agency (europa.eu)

ELSTAT (2019). Statistics Data of areas and production of plant products - Table 1: Arable, Legumes, Industrial & Aromatic Plants and Large Crop Plants. http://www.minagric.gr/index.php/el/the-ministry-2/statistikes-tekmhrioshs/8510-statistika-ekt-parag-fytikonproionton

Eurostat (2022). Economic accounts for agriculture by NUTS 2 regions - AGR_R_ACCTS. https://ec.europa.eu/eurostat/databrowser/view/AGR_R_ACCTS__custom_3279221/default/table?lang=en

Eurostat (2022). Economic accounts for agriculture – AACT. https://ec.europa.eu/eurostat/cache/metadata/en/aact_esms.htm.

Eurostat (2022). Gross domestic product at market prices - TEC00001. https://db.nomics.world/Eurostat/tec00001

Eurostat (2022). Water use by river basin district (RBD) - ENV_WATUSE_RB https://ec.europa.eu/eurostat/databrowser/view/ENV_WATUSE_RB__custom_3124490/default/table?lang=en

Eurostat (2022). Freshwater resources by river basin district (RBD) - ENV_WATRES_RB https://ec.europa.eu/eurostat/databrowser/view/env_watres_rb/default/table?lang=en

Eurostat (2022). Water use by river basin district (RBD) - ENV_WATUSE_RB https://ec.europa.eu/eurostat/databrowser/view/ENV_WATUSE_RB__custom_3124490/default/table?lang=en

Eurostat (2022). Share of energy from renewable sources - NRG_IND_REN. https://ec.europa.eu/eurostat/databrowser/view/nrg_ind_ren/default/bar?lang=en

Eurostat (2022). Energy imports dependency - NRG_IND_ID. https://ec.europa.eu/eurostat/databrowser/product/view/NRG_IND_ID

Flato, G., Marotzke, J., Abiodun, B., Braconnot, P., Chou, S. C., Collins, W., ... & Rummukainen, M. (2014). Evaluation of climate models. In Climate change 2013: the physical science basis. Contribution of Working Group I to the Fifth Assessment Report of the Intergovernmental Panel on Climate Change (pp. 741-866). Cambridge University Press.

Ford, J., King, D. (2013). A framework for examining adaptation readiness. Mitigation and Adaptation Strategies for Global Change. Springer. doi: 10.1007/s11027-013-9505-8.

Fritzsche, K., Schneiderbauer, S., Bubeck, P., Kienberger, S., Buth, M., Zebisch, M., & Kahlenborn, W. (2014). The Vulnerability Sourcebook: Concept and guidelines for standardised vulnerability assessments. https://uni-salzburg.elsevierpure.com/de/publications/the-vulnerability-sourcebook-concept-and-guidelines-for-standardi

García Novo, F. (1997). The ecosystems of Doñana National Park. The ecology and conservation of European dunes., 77-116.

Giannakopoulos, C., and Karali, A. (2019). Fire Weather Index (FWI) – Dataset Description. C3S_422_Lot2_TEC/C3S European Tourism. Copernicus Climate Change Service.

Giorgi, F. (2019). Thirty years of regional climate modelling: where are we and where are we going next?. Journal of Geophysical Research: Atmospheres, 124(11), 5696-5723. https://doi.org/10.1029/2018JD030094

Giorgi, F., Jones, C., & Asrar, G. R. (2009). Addressing climate information needs at the regional level: the CORDEX framework. World Meteorological Organization (WMO) Bulletin, 58(3), 175. http://wcrp.ipsl.jussieu.fr/cordex/documents/CORDEX_giorgi_WMO.pdf

Gómez-Baggethun, E. R. I. K., Mingorria, S., Reyes-Garcia, V., Calvet, L., & Montes, C. (2010). Traditional ecological knowledge trends in the transition to a market economy: empirical study in the Doñana natural areas. Conservation Biology, 24(3), 721-729. https://doi.org/10.1111/j.1523-1739.2009.01401.x

Hersbach, H., Bell, B., Berrisford, P., Biavati, G., Horányi, A., Muñoz Sabater, J., ... & Thépaut, J. N. (2018). ERA5 hourly data on single levels from 1979 to present. Copernicus climate change service (c3s) climate data store (cds), 10(10.24381).

Iglesias, A., Sánchez, B., Garrote, L., & López, I. (2017). Towards adaptation to climate change: Water for rice in the coastal wetlands of Doñana, Southern Spain. Water Resources Management, 31(2), 629-653. doi: 10.1007/s11269-015-0995-x

IPCC (2014). Climate Change 2014: Synthesis Report. Contribution of Working Groups I, II and III to the Fifth Assessment Report of the Intergovernmental Panel on Climate Change Core Writing Team, R.K. Pachauri and L.A. Meyer (eds.). IPCC, Geneva, Switzerland, 151 pp. https://ar5-syr.ipcc.ch/ipcc/ipcc/resources/pdf/IPCC_SynthesisReport.pdf

IPCC (2018). Annex I: Glossary [Matthews, J.B.R. (ed.)]. In: Global Warming of 1.5°C. An IPCC Special Report on the impacts of global warming of 1.5°C above pre-industrial levels and related global greenhouse gas emission pathways, in the context of strengthening the global response to the threat of climate change, sustainable development, and efforts to eradicate poverty [Masson-Delmotte, V., P. Zhai, H.-O. Pörtner, D. Roberts, J. Skea, P.R. Shukla, A. Pirani, W. Moufouma-Okia, C. Péan, R. Pidcock, S. Connors, J.B.R. Matthews, Y. Chen, X. Zhou, M.I. Gomis, E. Lonnoy, T. Maycock, M. Tignor, and T. Waterfield (eds.)].

Katragkou, E., García-Díez, M., Vautard, R., Sobolowski, S., Zanis, P., Alexandri, G., ... & Jacob, D. (2015). Regional climate hindcast simulations within EURO-CORDEX: evaluation of a WRF multi-physics ensemble. Geoscientific model development, 8(3), 603-618. doi:10.5194/gmd-8-603-2015.

Kiani, A.K., Sardar, A., Khan, W.U., He, Y., Bilgic, A., Kuslu, Y., Raja, M.A.Z., (2021) Role of Agricultural Diversification in Improving Resilience to Climate Change: An Empirical Analysis with Gaussian Paradigm. Sustainability, 13, 9539. https://doi.org/10.3390/ su13179539

Kiktev, D., J. Caesar, L. V. Alexander, H. Shiogama, and M. Collier (2007), Comparison of observed and multimodeled trends in annual extremes of temperature and precipitation, Geophys. Res. Lett., 34, L10702, doi:10.1029/2007GL029539

Klinges, D. H., Duffy, J. P., Kearney, M. R., & Maclean, I. M. (2022). mcera5: Driving microclimate models with ERA5 global gridded climate data. Methods in Ecology and Evolution, 13(7), 1402-1411.

Kotlarski, S., Keuler, K., Christensen, O. B., Colette, A., Déqué, M., Gobiet, A., ... & Wulfmeyer, V. (2014). Regional climate modeling on European scales: a joint standard evaluation of the EURO-CORDEX RCM ensemble. Geoscientific Model Development, 7(4), 1297-1333. doi:10.5194/gmd-7-1297- 2014.

McGarigla, K., and Marks, B. (1995). FRAGSTATS: spatial pattern analysis program for quantifying landscape structure. Gen. Tech. Rep. PNW-GTR-351. Portland, OR: U.S. Department of Agriculture, Forest Service, Pacific Northwest Research Station. 122 p.

McKee, T. B., Doesken, N. J., and Kleist, J. (1993). The relationship of drought frequency and duration to time scales, in: vol. 17, Proceedings of the 8th Conference on Applied Climatology, American Meteorological Society, Boston, MA, 179–183.

McSweeney R, Hausfather Z (2018) Q&A: How do climate models work? Available via CarbonBrief. https://www.carbonbrief.org/qa-how-do-climate-models-work. Accessed 18 October 2021.

McSweeney, C. F., Jones, R. G., Lee, R. W., & Rowell, D. P. (2015). Selecting CMIP5 GCMs for downscaling over multiple regions. Climate Dynamics, 44(11), 3237-3260. https://doi.org/10.1007/s00382-014-2418-8

Mullen, S. L., & Buizza, R. (2002). The impact of horizontal resolution and ensemble size on probabilistic forecasts of precipitation by the ECMWF ensemble prediction system. Weather and Forecasting, 17(2), 173-191. https://doi.org/10.1175/1520-0434(2002)017<0173:TIOHRA>2.0.CO;2

Nobakht, M., Hutjes R., Beavis, P., Hara, S. (2019). Agroclimatic Indicators. Product User Guide and Specification. C3S Global Agriculture SIS. Copernicus Climate Change Service.

OECD (2020). oecd-water-policies-country-note-turkey.pdf

OECD 2008: Handbook on constructing composite indicators: methodology and user guide. Technical Report. Paris: OECD Publishing.

Pisinaras, V., Panagopoulos, A., Herrmann, F., Bogena, H.R., Doulgeris, C., Ilias, A., Tziritis, E. and Wendland, F., (2018). Hydrologic and geochemical research at Pinios Hydrologic Observatory: Initial results. Vadose zone journal, 17(1), pp.1-16

Reisinger, A., Howden, M., Vera, C. (2020). The Concept of Risk in the IPCC Sixth Assessment Report: A Summary of Cross-Working Group Discussions. Intergovernmental Panel on Climate Change, Geneva, Switzerland. pp15

Riahi, K., Rao, S., Krey, V., Cho, C., Chirkov, V., Fischer, G., ... & Rafaj, P. (2011). RCP 8.5—A scenario of comparatively high greenhouse gas emissions. Climatic change, 109(1), 33-57.

Saaty, T. (1990). How to make a decision: The analytic hierarchy process. European Journal of Operational Research, 44(1). https://doi.org/10.1016/0377-2217(90)90057-I

Snyder, R.L and Melo-Abreu, J.P. (2005). Experimental Agriculture. Food and Agriculture Organization of the United Nations (FAO), Rome, Italy.

Strasser, L., & Stec, S. (n.d.). Transboundary Diagnostic Analysis Thematic Report on the Resource Nexus (Phase I of the Water-Food-Energy-Ecosystems Nexus Assessment of the Drin Basin). Project "Enabling Transboundary Cooperation and Integrated Water Resources Management in the Extended Drin River Basin".

Tabari, H., Marofi, S., Aeini, A., Talaee, P. H., & Mohammadi, K. (2011). Trend analysis of reference evapotranspiration in the western half of Iran. Agricultural and forest meteorology, 151(2), 128-136. https://doi.org/10.1016/j.agrformet.2010.09.009.

Tebaldi, C., & Knutti, R. (2007). The use of the multi-model ensemble in probabilistic climate projections. Philosophical transactions of the royal society A: mathematical, physical and engineering sciences, 365(1857), 2053-2075. https://doi.org/10.1098/rsta.2007.2076.

Termeer, C., Biesbroek, R., Van den Brink, M. (2012). Institutions for adaptation to climate change: comparing national adaptation strategies in Europe. European Policy 11.

The World Bank. (2021). World Bank Climate and Disaster Risk Screening Tools. climatescreeningtools.worldbank.org

Thomson, Allison & Calvin, Katherine & Smith, Steven & Kyle, Page & Volke, April & Patel, Pralit & Delgado Arias, Sabrina & Bond-Lamberty, Ben & Wise, Marshall & Clarke, Leon & Edmonds, Jae. (2011). RCP4.5: A pathway for stabilization of radiative forcing by 2100. Climatic Change. 109. 77-94. doi: 10.1007/s10584-011-0151-4.

UN Environment Programme World Conservation Monitoring Centre (UNEP-WCMC), World Database on Protected Areas (2023). https://www.protectedplanet.net/en/thematic-areas/wdpa?tab=WDPA

USAID (2020). Water Resources & Environment | Jordan | U.S. Agency for International Development (usaid.gov)

Vanuytrecht, E., Wouters, H., Maes, R., Bercjmans, K.R. (2020). Downscaled bioclimatic indicators for selected regions from 1950 to 20100 derived from projections. Product User Guide. Copernicus Climate Change Service.

Vicente-Serrano, S.M., Beguería, S., López-Moreno, S. (2010). A Multi-scalar drought index sensitive to global warming: The Standardized Precipitation Evapotranspiration Index - SPEI. Journal of Climate 23: 1696-1718.

World Resources Institute (2009). The National Adaptive Capacity Framework Key Institutional Functions for a Changing Climate.

World Bank (2022). Development Indicators - Agriculture, forestry, and fishing, value added. https://data.worldbank.org/indicator/NV.AGR.TOTL.CD